

MODIFICATION OF COMMERCIAL FAULT CALCULATION PROGRAMS FOR WIND TURBINE GENERATORS

**Power System Relaying and Control Committee
Report of Working Group C-24
of the
System Protection Subcommittee**

Members of the Working Group

Sukumar Brahma, Chair

Evangelos Farantatos, Vice-Chair

Members (Attendees and Contributors)

Sandro Aquiles-Perez, Siemens Industry Inc. (former Electrocon)
Sherman Chan, ASPEN
Ritwik Chowdhury, SEL
Ratan Das, GE
Alla Deronja, ATC
Charles Henville, Henville Consulting
Jim van de Ligt, CANA Energy Ltd
Dean Miller, POI Engineering
Manish Patel, Southern Company
Athula Rajapakse, University of Manitoba
Looja Tuladhar, Commonwealth
Mohammad Zadeh, ETAP
Amin Zamani, GE

Corresponding Members (Contributors – Non-Attendees)

Nicole Clock, Vestas
Ali Goharrizi, Manitoba Hydro International
Rajat Majumder, Siemens Gamesa Renewable Energy
Donald MacGregor, Siemens Industry Inc. (former Electrocon)
Robert Nelson, Siemens Gamesa Renewable Energy

ACKNOWLEDGMENTS

The Working Group is truly grateful for the support of our sponsoring subcommittee and committee.

KEYWORDS

Fault Calculation, Inverter, Phasor Domain Modeling, Short-Circuit, Wind Turbine Generator

CONTENTS

1. INTRODUCTION.....	1
2. FAULT RESPONSE OF DIFFERENT TYPES OF WTGS.....	2
2.1 Type-I and II	2
2.2 Type-III	4
2.3 Type-IV.....	5
2.3.1 Normal condition (terminal voltage between 0.9 pu to 1.1 pu)	6
2.3.2 Abnormal conditions (terminal voltage less than 0.9 pu or greater than 1.1 pu)	6
3. PROPOSED MODEL STRUCTURE AND DATA NECESSARY TO MODEL TYPE-III and TYPE-IV WTGS IN A PHASOR DOMAIN SHORT-CIRCUIT PROGRAM.....	8
3.1 Rationale	8
3.2 Data needed for modelling Type-III and IV WTGs.....	8
4. PROPOSED ALGORITHMS FOR SHORT-CIRCUIT MODELS of TYPE-III and TYPE-IV WTGS IN COMMERCIAL FAULT CALCULATION PROGRAMS.....	11
4.1 EPRI algorithms and validation results.....	11
4.1.1 Model and algorithm overview.....	11
4.1.2 Type-IV WTG model	12
4.1.3 Type-III WTG model.....	16
4.1.4 Model validation study for Type-III WTG plants	18
4.2 OneLiner model implementation	27
4.2.1 Introduction	27
4.2.2 Dynamic reactive current control mode	28
4.2.3 Implementation overview.....	29
4.2.4 Modeling considerations for a wind farm	30
4.2.5 Data needed for Type-IV generators	30
4.2.6 Experience on solution method for Type-IV generators.....	32
4.2.7 What is <i>not</i> modeled in ASPEN's Type-IV WTG.....	32
4.2.8 Benchmarking Type-IV wind generator model against EPRI model.....	33
4.2.9 Data needed for Type-III WTG model.....	34
4.2.10 Benchmarking Type-III WTG model against EPRI model	35
4.3 CAPE model implementation	36
4.3.1 Type-IV WTG model	37
4.3.2 Type-III WTG model.....	40
4.3.3 Voltage-Controlled Current Source (VCCS)	40
4.3.4 Iterative Algorithm	41
4.3.5 Reports	42
4.3.6 Examples	44
4.4 ETAP model implementation.....	47
4.4.1 WTG Type-I and II.....	47
4.4.2 WTG Type-III with crowbar.....	47

4.4.3	WTG Type-III without crowbar or Type-IV	47
5.	CONCLUDING REMARKS.....	51
6.	REFERENCES.....	52
	APPENDIX A: DATA GENERATED WITH PSCAD USING BLACK-BOX MODELS – TYPE-III AND IV.....	54
A.1	Type-III wind turbine results	54
A.1.1	Fault results on Bus 2	55
A.1.2	Fault results on Bus 4	56
A.2	Type-IV wind turbine results.....	59
A.2.1	Fault results on Bus 2	59
A.2.2	Fault results on Bus 4	61
A.2.3	Generic Type-IV WTG based on IEC standard 61400-27-1 (2015)	63
	APPENDIX B – DATA PROVIDED BY OEM – TYPE-IV WTG	65
	APPENDIX C – SIMULATION AND ANALYSIS OF SEQUENCE FAULT VOLTAGE-CURRENT CHARACTERISTICS OF A TYPE-III GE WTG	66
C.1	Simulation of Faults	66
C.2	Faults Performance Characteristics	67
	APPENDIX D – DATA PROVIDED BY VESTAS – TYPE-IV WTG	71
	APPENDIX E – TYPE-III WTG MODEL PARAMETERS	72

THIS PAGE LEFT BLANK INTENTIONALLY

1. INTRODUCTION

In 2015, Power System Relaying & Control Committee, jointly with Electric Machines and Transmission and Distribution committees, published a report entitled “Fault Contributions from Wind Farms”[1]. This report documented simulated and field data pertaining to different types of wind turbine generators (WTGs) and wind farms. The report showed the complexities of the short-circuit responses, especially from Type-III and Type-IV WTGs, which revealed that the existing phasor domain short-circuit models for WTGs in commercial fault analysis programs do not adequately capture the fault behavior of these WTGs. This led to the formation of this working group C24 - Modification of Commercial Fault Calculation Programs for Wind Turbine Generators. The scope of this working group was:

- 1) To survey WTG manufacturers to determine what parameters they could provide that could be used by steady-state short-circuit program developers to model the response of WTGs in various time frames.

- 2) To use the results of this survey to prepare a report that can be used by steady-state short-circuit program developers to refine their models.

Three major WTG manufacturers – Siemens Gamesa, Vestas and General Electric (GE) – were engaged to discuss the fault response characteristics of their WTGs and what data they would be able to provide without revealing their proprietary controls. Based on their response and further discussions, the working group members agreed to a dataset and model structure that would be sufficient to create accurate short-circuit models of Type-III and Type-IV WTGs.

Section 2 of this report provides the necessary background of the behavior of different types of WTGs. Based on this background and the discussions with WTG manufacturers, section 3 outlines the proposal of the WG about the data to be requested from and provided by the WTG and inverter manufacturers for creating accurate short-circuit models. Section 4 describes the implementation of such models by EPRI, ASPEN, Siemens and ETAP. Data from WTG manufacturers and from time-domain simulations of black-box models of Type-III and IV WTGs are provided in the appendices.

Nature of this work required close collaboration with WTG manufacturers for data and commercial software developers to demonstrate feasibility of the approach proposed by the working group. Therefore, their names appear in the report. This should not be construed as endorsement of these companies either by the Power System Relaying and Control Committee, or by the IEEE.

2. FAULT RESPONSE OF DIFFERENT TYPES OF WTGS

2.1 Type-I and II

Type-I WTGs, schematically shown in Fig. 2-1, use squirrel cage induction generators with switched shunt capacitors on the generator terminals for power factor correction. Several steps of shunt capacitors are typically used for different operating speeds of the turbine shaft. To produce power, the speed of the rotor needs to be greater than the rotation of the magnetic field created by the power system.

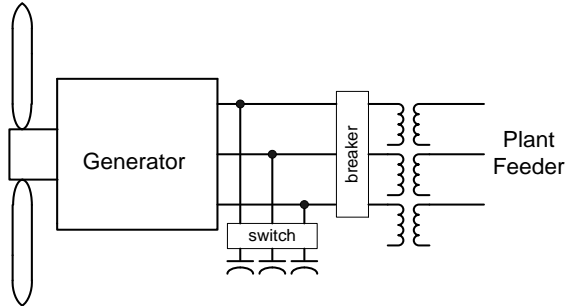


Fig. 2-1. Basic configuration of a Type-I wind turbine generator.

The performance of a Type-I WTG for a fault on the power system is dictated by the electromagnetic configuration of the generator. Fig. 2-2 is a diagram of the equivalent circuit for an induction generator for a fault on the system.

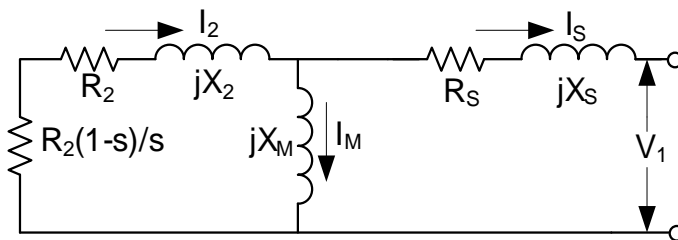


Fig. 2-2. Equivalent circuit of an induction generator.

Its parameters are:

- Stator resistance R_s
 - Stator leakage reactance X_s
 - Magnetizing reactance X_m
 - Rotor resistance R_2 referred to stator
 - Rotor leakage reactance X_2 referred to stator
 - Slip $s = (n_s - n_m) / n_s$; n_s = synchronous speed, n_m = machine speed
- The equivalent transient reactance that can be used to calculate the initial response of the WTG to a system fault is calculated using the following equation:

$$X' = X_s + \frac{X_m X_2}{X_m + X_2} \quad (1)$$

Since the rotor field is induced from the power system, the collapsed terminal voltage due to the fault and the internal resistance of the rotor causes the fault current contribution from the WTG to decrease with time. The maximum fault current that a typical Type-I WTG contributes to a collector system three-phase fault, with the WTG step-up transformer having 6% impedance, is typically in the range of 3.2 - 4.3 per unit. By the fourth cycle into the fault event the magnitude of that current normally drops to 1.4 - 2.0 per unit, and by the 30th cycle the current approaches zero [1].

Type-II WTGs, shown schematically in Fig. 2-3, use induction generators with wound rotors and variable external resistance inserted in the rotor circuits. To produce power, the Type-II WTGs, like the Type-I WTGs, have the rotor turning faster than the magnetic field created by the power system. With the external resistors, the Type-II WTG can produce power over a wider range of wind speeds compared to the operating speed-range of the Type-I WTG.

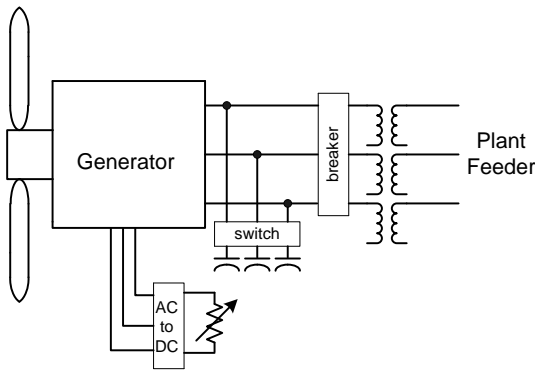


Fig. 2-3. Basic configuration of a Type-II wind turbine generator.

The same equivalent circuit of an induction machine, as shown in Fig. 2-2, can be used for the Type-II WTG, but the rotor resistance R_2 , which represents the actual rotor resistance R_r referred to stator for Type-I machine, represents the rotor resistance R_r plus the external rotor resistance R_{ext} for the Type-II machines. Generally, it is not critical to model the controls for this external rotor resistance. The maximum fault contribution always occurs for an external resistance value of zero. The higher the slip the larger the value of the external resistance. With larger values of the external resistance the maximum initial fault current contributed from the Type-II WTG is reduced and the amount of damping of the current is increased. With the increased damping the duration of the fault current is reduced.

If the maximum fault current is the quantity needed for the analysis being performed, then the Type-II WTG can be modeled using the same Equation (1) as used for the Type-I WTGs. For the same WTG step-up transformer with 6% impedance, as used in the Type-I WTG description, the fault current contribution from a Type-II WTG for a three phase fault on the terminal of the transformer is typically in the range of 2.7 - 4.3 per unit current. By the fourth cycle into the fault event the magnitude of that current normally drops to 1.0 - 2.0 per unit and by the 30th cycle the current approaches zero.

2.2 Type-III

Type-III WTG provides independent control of active and reactive power over a wider range of operating slips ($\pm 30\%$) using back to back converters between the rotor and the grid. Stator winding in the Type-III WTG is connected directly to the grid. Type-III WTG is made up of the following components: wind turbine, wound rotor induction generator (WRIG) – typically doubly-fed induction generator (DFIG), rotor side converter (RSC) and grid side converter (GSC) as shown in Fig. 2-4. RSC is normally set to control active and reactive power injection into the grid through the stator. GSC keeps the DC link voltage constant and provides reactive power to the grid, thus, reducing the need for external capacitors. Both GSC and RSC have insulated-gate bipolar transistor (IGBT) switches that are controlled via a pulse width modulation (PWM) scheme. Type-I and Type-II WTGs can transfer wind power to the system only at supersynchronous speeds, and the maximum value of the slip is determined by the rotor resistance. Type-III WTGs on the other hand facilitate bidirectional transfer of real power between power system and the rotor, allowing large variations of slip at both subsynchronous and supersynchronous speeds. At supersynchronous speed the wind power is pushed out via the converters into the power system, while at subsynchronous speeds the real power is absorbed from the grid via converters. Since severe faults in the network can induce high stator and rotor currents, the converters used in the Type-III WTG characteristically have protection which is provided by a crowbar circuit that gets activated if the rotor current increases beyond a certain threshold. The rotor currents can reach three times the nominal value without a crowbar activation, which could lead to a high DC link voltage. When the crowbar gets activated, it shorts the rotor which in effect isolates the converter, making the WTG perform similar to what was described above for a Type-I or Type-II WTG, causing a short-circuit model described by equation (1). This model produces the highest fault currents which can be used for equipment ratings and withstand capabilities. [1]

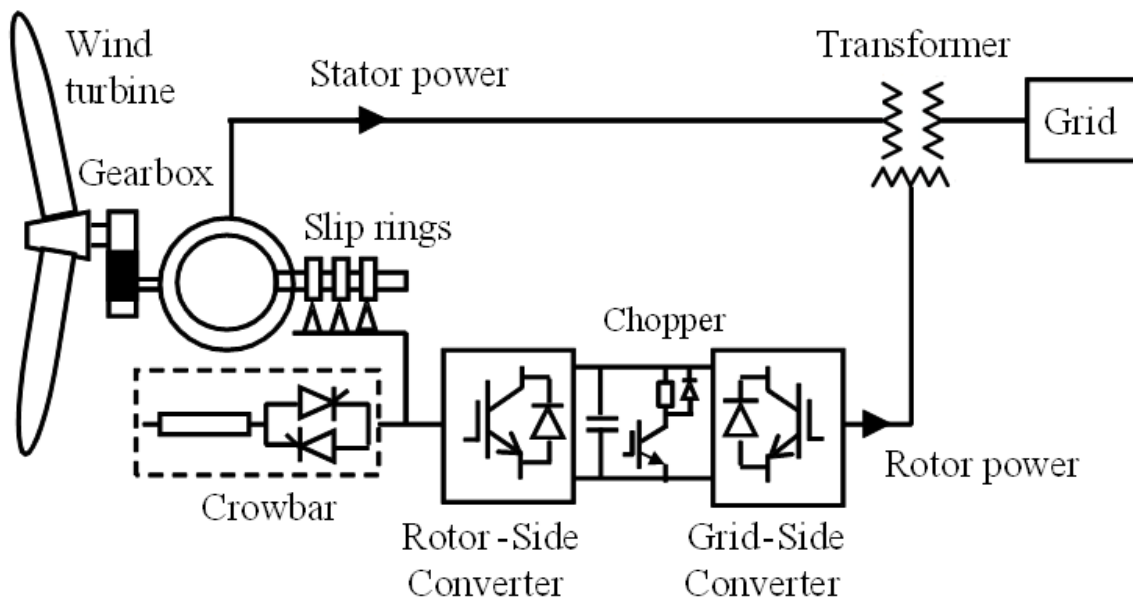


Fig. 2-4. Typical Type-III WTG configuration.

On the other hand, when the crowbar does not activate, it is much more difficult to model the Type-III WTG. The controls are very design dependent, and to accurately model the behavior, normally one would need access to proprietary data from the manufacturer that describe the operation of the WTG when not under crowbar. Controls for the WTG, for example, may be configured for current limiting operation. This current can be estimated at 1.1 to 2.5 times the rated current at known angle. Recent designs of Type-III WTGs allow the crowbar to intermittently activate during a fault. This allows effective control of the fault current from the WTG throughout the duration of the fault.

To summarize, it is important to determine whether the crowbar gets activated or not during a fault, as it can significantly impact the short-circuit behavior of the machine. When the crowbar is inactive, current magnitude and angle are dependent on control design. Due to the different designs, a general short-circuit model is difficult to create.

2.3 Type-IV

A Type-IV WTG consists of an induction machine (IM) or a permanent magnet synchronous generator (PMSG) connected to the grid via a full power electronic converter as shown in Fig. 2-5. This essentially decouples the machine from the grid, and the fault response of this type of WTG is dictated by the behavior of the converter [1]. Typically, these converters do not produce negative sequence currents, even during unbalanced faults on the grid, although in some countries the converters are designed to produce negative sequence currents if mandated by the grid code (for example German grid code [2]). In addition, in order to protect the component devices, the magnitude of the output current is quickly controlled to a value close to the rated current of the converter.

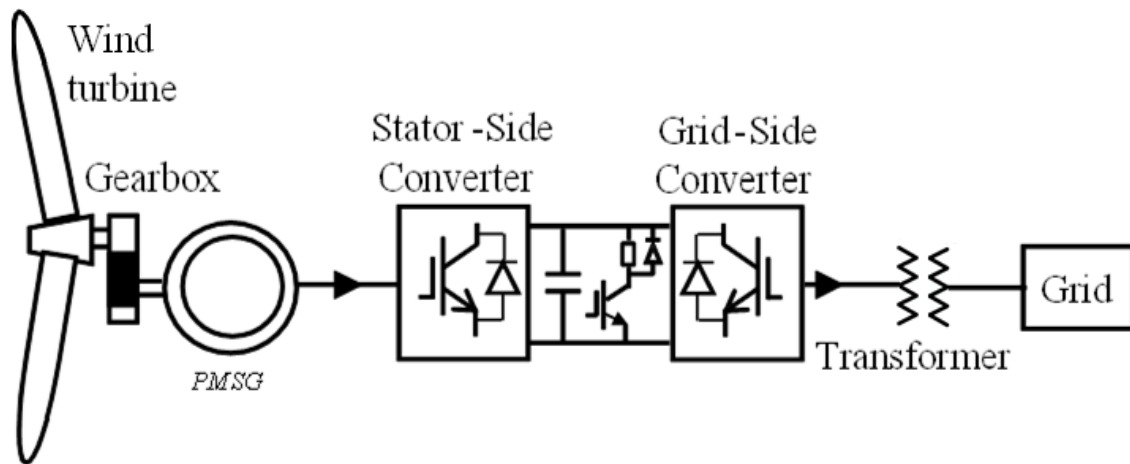


Fig. 2-5. Typical Type-IV WTG configuration.

The controls for the Type-IV WTG converters can make it possible for the WTG to ride through faults and provide reactive power to support voltages during faults. Therefore, the controls facilitate a range of power factors to operate the WTG during normal and faulted conditions. Based on the input received by this working group from Siemens, the following operating conditions are typical.

2.3.1 Normal condition (terminal voltage between 0.9 pu to 1.1 pu)

WTGs are typically in voltage regulation mode. They are given terminal voltage set-points by the wind-park controller, which is usually regulating voltage at a node on the transmission system. The turbines can usually regulate from 90% to 110% of their nominal voltage. Real power is given priority in this range, but the turbines can typically operate with enough reactive power to provide ± 0.9 pf at their terminals at rated voltage. Settings of the converter output are typically designed in the synchronous, or dq reference frame, though control is also possible in phase domain. Conversion of phase quantities to synchronous reference frame transforms voltage and current to a frame that rotates synchronously with the grid voltage vector, making three-phase time-varying signals appear as DC signals. Details of the inverter control in dq frame can be found in [3].

The portion of the current in phase with the converter output voltage is denoted I_{active} in this section, and the quadrature component is the reactive part of the current, denoted $I_{reactive}$ in this section. The total output current is $I = I_{active} + jI_{reactive}$, which is restricted to a magnitude close to the nominal current, values between 1.1 pu to 1.3 pu being typical. Following is the setting procedure illustrated with an example:

Active current is set as: $I_{active} = P_{pu} / V_t^{(1)}$ pu, where P_{pu} is the real power output in per unit and $V_t^{(1)}$ is the positive sequence voltage magnitude at the converter terminal. If converter is supplying rated power at nominal voltage, $I_{active} = I/I = 1$ pu. For half the rated power at 95% voltage, $I_{active} = 0.5/0.95 = 0.526$ pu, and so on. In the normal operating condition, $I_{reactive}$ can be adjusted to any value up to $\sqrt{I_{max}^2 - I_{active}^2}$ leading or lagging. I_{max} is the limit imposed on the output current magnitude.

2.3.2 Abnormal conditions (terminal voltage less than 0.9 pu or greater than 1.1 pu)

2.3.2.1 Low Terminal Voltage

For a terminal voltage lower than 0.9 pu, certain reactive current is expected to be supplied by the converter. Several different control strategies are available, but one that is commonly used is: $I_{reactive} = I_{reactive, PreFlt} + K(I - V_t^{(1)})$ pu for $V_t^{(1)} < 0.9$ pu. K is a multiplier from 1 to 10, typically set to 2, and $I_{reactive, PreFlt}$ is the pre-fault value of the reactive current.

Given that the maximum total current magnitude allowed during a fault is limited (say, to 1.1 pu), for a measured voltage $V_t^{(1)}$, $I_{reactive}$ is known for set values of K . Since the inverter current I equals $I_{active} + jI_{reactive}$, the active current I_{active} can be found, and hence the power factor of the total current can be determined. However, there are nuances to these settings that depend on the available real power and/or the positive sequence voltage at the converter terminal during fault. The total current is at its limit (e.g. 1.1 pu) only if the active power is high or the voltage is low. In the examples that follow, generated reactive current is considered positive going *out* of the source, and the corresponding power factor is considered lagging.

For example, if the turbine is operating at unity power factor prior to a fault, the pre-fault active power is 5% (at nominal voltage) and the voltage drops to 70%, then, for K factor equal to 2, $I_{reactive} = 2(I - 0.7) = 0.6$ pu. If it is a remote balanced fault, the $I_{active} =$

0.05 / 0.7 = 0.07 pu, and the total current is $\sqrt{0.6^2 + 0.07^2} = 0.604$ pu, which is below the maximum allowed. On the other hand, if the active power is at its nominal value at unity pf and the voltage drops to 0.7 pu, then the desired currents are $I_{active} = 1/0.7 = 1.43$ pu and $I_{reactive} = 2(1-0.7) = 0.6$ pu. Since the total current equaling $\sqrt{1.43^2 + 0.6^2}$ exceeds the 1.1 pu limit, the active current is limited to $\sqrt{1.1^2 - 0.6^2} = 0.92$ pu. Thus, the reactive power gets priority during the fault. If the voltage drops even further to 0.4 pu and the active power is nominal, then the desired currents are $I_{active} = 1/0.4 = 2.5$ pu, and $I_{reactive} = 2(1-0.4) = 1.2$ pu. Obviously, the limit is hit again, and with the Q-priority imposed upon the current limiter function, the currents are $I_{reactive} = 1.1$ pu and $I_{active} = 0$.

2.3.2.2 High terminal voltage

For terminal voltages higher than 1.1 pu, the converter loses its ability to export reactive power, but it can typically operate at a low power factor to absorb reactive power. Since the converter is current-limited, it can operate, for example, roughly at 0.8 pf at 110% voltage and 0.75 pf at 120% voltage, though the permissible time at terminal voltages above 110% is usually limited. Given the existence of two transformers between the WTG and the system (usually, there is a WTG transformer and a wind-farm transformer), these control methods are quite effective at pulling the system voltage down. Of course, the same transformers are slightly detrimental when the turbines provide reactive power. Some examples illustrating this behavior follow.

At 1.2 pu voltage and nominal pre-fault power, $I_{active} = 1/1.2 = 0.833$ pu, so, if $I_{max} = 1.1$ pu, $I_{reactive} = -0.7181$ pu (negative because it absorbs reactive power), the power factor is 0.76 (leading). At 1.1 pu voltage and nominal pre-fault power, $I_{active} = 1/1.1 = 0.9091$ pu, so $I_{reactive} = -0.6193$ pu, a power factor is 0.83 (leading). At 1.1 pu voltage and half the nominal pre-fault power, $I_{active} = 0.5/1.1 = 0.4545$ pu, so $I_{reactive}$ can go all the way up to -1.002 pu or to a power factor of 0.41 (leading).

3. PROPOSED MODEL STRUCTURE AND DATA NECESSARY TO MODEL TYPE-III and TYPE-IV WTGS IN A PHASOR DOMAIN SHORT-CIRCUIT PROGRAM

3.1 Rationale

As described in section 2, the fault response of Type-III and Type-IV wind power plants depends on the control system of the converters and the associated control settings that define the real and reactive power control of the wind power plant. Phasor domain programs can model converter interfaced renewable resources using an iterative method to consider the nonlinear fault response of these devices due to the converter controls. A renewable resource may be modeled in short-circuit programs as a voltage dependent current source. This is the main “modification of the commercial short-circuit program” compared to the traditional voltage source behind an impedance model used for synchronous generators. The voltage dependency of the current can be indicated using tabular data structures. A formal data structure format is provided in Section 3.2 to allow software vendors to implement the iterative solution of the voltage dependent current source model based on the terminal conditions at the WTG. It is recognized that Type-I and II WTGs are adequately modeled in commercial short-circuit programs, and no modifications are discussed further.

Considering that short-circuits may be balanced or unbalanced, information may be provided in the sequence domain (positive, negative and zero sequence) or in the phase domain (phase A, B and C), although the sequence domain is preferred. Also, considering that the short-circuit presents reduced voltages to the WTG, and the converter response depends on the voltage magnitude, the information is necessary at various voltage levels. It is also realized that the zero-sequence network of a WTG is typically isolated from the power system via a delta-wye grounded transformer. So, zero sequence voltages on the power system would not affect the output of the WTG.

It is also realized that some control systems may be time dependent, thus the fault response of the WTG may vary for different time instants while commercial fault calculation programs provide steady-state solutions. This is done for synchronous generators because the impedance of the generators increases with time during a fault. In commercial programs, it is possible to specify different time frames for which the analysis is performed.

3.2 Data needed for modelling Type-III and IV WTGs

A tabular data format shown in Table 3-1 is proposed, and the manufacturers can provide the data in the suggested tables without disclosing any proprietary information. All units are in per unit, based on the continuous rating of the WTG. The values in the tables can be obtained as follows:

- a) Provided by a manufacturer.
- b) Obtained via simulation models, preferably detailed Electromagnetic Transient (EMT) models and simulations.
- c) Generated through algorithms for generic control modes/logic of the wind power plant.

Guidance needed to provide the tabular data is provided below.

Item 1. Specify the fault type.

Item 2. The fault response is time dependent. Therefore, complete a separate table (Table 3-1) for each time frame that may be considered “steady-state” for a phasor domain solution.

Table 3-1. Proposed Tables for WTG Short-Circuit Model in Commercial Platforms

Time frame 1 (seconds or cycles)		Fault Type:
Positive sequence voltage (pu)	Positive sequence current (pu)	Positive sequence current angle with respect to positive sequence voltage (deg)
1.0		
0.9		
0.8		
0.7		
0.6		
0.5		
0.4		
0.3		
0.2		
0.1		

Time frame 1 (seconds or cycles)		Fault Type:
Negative sequence voltage (pu)	Negative sequence current (pu)	Negative sequence current angle with respect to negative sequence voltage (deg)
1.0		
0.9		
0.8		
0.7		
0.6		
0.5		
0.4		
0.3		
0.2		
0.1		

Item 3. Complete the fields shown in Table 3-1 to specify the response of the current control system at various per unit values of the measured voltage (one for each time frame longer than 1 cycle). Similar tables are expected to be provided for time frame 2 and additional time frames if necessary. The positive sequence current angle with respect to positive sequence voltage is negative if the reactive power is generated and positive if it is absorbed.

Item 4. It is realized that the response of the control system (and consequently the fault response) depends on the control settings of the converter and may vary depending on those. The manufacturers may provide a separate table (or sets of tables) (Table 3-1) for different control modes of the converter.

Item 5. It is realized that the values in the tables above (Table 3-1) depend on the pre-fault active power generated by the WTG. Thus, the pre-fault active power level for which the values in the tables were generated, is necessary to be specified. One common practice is to keep the pre-fault active power at nominal value.

Appendices A through D display such tables filled out by WTG manufacturers, provided as realistic examples of typical data.

4. PROPOSED ALGORITHMS FOR SHORT-CIRCUIT MODELS of TYPE-III and TYPE-IV WTGS IN COMMERCIAL FAULT CALCULATION PROGRAMS

This section reports work performed in developing phasor-domain short-circuit models using validated time-domain models for Type-III and Type-IV WTGs. As mentioned in Section 3.2, these models can be one of the options to create accurate short-circuit models. It is noted that there are no guarantees that all models for all manufacturers exhibit behavior similar to that described by these models, but in absence of specific data from manufacturers, these models can provide enhanced support.

4.1 EPRI algorithms and validation results

As described in the previous sections, the power electronics associated with the WTGs can produce current waveform signatures that are significantly different from those of traditional synchronous or asynchronous generators. The short-circuit characteristics of electronically coupled generators can be determined with high precision using time-domain simulation methods and tools such as EMTP, provided the controls are known. On the other hand, it is common practice for protection and planning engineers to perform short-circuit analysis in the phasor domain. It is therefore important to develop and include accurate phasor models of renewable powered generating plants in the existing fault and protection analysis tools.

Recognizing this industry gap, EPRI in collaboration with Polytechnique Montreal has developed phasor domain steady-state short-circuit models for renewable powered generating plants coupled to the grid by means of power converters, i.e. wind parks employing Type-III and Type-IV WTGs. The EMTP models developed to benchmark the steady-state short-circuit analysis models use thoroughly researched generic controls and have been validated against some field data. The models can be used to simulate both balanced and unbalanced faults. The models are summarized in section 4.1.1. Details of the models, the algorithms and demonstrating examples can be found in [3]-[10].

4.1.1 Model and algorithm overview

The proposed phasor models are based on the concept of control based equivalent circuits. The WTG is represented by a voltage-controlled current source and the impact of WTG control is accounted through iterative solutions considering the mode of operation and the associated limiter constraints. Classical short-circuit solvers perform short-circuit analysis in one step by linearizing the network. However, the nonlinear nature of WTG controls necessitates an iterative solution, so in the proposed model the network is linearized at each iteration.

The overall structure of the iterative short-circuit algorithm is shown in Fig. 4-1. The analysis is initialized with a power flow solution (this is optional). The network is linearized and the WTGs are represented with current sources using the power flow solution. A given short-circuit scenario is afterwards produced by applying a fault on the network. Then, the current injection of the WTGs is computed iteratively using the network voltage conditions as an input until convergence, i.e., until the network voltages

and WTG current injections settle and the variations between two consecutive iterations fall under the pre-specified convergence tolerance.

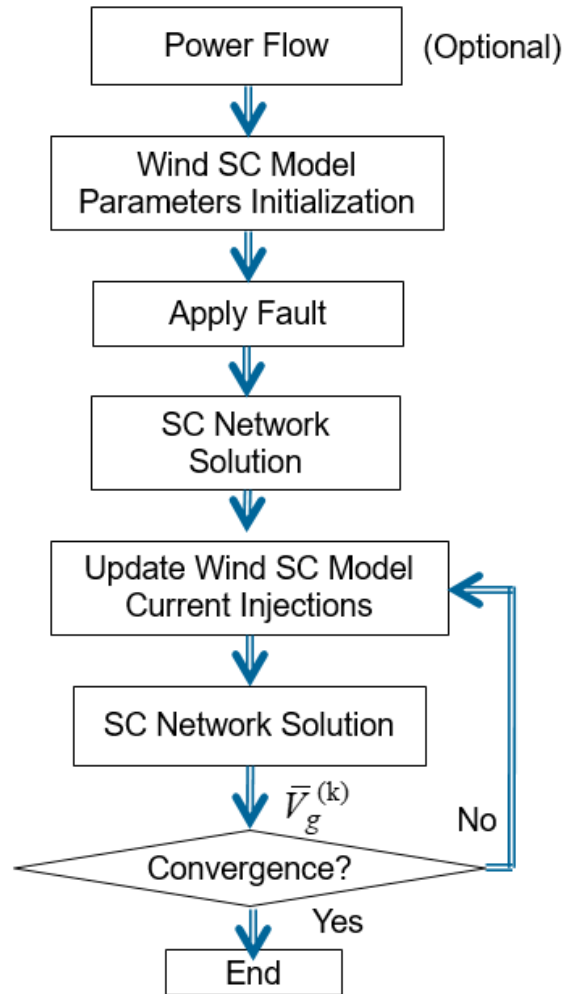


Fig. 4-1. Iterative Solution.

The “Update Wind SC Model Current Injections” block can be updated using the tabular data obtained from the manufacturer as described in section 3. The generic models created at EPRI for Type-III and Type-IV WTGs that can be used when such data are unavailable are described next. Sections 4.1.2 and 4.1.3 summarize the controls employed in the generic EMT models and validate the phasor domain equivalent models through simulation results for the IEEE 39-bus system. Section 4.1.4 shows that the model for Type-III, with appropriate tuning, can replicate the recorded fault response of a Type-III wind farm.

4.1.2 Type-IV WTG model

The fault response of the Type-IV WTG is governed by the GSC. The GSC control has 3 blocks: outer voltage/current control, current limiter and inner control. The outer control calculates the reference dq -frame currents. The reference currents are limited according to the P or Q priority and the current-limiting logic discussed in section 2.3.

The inner control allows controlling the converter AC voltage used to generate the modulated switching pattern. In the developed short-circuit model, Table 4-1 presents the generic control modes that are considered for the inverter in the developed short-circuit model.

Table 4-1. Generic Converter Control Modes of Inverter

Function	Control Mode	Performance/Description
Reactive power/voltage control during ride-through	Constant power factor	Allows for injection/absorption of reactive power based on a desired power factor
	Constant Q	Allows for fixed desired value of reactive power injection/absorption
	V Control	Allows for control of voltage to desired value
	Dynamic reactive current control based on reference curve	Allows for reactive current injection based on a reference curve (e.g. grid code)

For the dynamic reactive current control, a typical curve used is depicted in Fig. 4-2 which shows that the reactive current injection is proportional to the voltage deviation from 1pu, for values outside the deadband.

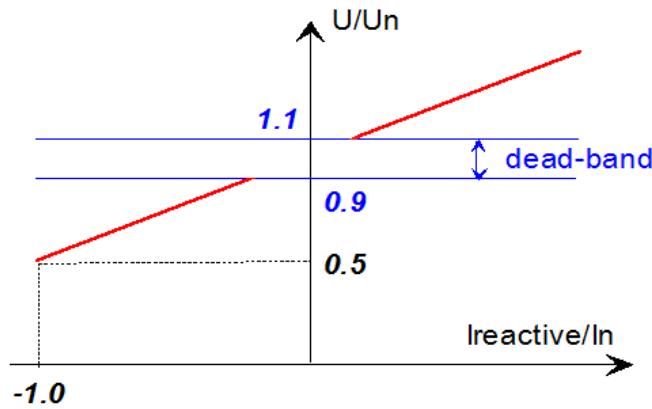


Fig. 4-2. Dynamic Reactive Current Injection Curve [10].

During a fault, the active power injection depends on the wind speed and maximum power point tracking control whereas the reactive power injection depends on the control mode. All the control modes use positive sequence voltages and currents. Some converters may allow negative sequence current injection by default or based on control settings during unbalanced fault. Various industries are exploring the need of such a feature to enhance the system performance during unbalanced faults. The data model proposed in Section 3.2 can cover such feature. However, algorithms, models and software implementations discussed in this report do not cover negative sequence current injection for Type-IV.

Independent of the control mode, the controller can give the priority to active power or reactive power. This is important when the reference current calculated by the control mode exceeds the thermal capacity of the semiconductor elements. In such a case, the active or reactive component of current needs to be reduced. If the reactive current output has priority, the converter current reference values are limited based on the following equations.

$$\begin{aligned} i_{react-ref} &\leq i_{react-lim} , & i_{react-lim} &= 1pu \\ i_{act-ref} &\leq i_{act-lim} = \sqrt{i_{lim}^2 - i_{react-ref}^2} , & i_{lim} &= 1.1pu \end{aligned}$$

where, $i_{react-lim}$ is the reactive (q-axis) current reference limit, $i_{act-lim}$ is the active (d-axis) current reference limit and i_{lim} is the converter current reference limit. Note that $i_{act-lim}$ is dynamic and changes with the reactive current reference $i_{react-ref}$. If the active current output has priority, the converter current reference values are limited based on the following equations:

$$\begin{aligned} i_{act-ref} &\leq i_{act-lim} , & i_{act-lim} &= 1pu \\ i_{react-ref} &\leq i_{react-lim} = \sqrt{i_{lim}^2 - i_{act-ref}^2} , & i_{lim} &= 1.1pu \end{aligned}$$

In this case note that, $i_{react-lim}$ is dynamic and it changes with the active current reference $i_{act-ref}$. In these equations, the values for $i_{react-lim} = i_{act-lim} = 1.0 pu$, and $i_{lim} = 1.1 pu$ are typical values and depend on the WTG manufacturer. Numerical examples of the current limiting logic are described in Section 2.3.

If the fault is balanced, the current injection is comprised of only positive sequence component. If the fault is unbalanced, there might also be a negative sequence component depending on the WTG control. In case of coupled control where there is no specific control for negative sequence component, a small negative sequence component typically appears due to the filtering of measured input data in the control system. The presence of negative sequence results in double network frequency oscillations in the dq frame. When there is a decoupled control, the negative sequence can be computed depending on the imposed control, but typically the negative sequence outer controller of the WTG-IV is used to eliminate the negative sequence current output of the WTG. Given that, for the EPRI Type-IV models presented in this report it was assumed that, even for unbalanced faults, the negative sequence current contribution is zero.

The WTG-IV is modeled with a controlled current source as shown in Fig. 4-3. The positive sequence current is computed by taking into account the controls of the WTG. The current output of WTG-IV (I_{fc}) is calculated using the iterative solution described in 4.1.1. More details on the algorithm can be found in [2]-[9].

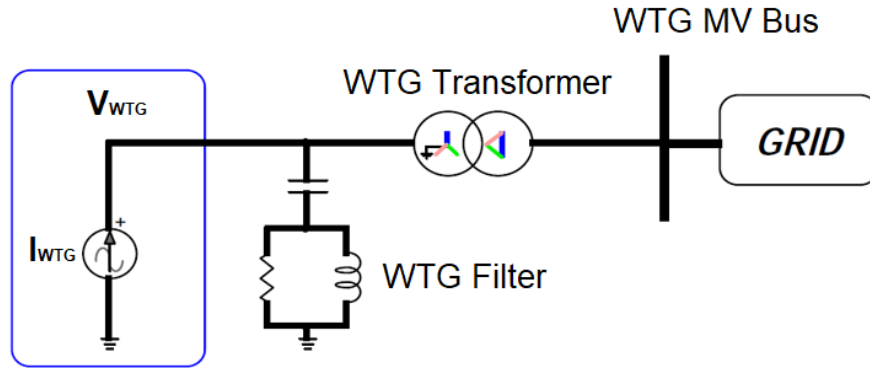


Fig. 4-3. WTG-IV controlled current source model.

Test results are given next, using the network of Fig. 4-4, which is the IEEE 39 bus system, with two synchronous generators replaced by wind farms (WF1, WF2) of equal capacities. For faults simulated at locations F1, F2, and F3, the phasor model results are compared to detailed time domain EMTP-RV simulations at the 3rd cycle during the fault. Table 4-2 and Table 4-3 present the comparison of the magnitude (in pu) and angle (in degrees) for the currents and voltages.

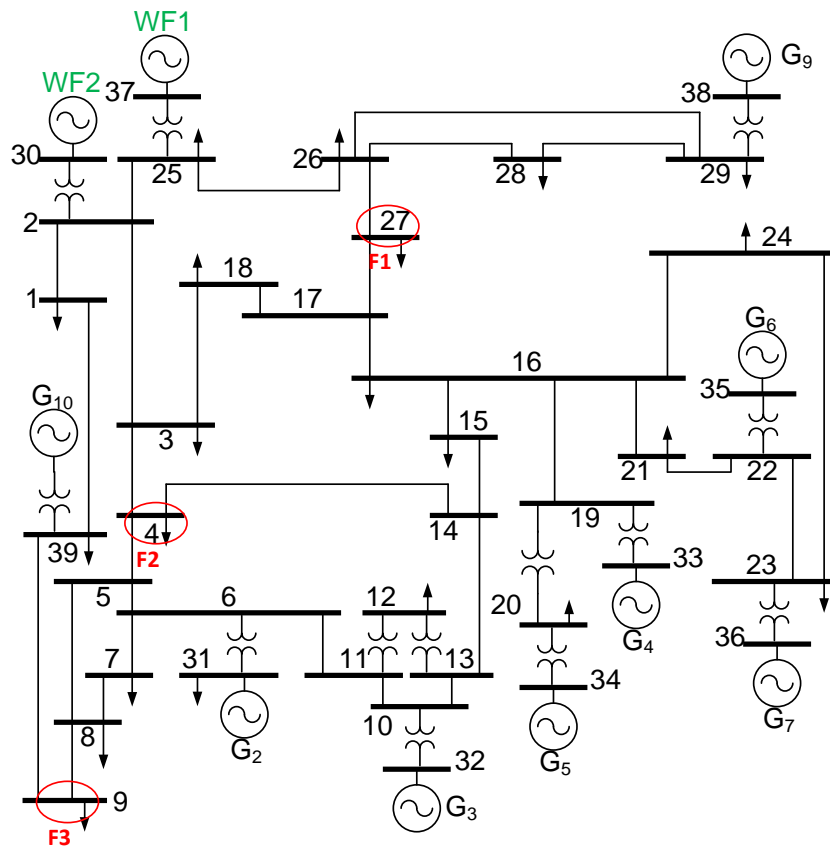


Fig. 4-4. Test System

Table 4-2. IEEE 39 Bus System - LL Fault at F1 – Type-IV WTG

WTG variable	WP1		WP2	
	EMTP-RV	Phasor Solution	EMTP-RV	Phasor Solution
\bar{I}_{fc}^+	1.039 \angle -4.0°	1.039 \angle -3.9°	1.035 \angle -6.6°	1.035 \angle -6.6°
\bar{V}_{fc}^+	0.858 \angle 11.8°	0.858 \angle 11.9°	0.866 \angle 8.3°	0.866 \angle 8.4°

Table 4-3. IEEE 39 Bus System - SLG Fault at Point of Interconnection (POI) of WP1 – Type-IV WTG

WTG variable	WP1		WP2	
	EMTP-RV	Phasor Solution	EMTP-RV	Phasor Solution
\bar{I}_{fc}^+	1.101 \angle -15.8°	1.100 \angle -15.2°	1.061 \angle -15.0°	1.058 \angle -14.9°
\bar{V}_{fc}^+	0.752 \angle 10.6°	0.764 \angle 10.2°	0.823 \angle 4.3°	0.828 \angle 4.1°

4.1.3 Type-III WTG model

In the model developed by EPRI, the Type-III WTG control is achieved by controlling the RSC and the GSC through vector control techniques. The RSC controls the active and reactive powers delivered to the grid and follows a tracking characteristic to adjust the generator speed for optimal power generation depending on the wind speed. The same control modes and generic control schemes as in the GSC control of WTG-IV apply for the RSC of WTG-III. Independent of the control mode, the controller can give priority to active power or reactive power. On the other hand, the GSC is used to maintain the DC bus voltage at nominal value. The GSC may be used to support the grid with reactive power during faults.

The short-circuit behavior is complex and determined by the combined and coupled response of the induction generator (IG) with the RSC and GSC. Note that the fault contribution is from both the stator of the IG and the GSC. As in the case of Type-IV WTG, the stator currents are calculated according to active power production and the control mode of the WTG. The currents imposed by the control cannot be used directly because the current limitations of the RSC need to be satisfied. In other words, the currents on the stator are used to calculate the corresponding rotor currents which are then checked against the current limits. The active and reactive components of the rotor current need to conform to their limits and the total current limit of the RSC. The active component of the GSC current depends on the active power flow in the RSC. This power can be obtained from the rotor and stator currents. This power transfer needs to be considered to calculate the active component of the desired stator-current. The total amount of active power produced is defined by the wind speed.

For unbalanced faults, the Type-III WTG has a negative sequence contribution as well. By analyzing the behavior of the control system and the machine equations, a

relation has been formulated between the negative sequence stator current and the negative sequence voltage on the stator. Due to the negative sequence, oscillations at twice the network frequency are observed in the dq frame. Because of these oscillations, an additional active power transfer occurs on the RSC. This active power needs to be considered to determine the active current of the GSC. In other words, the negative sequence parameters on the RSC impacts the positive sequence active power of the GSC.

An equivalent controlled current source model has been developed for WTG-III (Fig. 4-5) that uses an iterative algorithm to compute the short-circuit current contribution. The stator and GSC negative sequence current outputs are calculated separately using the IG - RSC and GSC control mode. More details on the algorithm can be found in [2]-[9].

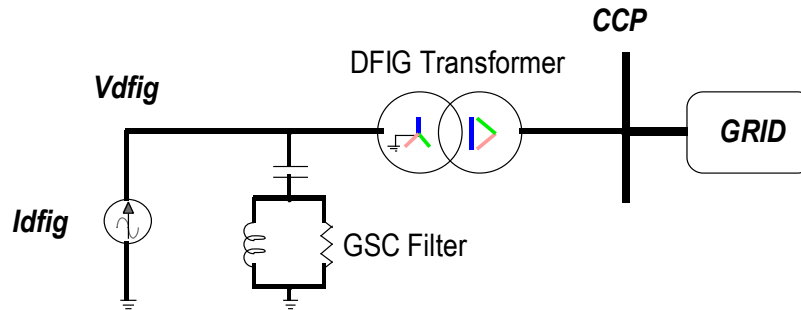


Fig. 4-5. WTG-III controlled current source model.

Test results are given in Table 4-4 and Table 4-5. The IEEE 39 bus system in Fig. 4-4 is used again as the test system. The phasor model results are compared to detailed time domain EMTP-RV simulations.

Table 4-4. IEEE 39 Bus System - LL Fault at F1 – Type-III WTG

DFIG variable	WP1		WP2	
	EMTP-RV	Phasor Solution	EMTP-RV	Phasor Solution
\bar{I}_{dfig}^+	1.025 \angle 1.6°	1.025 \angle 1.1°	1.018 \angle -1.3°	1.020 \angle -1.6°
\bar{V}_{dfig}^+	0.805 \angle 13.8°	0.808 \angle 13.7°	0.817 \angle 9.7°	0.820 \angle 9.8°
\bar{I}_{dfig}^-	0.381 \angle -33.3°	0.384 \angle -35.2°	0.329 \angle -30.2°	0.331 \angle -31.6°
\bar{V}_{dfig}^-	0.128 \angle -145.1°	0.127 \angle -143.1°	0.110 \angle -141.2°	0.110 \angle -139.6°

Table 4-5. IEEE 39 Bus System - SLG Fault at POI of WP1 – Type-III WTG

DFIG variable	WP1		WP2	
	EMTP-RV	Phasor Solution	EMTP-RV	Phasor Solution
\bar{I}_{dfig}^+	1.088 \angle -11.0°	1.089 \angle -10.2°	1.069 \angle -9.3°	1.041 \angle -10.7°
\bar{V}_{dfig}^+	0.701 \angle 12.9°	0.700 \angle 13.2°	0.770 \angle 5.8°	0.774 \angle 5.4°
\bar{I}_{dfig}^-	0.634 \angle 38.9°	0.637 \angle 36.6°	0.444 \angle 46.7°	0.446 \angle 45.0°
\bar{V}_{dfig}^-	0.213 \angle -73.3°	0.211 \angle -71.3°	0.149 \angle -64.6°	0.148 \angle -62.9°

4.1.4 Model validation study for Type-III WTG plants

This section presents a validation study of the proposed phasor model for Type-III WTG using fault record data. Two sets of actual relay recordings were used corresponding to the fault response of two Type-III wind plants connected to 115 kV and 230 kV transmission systems [1]. The validation study shows qualitatively that the proposed generic model, with generic controls, when tuned, can reproduce the actual fault responses in simulation with high accuracy. This is especially helpful for existing wind farms since the tabular data from the manufacturer may not be available, but some fault records are most likely available.

Fault 1 (230 kV system)

Fig. 4-6 depicts the system analyzed for a fault on the 230 kV tie line shown in the figure, referred as Fault 1. The wind park embeds 66×1.667 MVA Type-III wind turbines connected to a collector substation through three 34.5-kV collector circuits and a YG- Δ -YG, 34.5/230 kV step-up transformer. An 18.7 km tie-line connects the collector substation to the 230 kV interconnection (POI) substation. The fault is a B-to-C phase-to-phase fault occurring on the tie-line, 3.5 km from the POI substation. Prior to the fault, all 66 WTGs were connected to the system; the park was delivering 25.69 MW and absorbing 1.35 MVar from the 230 kV system at the collector substation, and the wind speed was 6.5 m/s. The fault event was recorded by the line relays on the 230 kV tie line. The current differential relays recorded the currents at both terminals of the line.

Fig. 4-7 shows a reduced equivalent model of the test system developed in EMTP-RV. The model represents the wind park using a generic Type-III WTG model, the tie-line using a PI section model, and the rest of the transmission grid represented by an ideal source behind an impedance. Appendix E presents the parameters of the wind park model which have been tuned such that the simulation results match the actual fault recordings as closely as possible.

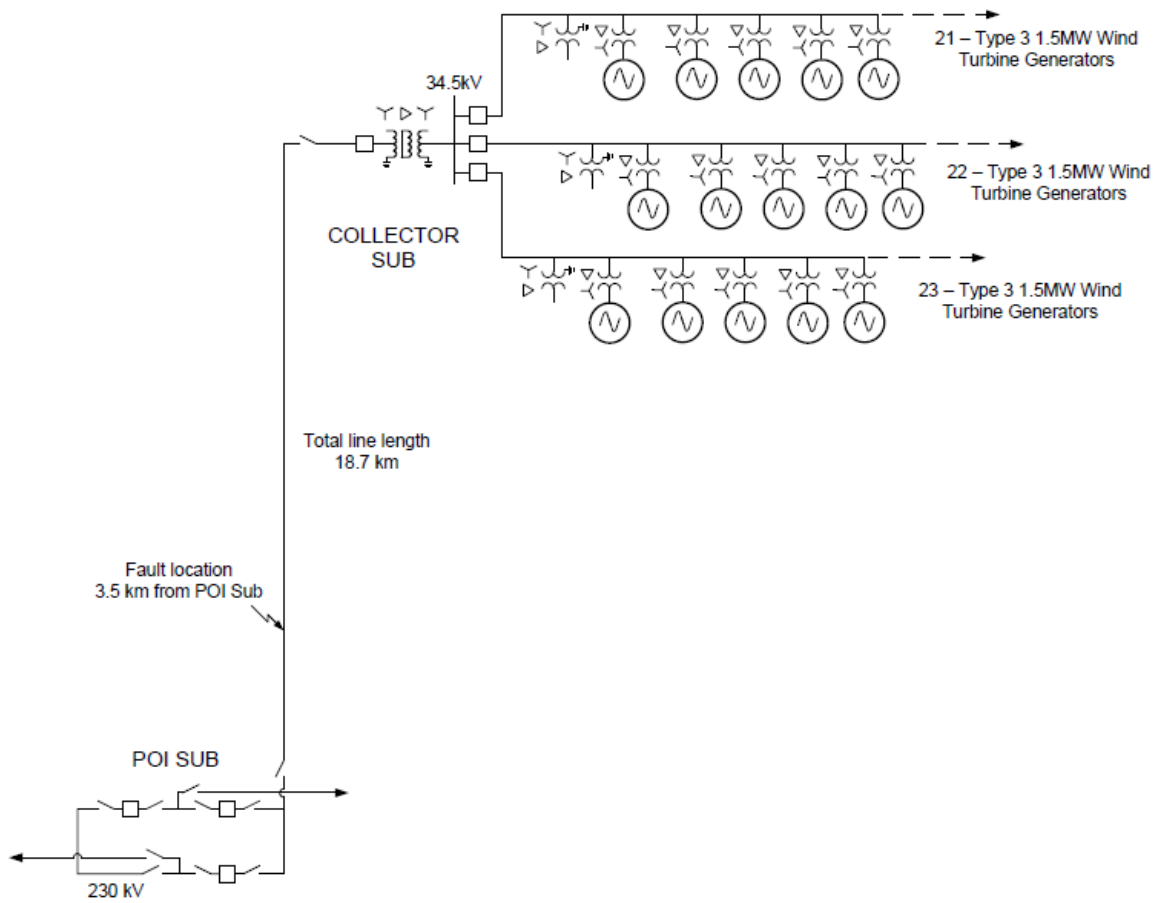


Fig. 4-6. Test system for Fault 1.

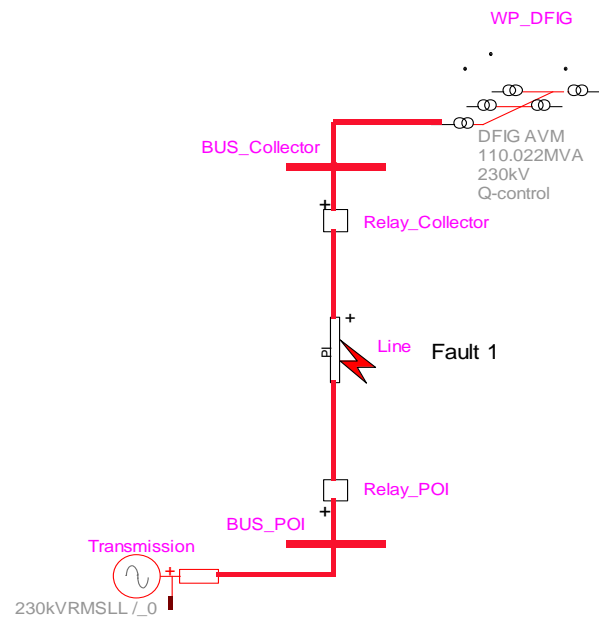


Fig. 4-7. Equivalent model of test system for Fault 1 in EMTP-RV.

Fig. 4-8 to Fig. 4-11 compare the actual response of the wind plant as recorded by the relays (dashed line) against simulation results (solid line). The results are scaled so that the RMS magnitudes for the waveforms are displayed as peak values. Fig. 4-8 shows the unfiltered phase currents from the wind plant. The "unfiltered phase currents" from the relay records correspond to the lack of digital filtering, but not analog filters which remove the high frequency transients observed in the simulation results. The fault occurs 3.8 cycles into the simulation and is cleared within 3 cycles. Fig. 4-9 illustrates the magnitude of the sequence currents from the wind plant. Fig. 4-10 presents the unfiltered phase voltages on the line side of the collector substation. Fig. 4-11 depicts the magnitude of the sequence voltages at the collector substation. As shown, the simulation results exhibit a close agreement with the actual recordings.

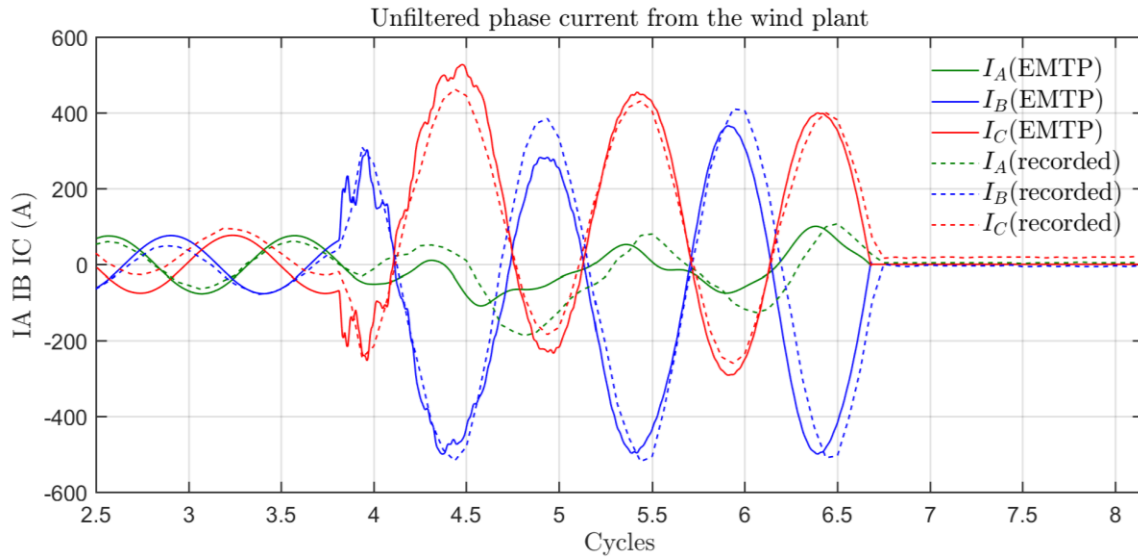


Fig. 4-8. Unfiltered phase currents from wind plant for Fault 1.

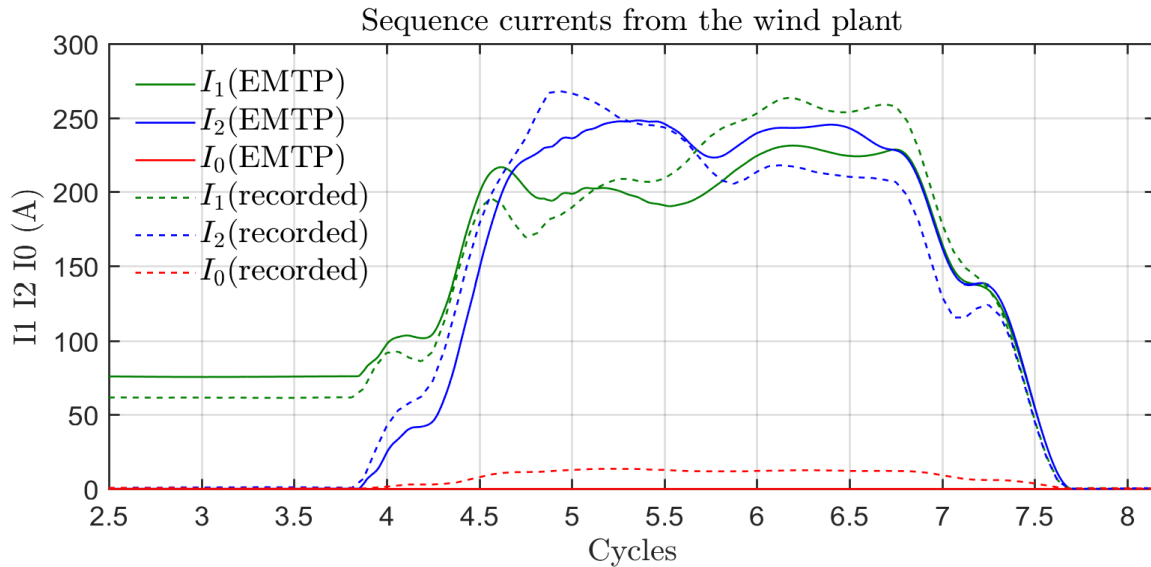


Fig. 4-9. Sequence currents from wind plant for Fault 1.

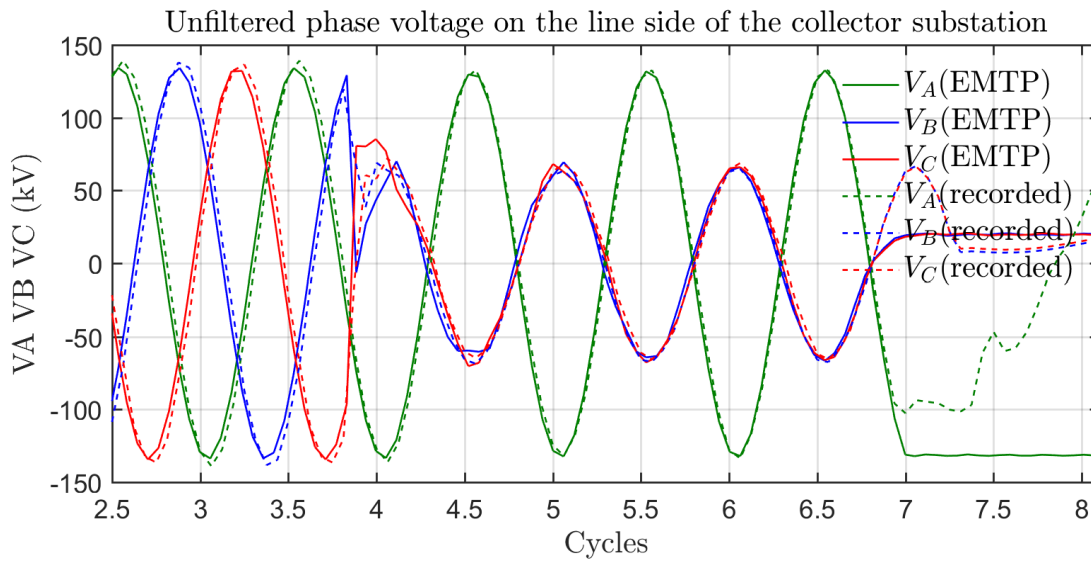


Fig. 4-10. Unfiltered phase voltage on line side of collector substation for Fault 1.

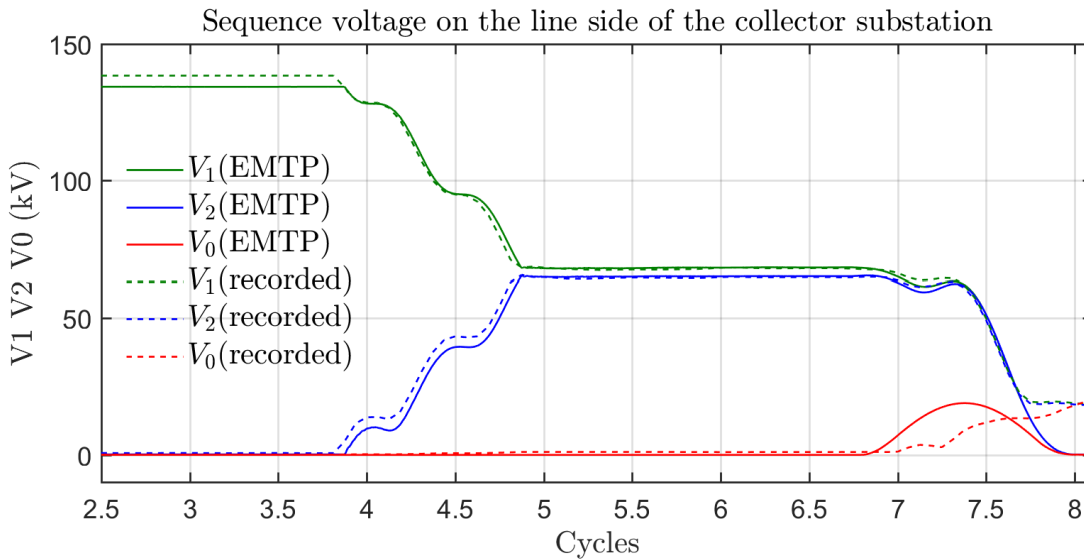


Fig. 4-11. Sequence voltages at collector substation for Fault 1.

To validate the accuracy of the phasor domain generic model, the reduced model of Fig. 4-7 was simulated in phasor domain by representing the wind park using the proposed phasor-domain generic model described in section 4.1.3. The simulation scenario is the same except that the fault is assumed to be permanent to enable comparison between EMTP and phasor domain results. Table 4-6 compares the simulation results of the EMTP with the phasor calculated at 2 cycles after the fault and the phasor-domain generic models. The results show a reasonable match.

Table 4-6. Positive and Negative Sequence Quantities at Collector – Fault 1 – EMT-Type Generic Model vs Phasor-Domain Generic Model

Variable	Collector			
	EMT Model		Phasor Model	
Positive-sequence current	$0.825 \angle -39.7^\circ$	228 A	$0.810 \angle -56.4^\circ$	223.8 A
Positive-sequence voltage	$0.509 \angle 1.5^\circ$	67.6 kV	$0.509 \angle 0.6^\circ$	67.63 kV
Negative-sequence current	$0.858 \angle 105.8^\circ$	237 A	$0.862 \angle 98.4^\circ$	238 A
Negative-sequence voltage	$0.488 \angle 0.4^\circ$	64.8 kV	$0.486 \angle 0.1^\circ$	64.5 kV

Fault 2 (115 kV system)

Fig. 4-12 shows the test system of Fault 2, for another set of field data. The wind plant in this case embeds 11×1.667 MVA Type-III wind turbine generators connected to a 34.5kV collector circuit. A YgDYg 34.5/115 kV step-up transformer connects the collector circuit to a 115-kV POI/Collector substation. A 10.7-km tie-line connects the POI/Collector substation to a network substation. The fault was a phase-A-to-ground fault occurring on the line to the network substation, 3.8 km from the network substation. Prior to the fault, all 11 wind turbine generators were connected to the system, and the plant was supplying 17.7 MW and 3.2 MVar into the grid.

Fig. 4-13 shows a reduced equivalent model of the test system of Fig. 4-12 developed in EMTP-RV. The parameters of the wind park model, which have been tuned such that the simulation results match the actual fault recordings as closely as possible, are provided in Appendix E.

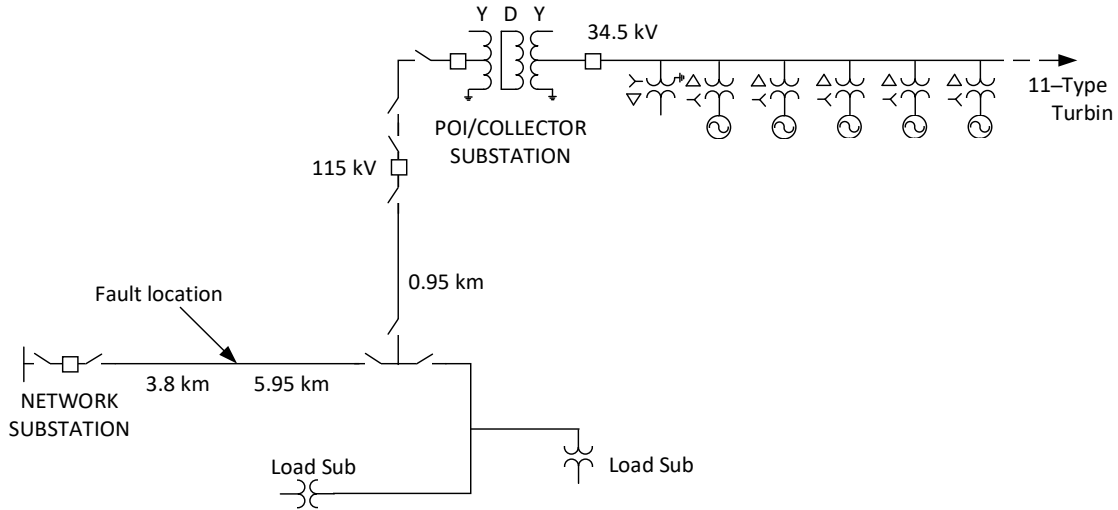


Fig. 4-12. Test system for Fault 2.

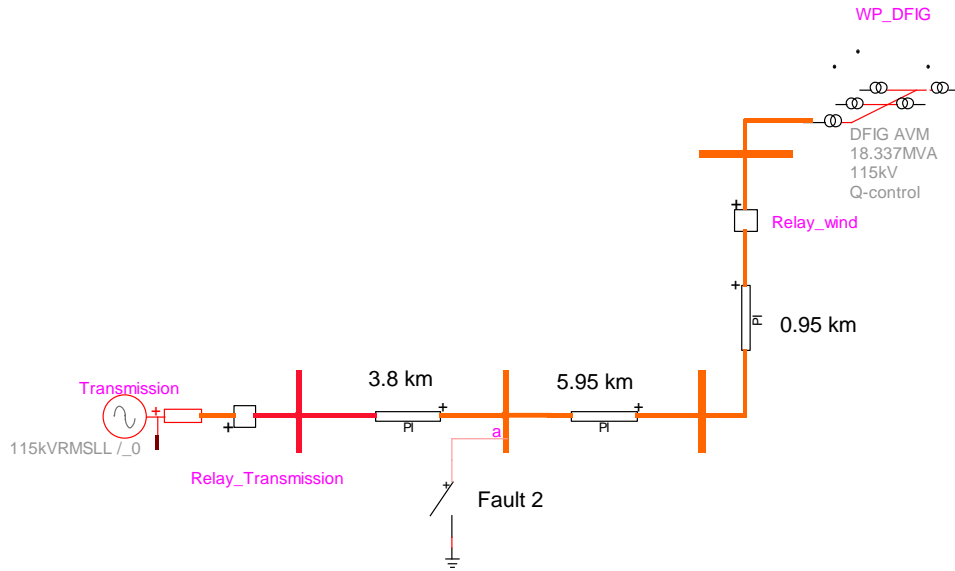


Fig. 4-13. Equivalent model of test system for Fault 2 in EMTP-RV.

Fig. 4-14 to Fig. 4-20 compare the actual response of the wind plant recorded by the relays (dashed line) against the simulation results (solid line). The results are scaled so that the RMS magnitudes for the waveforms are displayed as peak values. The fault event was recorded by the line relays at the network and the POI/collector substations. As shown, the simulation results closely match the actual fault records.

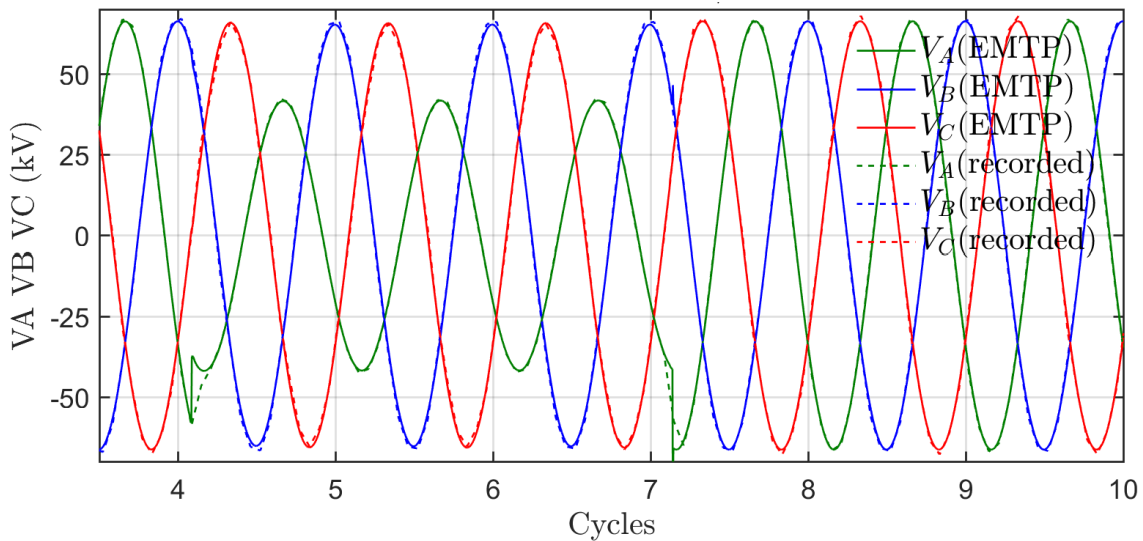


Fig. 4-14. Unfiltered phase voltage at network substation for Fault 2.

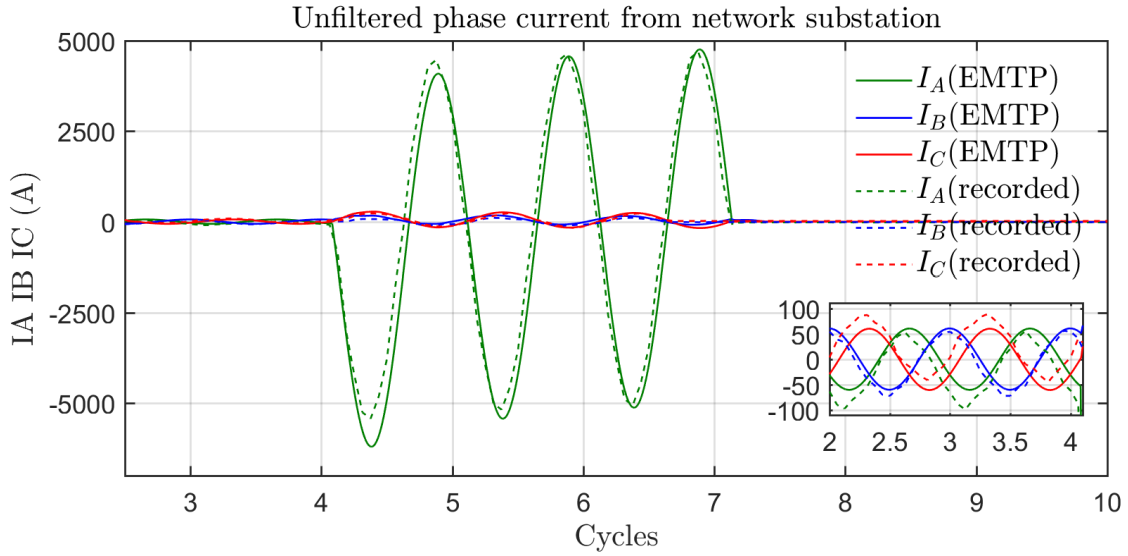


Fig. 4-15. Unfiltered phase currents from network substation for Fault 2.

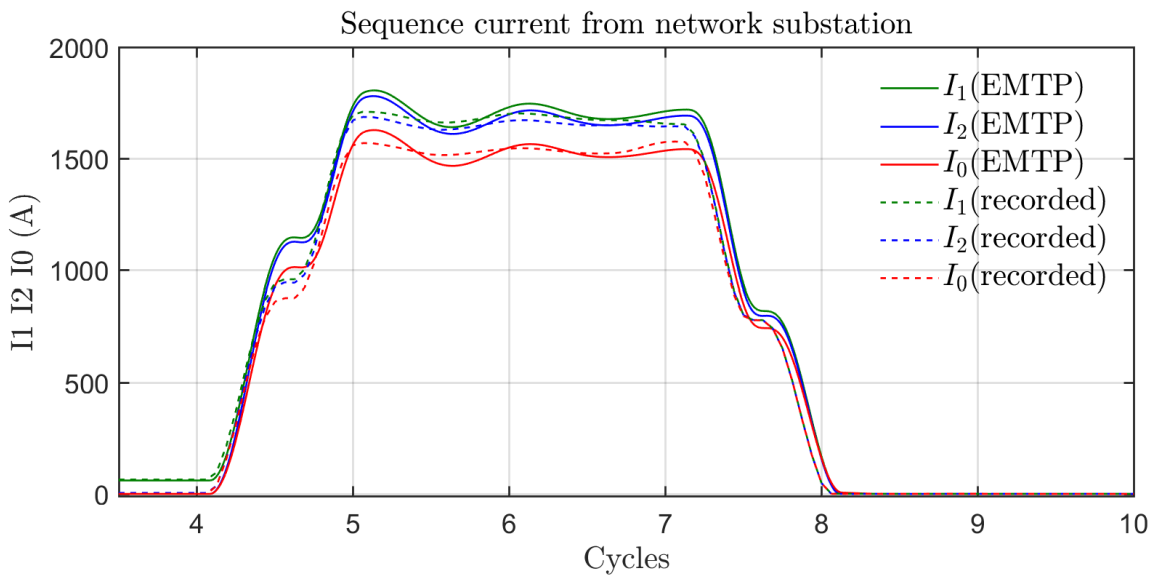


Fig. 4-16. Sequence currents from network substation for Fault 2.

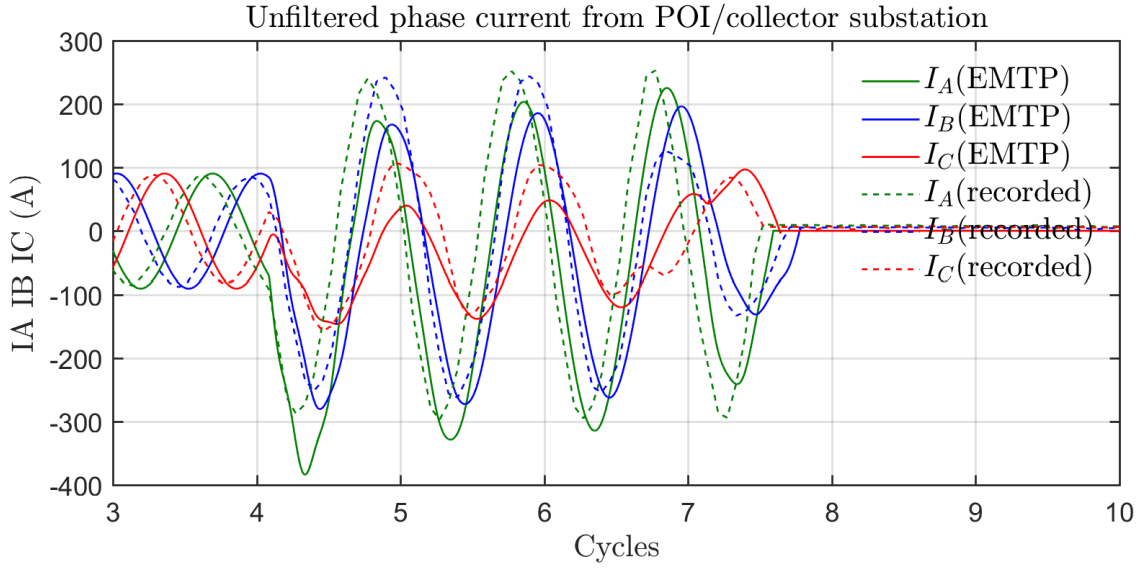


Fig. 4-17. Unfiltered phase currents from wind plant at POI/Collector substation for Fault 2.

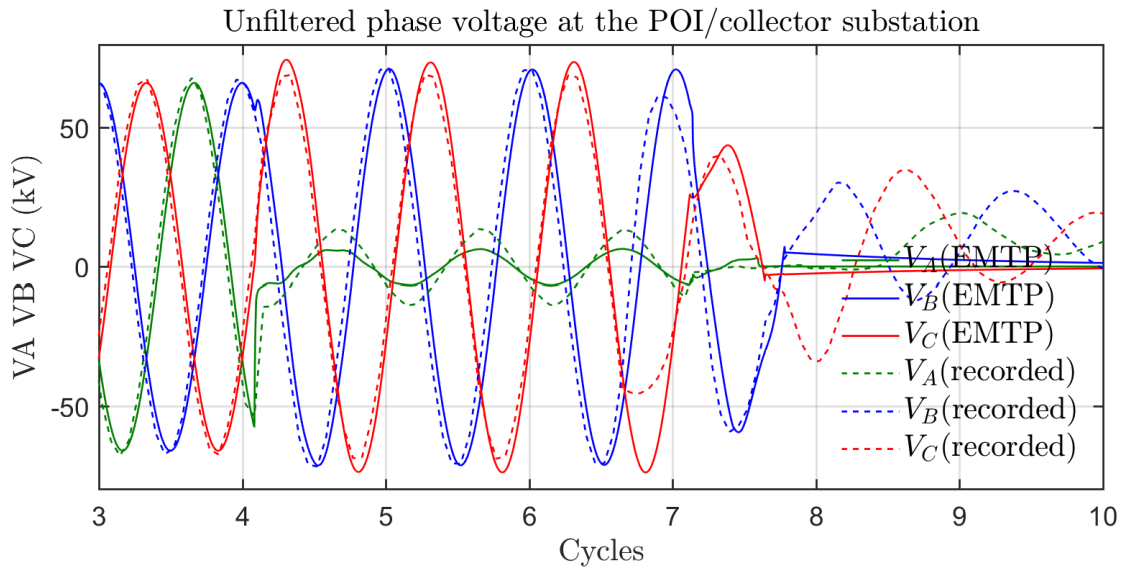


Fig. 4-18. Unfiltered phase voltages at POI/Collector substation for Fault 2.

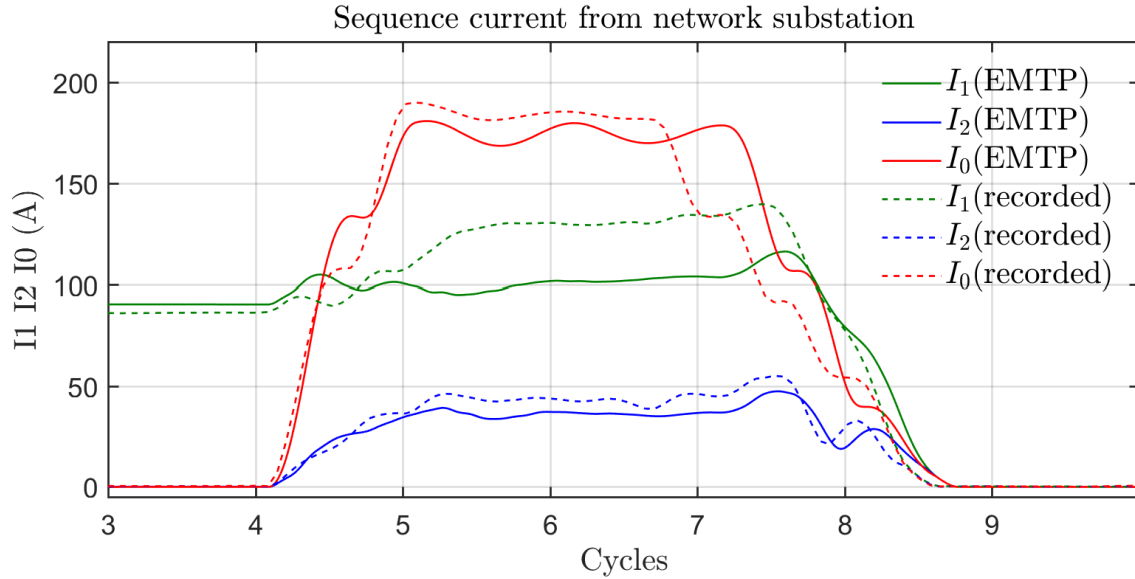


Fig. 4-19. Sequence currents from wind plant at POI/Collector substation for Fault. 2

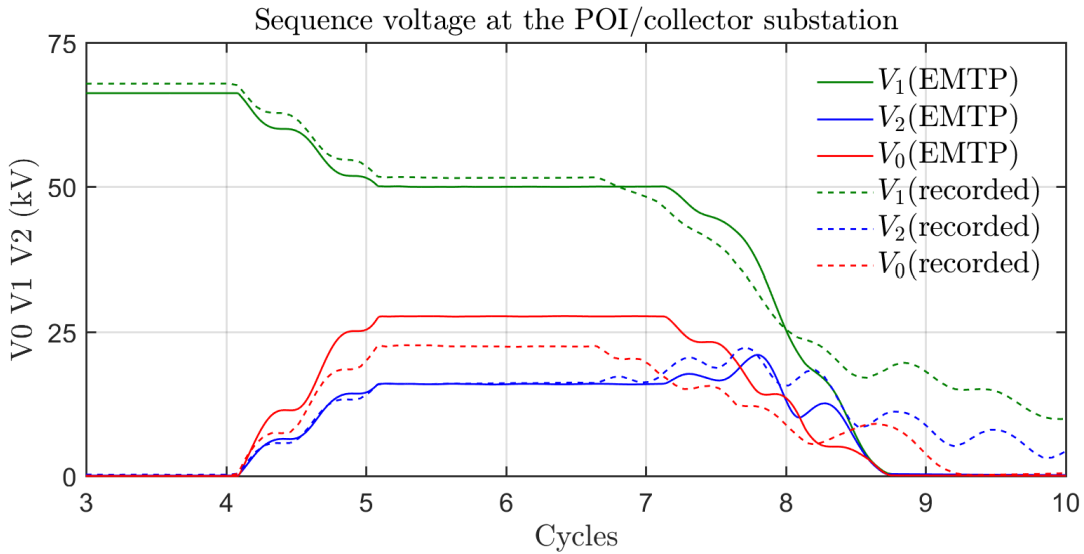


Fig. 4-20. Sequence voltages at POI/Collector substation for Fault 2.

Table 4-7 compares the simulation results of the EMT (phasor computed at 2 cycles after the fault) and phasor-domain generic models. The results show a reasonable match.

Table 4-7. Positive and Negative Sequence Quantities at POI/Collector – Fault 2 – EMT-Type Generic Model vs Phasor-Domain Generic Model

Variable	POI/Collector			
	EMT Model		Phasor Model	
Positive-sequence current	1.109 \angle -18.5°	102.1 A	1.082 \angle -28.0°	99.61 A
Positive-sequence voltage	0.762 \angle 1.1°	50.6 kV	0.762 \angle 0.6°	50.58 kV
Negative-sequence current	0.394 \angle -76.9	36.3 A	0.364 \angle -81.2°	33.51 A
Negative-sequence voltage	0.242 \angle -178.0	16.1 kV	0.242 \angle -178.3°	16.07 kV

4.2 OneLiner model implementation

4.2.1 Introduction

This section describes the modeling and simulation of utility-scale Type-III and Type-IV wind plants in ASPEN’s short-circuit program.

For Type-III and Type-IV wind plants, there is an initial transient following the onset of a fault that lasts about half of a cycle [11]. Short-circuit programs are typically designed to provide snapshots of the system at pre-determined and configurable instants in time at a specified frequency. This makes them unsuitable for simulating the initial transient, but it has been shown that they are capable of simulating the controlled response that follows.

About a year prior to the formation of the C24 working group (see report [1]), ASPEN implemented a model for voltage source converters (VSC) in its short-circuit program at the urging of two large electric utilities in the US. As per the guidance of a major European converter manufacturer, the converter was modeled as an ideal current source, the output of which followed a schedule in the form of a table of current magnitudes and power-factor angles at various terminal voltages. It is reasonable to postulate that this model would also capture the phasor response of a Type-IV WTG. The proposed data requirements are outlined in section 3.2.

EPRI’s work presented in section 4.1 describes the possible control modes for a Type-IV WTG - constant real power, constant power factor, constant voltage, and dynamic reactive current injection. The different control modes are not mutually exclusive. For instance, the dynamic reactive current control strategy is identical to that of the constant-voltage control mode, except the current-versus-voltage curve in the first mode usually has a slope of 2 whereas the current-versus-voltage curve in constant-voltage mode is set equal to the admittance of the network as seen from the converter terminal. The dynamic reactive current control mode also has elements of the constant MW control mode when the voltage is relatively high. For any given control mode, it is expected that there are variations in the control strategy between different converter manufacturers as evidenced by the data provided in Appendices A-D of this report.

In ASPEN’s Type-IV WTG model, it is assumed that the generator is regulated to maintain constant real power when the terminal voltage of the WTG is within a narrow voltage deadband (from 0.9 pu to 1.1 pu by default). It is assumed that the converter follows the dynamic reactive current control mode when the terminal voltage is outside the deadband. This control strategy is in line with details provided by Siemens (section

2.3) and also confirmed by another inverter manufacturer, SMA. It is appropriate because a priority is given into the task of supporting voltage by injecting reactive power to the network when the voltage is low and it absorbs reactive power when the voltage is high (up to 1.2 pu). This approach should simulate most Type-IV WTGs with reasonable accuracy, but, due to variations in different model-responses, as evidenced by the manufacturer-data provided in Appendix D, the software also allows the user to enter manufacturer-generated data in a tabular form as described in section 3.

As for Type-III WTG, ASPEN lets the user specify whether the crowbar mechanism is engaged. When the crowbar option is turned on, the model behaves as a passive induction machine. When the crowbar option is turned off, the WTG is modeled as a doubly-fed generator with its back-to-back converter and the associated control logic. Controlled response of the WTG is based on the EPRI's generic control and phasor domain short-circuit model described in section 4.1. In this case, the response is more complicated, and prone to more variations based on the individual manufacturer's control. The tabular data entry approach can be enabled for this model as well but not yet implemented.

4.2.2 Dynamic reactive current control mode

The dynamic reactive current control strategy is used in both Type-III and Type-IV WTGs. This section gives a brief description of how it works.

The following variables are used in this section:

V_{dpf} : the d-axis positive sequence voltage at the converter terminal in per-unit before the fault.

I_{dpf} : the d-axis current being injected into the network in per-unit before the fault.

V_{d} : the d-axis positive sequence voltage at the converter terminal in per-unit.

I_{d} : the d-axis current being injected into the network in per-unit.

I_{q} : the q-axis current being injected into the network in per-unit.

First, the reactive current I_{q} injected by the converter is computed as:

$$I_{\text{q}} = -2 (1.0 - V_{\text{d}}) \quad (4.2.1)$$

I_{q} is limited to the reactive current limit, which is assumed to be 1.1 pu in this example. In ASPEN's implementation, the reactive current limit and the maximum current magnitude are assumed to be the same. The user can enter this limit under "Maximum current" in the information dialog box for the Type-IV WTG. Note that equation (4.2.1) causes a *negative* I_{q} to be injected into the network during a low-voltage condition. This condition of lagging power factor (i.e., current lagging the voltage) during a fault is similar to the response of a conventional synchronous generator.

Next, a d-axis current injection, I_{d} is computed by the following equation, with the aim of maintaining constant real power:

$$I_{\text{d}} = I_{\text{dpf}} / (V_{\text{d}} / V_{\text{dpf}}) \quad (4.2.2)$$

The current given by equation (4.2.2) then goes into a limiter, so that the magnitude of $I_{\text{d}} + j I_{\text{q}}$ is no larger than the maximum current limit (which is 1.1 pu in this example). This is done by comparing the value of I_{d} to the limit $[(1.1)^2 - (I_{\text{q}})^2]^{0.5}$. The direct-axis current I_{d} is held to this limit if it is too large.

The angle of $I_{\text{d}} + j I_{\text{q}}$ is the *power factor angle*. A positive power factor angle means the current leads the voltage, and *vice versa*. Table 4-8 shows the current magnitudes and power factor at different terminal voltages. This table assumes that the generator is

generating 1.0 pu real power and no reactive power when the voltage is 1.0 pu, and the maximum phase current and the maximum q-axis current are both set to 1.1 times the full load current.

Table 4-8. Example Input Data for Tabular Input of Voltage-Controlled Current Source Model

Magnitude of V_d in pu	d-axis current I_d in pu	q-axis current I_q in pu	$ I_q + j I_d $ in pu	Power factor angle in degrees
1.0	1.000	0.00	1.0	0
0.9	1.000	-0.20	1.02	-11.31
0.7	0.922	-0.60	1.10	-33.06
0.5	0.458	-1.00	1.10	-65.38
0.3	0.0	-1.10	1.10	-90.00
0.1	0.0	-1.10	1.10	-90.00

4.2.3 Implementation overview

Both Type-III and Type-IV WTGs are simulated in the pre-fault condition if “start from linear network solution” or “start from a power flow solution” option is in effect. By doing this the power they generate is fully accounted for in the computation of the pre-fault voltages. Type-III and Type-IV WTGs are assumed to output zero pre-fault current if the “flat start” option is in effect.

The simulation in a short-circuit program has to be iterative because change in the current injection in each iteration alters the terminal voltage magnitude, which, in turn, changes the current injection. The modeling of nonlinear devices in ASPEN’s short-circuit program is not new. It has been successfully implemented to model MOV-protected series capacitors and other non-linear models. ASPEN’s short-circuit program is based on a method described in a paper by V. Brandwajn and W.F. Tinney in 1985 [12]. The following is a synopsis of the iterative solution method:

1. The program computes the pre-fault voltage for all the buses in the network. Iterations are necessary to model the effects of non-linear circuit elements and contributions from unconventional generation sources such as Type-III or Type-IV wind plants.
2. The program reduces the sequence networks to the faulted buses and terminal buses of nonlinear devices.
3. Any balanced network modifications, such as line outages, are performed on the reduced sequence network model.
4. The reduced sequence networks are transformed to the phase domain, yielding a phase admittance matrix.
5. The program modifies the phase admittance matrix to simulate short-circuit conditions such as the short-circuiting and grounding of one or more phases.
6. The program solves the modified phase equations, yielding a voltage solution for the nodes in the reduced network. If nonlinear network elements are present, the voltage solution at the terminal buses of these elements are compared to that of the previous iteration. If the solution has not converged, some elements of the phase network equations are modified to reflect the latest change in voltage or current flow, and this

step is repeated. Usually less than 10 iterations are adequate. This step takes very little time because it involves the manipulation and solution of a relatively small matrix.

7. Changes in the reduced phase network are reflected back into the full sequence networks in the form of a compensation current vector. The principle behind this step is called the Network Compensation Theorem [13].

Iterative solution of Type-III and Type-IV wind generator is handled in step 6, along with the iterative solution of other non-linear elements.

4.2.4 Modeling considerations for a wind farm

For short-circuit studies involving plants with large number of WTGs, it is a convenient practice that the generating units in a plant be aggregated into a small number of wind generators. Modeling the units individually does not appreciably improve the accuracy of studies for faults in the utility system. This was demonstrated in a study at New Mexico State University with a model of Type-II wind turbines [14],[15]. Following this proposed approach for Type-III and Type-IV wind generators lessens the possibility of convergence difficulties, degradation in solution speed, and increase in computer storage resources.

An example wind plant model is shown in Fig. 4-21. In this network, all the generating units are lumped into a single voltage-controlled current source. If this aggregation is too drastic for a user's application, an alternative model of the plant can be created as a collection of several WTGs connected by the main trunk of the collector network.

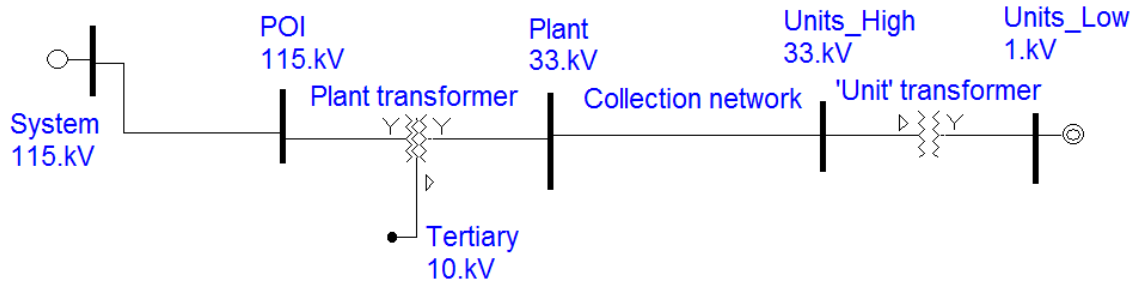


Fig. 4-21. A sample network model in which all the generating units are lumped into a single wind generator.

4.2.5 Data needed for Type-IV generators

The dialog box for the Type-IV wind plant model is shown in Fig. 4-22. Note that the “number of units” is one of the input parameters. This is intended to encourage the user to use each Type-IV generator to represent multiple units. It is assumed that the generator is producing only real power before the fault is applied. Hence the dialog box asks only for the kW generation. The model has the option to reduce the magnitude of the current injection when the voltage drops below a certain value.

The second dialog box is brought up by pressing the “Advanced Settings” button in the first dialog box. It contains parameters that are unlikely to be changed from one generator to another. The “voltage deadband extent” of 0.2 in this dialog box means that

the generator maintains constant real power when the terminal voltage is between 0.9 pu and 1.1 pu. The fault ride-through (FRT) mode is turned on once the terminal voltage goes outside of this deadband. The rest of the self-explanatory parameters are shown in Fig. 4-22.

Note that the converter-interfaced generator model also has the option of constant real-power control mode, subject to the maximum-current constraint.

Converter-Interfaced Generator

At 9 PGC 0.575kV

Name= WindType4-Sola

Number of units= 10

Unit kVA rating= 750.

Unit kW generation= 700.

Advanced Settings

FLC

Max current (in multiple of full-load current)

When V (pu) > 0.4 Max I= 1.1

Otherwise, reduce current to Max I= 0.5

Control method outside of deadband

Fault ride through (FRT)

Constant real power

Memo

OK Cancel Help

Advanced Parameters of Converter-Interfaced Generator

Voltage deadband extent= 0.2 pu

Slope for FRT characteristics= 2.

Generator Shuts Down

When a phase voltage exceeds 1.5 pu

When a phase voltage drops below 0.05 pu

OK Cancel Help

Fig. 4-22. ASPEN dialog boxes for the Type-IV wind generator model.

4.2.6 Experience on solution method for Type-IV generators

A simple solution method for Type-IV wind generator model was tried at first. At each iteration, based on the magnitude of the voltage phasor V_d at the generator terminal, equations in Section 4.2.2 were used to arrive at the corresponding current magnitude and power factor angle. The magnitude of the current-injection phasor was then updated to the calculated value, and its angle to the sum of the calculated power-factor angle and the latest angle of V_d . This method did *not* work reliably. It worked as expected only for faults away from the generator terminal but not for close-in faults that cause low voltages at generator terminals. In cases where the solution failed to converge, it was observed that the angle of the voltage and current phasors rotated around in circles without ever settling to a fixed position.

The principal flaw of this simple method is that the voltage phasor was allowed to wander aimlessly from iteration to iteration without tethering it to any fixed reference. Designers of converters are aware of the importance of maintaining a fixed phase reference because, in detailed time-domain models of converters, there is always a phase-locked loop that is synchronized to the grid frequency. The phase-locked loop is used for the converter to maintain synchronism even when there is 3-phase fault near the generator terminal. With this in mind, an alternative solution method was devised that proved to be extremely reliable. The method is shown in the following pseudo-code (Note: *PF* stands for “power factor”, and the variable “*PF Angle Offset*” is initialized to 0 at the beginning of the iterative loop.):

```
Actual PF Angle = IAng - Vang; //Difference in current phasor angle and
voltage
//phasor angle
PF Angle Error   = Actual PF Angle - Calculated PF angle of previous
iteration;
PF Angle Offset -= 0.8 * PF Angle Error; // 0.8 is a deceleration factor
New PF Angle     = Pre-fault voltage angle + PF Angle Offset + calculated PF
angle
in the current iteration;
```

Note in the line for new PF angle, the power factor angle is always calculated starting with the pre-fault voltage angle of the generator bus. The use of the “PF Angle Offset” variable allows the solution to converge in cases where the power-factor angle converges to a value that is different from the calculated value.

4.2.7 What is *not* modeled in ASPEN’s Type-IV WTG

ASPEN’s Type-IV generator model does not have any negative-sequence current output for unbalanced faults. Negative-sequence current output was omitted for the simple reason that it cannot be predicted. The manufacturer data in Appendix A, B and C support this assumption. Harmonic filters were omitted in the sample network of Fig. 4-21. Within the converter enclosure, there are usually two banks of harmonic filters, with cutoff frequency set at the first and second harmonics of the converter’s switching frequency (between 2 to 5 kHz). In the EPRI model, each filter consists of a capacitor in series with the parallel combination of a reactor and a small resistor. At the power frequency of 50 or 60 Hz, the filters are capacitive. With the two harmonic filters in

parallel, the combined shunt admittance (in per-unit based on the wind plant’s aggregate MVA rating) is around $j0.1$ pu. Thus, if needed, filters can be modeled by adding a shunt object on the Unit_Low 1kV bus in Fig. 4-21.

4.2.8 Benchmarking Type-IV wind generator model against EPRI model

The output from ASPEN’s Type-IV generator model was benchmarked against the EPRI model for different faults in a sample 9-bus network shown in Fig. 4-23.

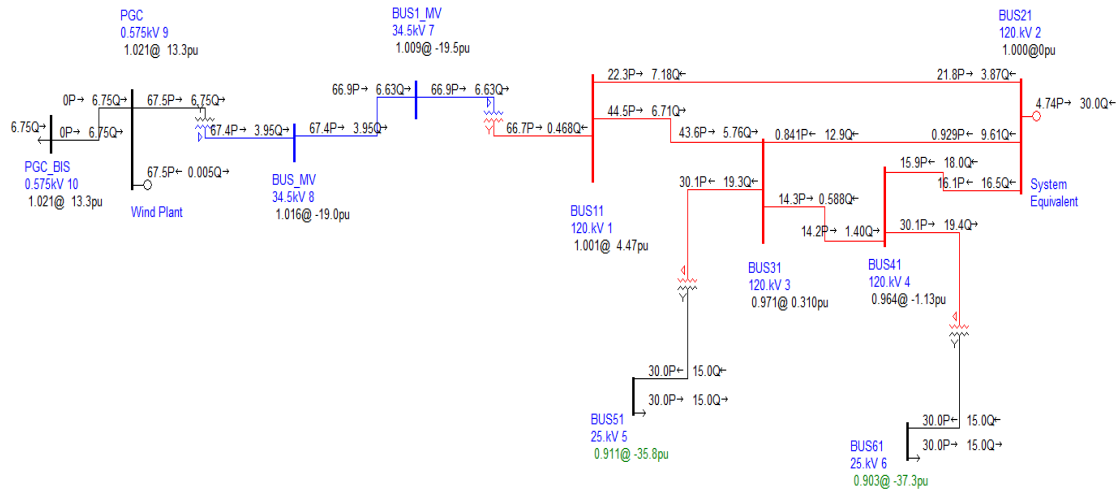


Fig. 4-23. Power flow solution of 9-bus test network.

Note: The wind generator is on the bus named PGC. The 3-line-to-ground short-circuit results are shown in the following tables.

Table 4-9. EPRI WTG-IV Results for 9 Bus System

EPRI Model					
Faulted Bus	V	Id	Iq	Id + jIq	PF Angle
BUS31	0.498	0.456	-1.000	1.099	-65.5°
BUS41	0.650	0.850	-0.698	1.099	-39.4°
BUS51	0.842	1.000	-0.315	1.048	-17.5°
BUS61	0.891	1.000	-0.214	1.023	-12.1°

Table 4-10. ASPEN WTG-IV Results for 9 Bus System

ASPEN Model					
Faulted Bus	V	Id	Iq	Id + jIq	PF Angle
BUS31	0.498	0.449	-1.004	1.100	-65.9°
BUS41	0.651	0.833	-0.718	1.100	-40.8°
BUS51	0.833	0.993	-0.332	1.047	-18.5°
BUS61	0.883	1.000	-0.233	1.027	-13.1°

4.2.9 Data needed for Type-III WTG model

The dialog box for the Type-III wind plant model is shown in Fig. 4-24. This design is similar to that of Type-IV WTG. The second dialog box is brought up by pressing the “Advanced Settings” button in the first dialog box. It contains parameters that are unlikely to change from one generator to another. There are two data fields that are not in the Type-IV dialog box: The *crowbarred* check box and the “unit rated kW” edit box.

Doubly-Fed (Type-3) Wind Generator

At 9 PGC 0.575kV

Name= Type-3 WindGen

Number of units= 10

Unit kVA rating= 750.

Unit rated kW= 700.

Unit kW generation= 700.

Advanced Settings

FLC

Converter current limits

Rotor-side limit= 1.1 pu

Grid-side limit= 0.35 pu

Crowbarred

Memo

OK Cancel Help

Advanced Parameters of Type-3 Wind Generator

Voltage Deadband

Voltage deadband extent= 0.2 pu

Generator Shuts Down

When a phase voltage exceeds 1.5 pu

When a phase voltage drops below 0.05 pu

Machine parameters in pu

Rotor R= 0.03

Stator R= 0.03

Rotor leakage L= 0.2

Stator leakage L= 0.2

Mutual L= 3.

Misc Parameters

Slip at rated kW= -0.2

Filter X= -20. pu

OK Cancel Help

Fig. 4-24. Dialog boxes for the Type-III wind generator model.

The *crowbarred* check box, when marked, instructs the short-circuit program to treat the generator as a passive induction machine. This option is usually used for models allowing crowbarring action in conjunction with a 3-phase fault that is close to the generator – either inside the plant or at a point very close to the high side of the plant transformer – for the purpose of designing the circuit breakers and related equipment. A megawatt-sized Type-III crowbarred generator injects roughly 5 times full-load current when crowbarred.

When the crowbar is not engaged, the rotor current is fed by a computer controlled back-to-back converter. During an unbalanced fault, the generator injects both positive and negative sequence current into the network. The magnitude of these currents is limited only *roughly* by the converter electronics. The reason is that the back-to-back converter controls only the rotor current, and it does not directly control the generator’s current injection into that grid. The crowbar of an actual generator engages when the current exceeds 2 to 2.5 times full-load current to prevent damage to the converter electronics.

In the Advanced Parameters dialog box, the “slip at rated kW” parameter and the rated kW generation (in the first dialog box) are used to calibrate a curve that relates the torque to the slip of the rotor. In this dialog box, there are other parameters unique to Type-III wind generators which include the induction-machine parameters. “Typical” parameters are provided that are expected to be commonly used for studies because it is highly unlikely that the manufacturer of the WTG provides them readily. Unlike Type-IV wind generators, the harmonic filters of Type-III WTG cannot be modeled externally. Hence a finite reactance is necessary for the filters in the second dialog box if they need to be modeled.

4.2.10 Benchmarking Type-III WTG model against EPRI model

The output from ASPEN Type-III generator model was benchmarked against the EPRI model for different 3-line-to-ground and single-line-to-ground faults in the 9-bus network shown in Fig. 4-23. The results are shown in Table 4-11, Table 4-12, Table 4-13, and Table 4-14. *Ipgc_pos* and *Ipgc_neg* are the positive and negative sequence current injections, respectively, from the Type-III generator.

Table 4-11. Three-Phase Fault – Bus 3 – WTG-III

WTG Variables	EPRI	ASPEN
Vpgc_pos (pu)	0.477 $\angle 34.7^\circ$	0.481 $\angle 32.3^\circ$
Ipgc_pos(pu)	1.201 $\angle -23.1^\circ$	1.189 $\angle -25.4^\circ$
Positive sequence pf angle (deg)	-57.8°	-57.7°

Table 4-12. Three-Phase Fault – Bus 6 – WTG-III

WTG Variables	EPRI	ASPEN
Vpgc_pos (pu)	0.884 $\angle 22.9^\circ$	0.899 $\angle 21.8^\circ$
Ipgc_pos(pu)	1.049 $\angle 8.3^\circ$	1.028 $\angle 8.6^\circ$
Positive sequence pf angle (deg)	-14.6°	-13.2°

Table 4-13. Single-Phase Fault – Bus 3 – WTG-III

WTG Variables	EPRI	ASPEN
V _{pgc_pos} (pu)	0.877 ∠20.6°	0.883 ∠20.0°
I _{pgc_pos} (pu)	1.058 ∠5.6°	1.052 ∠5.5°
Positive sequence pf angle (deg)	-15.0°	-14.5°
V _{pgc_neg} (pu)	0.112 ∠178.0°	0.124 ∠178.6°
I _{pgc_neg} (pu)	0.221 ∠-82.9°	0.243 ∠-82.4°
Negative sequence pf angle (deg)	99.1°	99.0°

Table 4-14. Single-Phase Fault – Bus 6 – WTG-III

WTG Variables	EPRI	ASPEN
V _{pgc_pos} (pu)	0.913 ∠18.5°	0.944 ∠17.2°
I _{pgc_pos} (pu)	0.981 ∠18.5°	0.953 ∠17.2°
Positive sequence pf angle (deg)	0°	0°
V _{pgc_neg} (pu)	0.040 ∠-135.7°	0.041 ∠-137.4°
I _{pgc_neg} (pu)	0.079 ∠-36.6°	0.0809 ∠-38.3°
Negative sequence pf angle (deg)	99.1°	99.1°

4.3 CAPE model implementation

This section summarizes the CAPE modeling of wind plants with a steady-state phasor solution. The CAPE implementation includes Type-IV WTG as developed by EPRI and described in section 4.1, with generic control modes - constant real power, constant power factor, constant voltage, and dynamic reactive current injection.

For Type-III wind plants, CAPE treats the DFIG as a conventional synchronous generator with the largest phase current limited and the other phase currents reduced in proportion. This model is based on earlier ANAFAS models [19,20], which suppress negative- sequence and zero-sequence currents. The EPRI Type-III model of section 4.1 has positive-sequence and negative-sequence controls. It is under implementation in CAPE and is not included in this report.

CAPE also accepts the tabular data structure (Voltage-Controlled Current Source or VCCS) as proposed in this report. Constant-current injection is a special case.

In CAPE the wind plant models can be found in the “Generator Data” form, under the “Current Limit” tab shown in Fig. 4-25. "No Limit" is a conventional synchronous generator model. “TYPE-3” is the synchronous generator with limited current. “Constant Current” and “Voltage-controlled Current Source” are based on the tables described in section 3.

Fig. 4-25. Generator Data Form.

4.3.1 Type-IV WTG model

A typical configuration of a wind plant is shown in Fig 4-26. Note that this represents an aggregate model with all wind turbines and their corresponding transformers and filters aggregated. The collector grid can be also aggregated or modeled in detail. PGC is the point of generator connection (low voltage – e.g. 0.6kV) and POI is the point of interconnection of the plant.

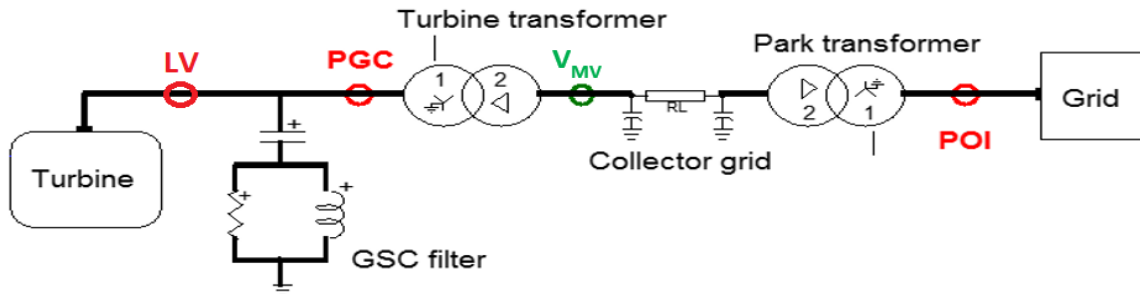


Fig. 4-26. Type-IV controlled generator with full power conversion inverter.

CAPE models the wind plant from the turbine (at low voltage) to the medium voltage (MV) bus of the equivalent turbine transformer. The collector grid and the transformer from MV to high voltage (HV) are modeled separately in the network database. The wind plant is modeled as a voltage dependent current source that injects positive-sequence AC current at the network frequency. This nonlinear model is used to capture the fact that the fault response of the wind plant is governed by the inverter controller. An iterative solution is used. The controls are applied to the currents and voltages at the point marked “LV” (low voltage). This model differs from a synchronous generator, which is modeled as a linear device with a constant subtransient or transient impedance and a constant internal EMF.

Fig. 4-27 shows the data form for a wind-turbine generator once the “EPRI WTG (Type-IV)” model is selected.

Fig. 4-27. EPRI WTG (Type-IV) Wind Model Data Form.

The user enters the following:

1) Turbine Parameters

- **Turbine Type:** Only Type-IV full converter (FC) is implemented on this form.
- **Number of Turbines:** The user can specify the number of turbines within the plant, which CAPE combines in parallel and model as an aggregate model.
- **S:** Nominal apparent power (MVA) of one turbine: The power base for the entire plant is set as: (Number of turbines) * (S for one turbine)
- **P:** Pre-fault real power generation (MW) from one turbine
- **Q:** Pre-fault reactive power generation (MVA_r) from one turbine
- **V:** Base (reference) line-to-line voltage for the MV side of the turbine transformer

2) Control Parameters

- **Control Mode**
The options are:
 - Voltage control (V)
 - Reactive power control (Q)
 - Power factor control (PF)

- Fault ride-through control (FRT)

For the control modes above, depending on the selection, additional inputs are necessary. In particular:

- For V control: the desired bus voltage (in pu) (default value: 1.0).
- For Q control: the desired reactive power generation (in pu) (default value: -0.1).
- For PF control: the desired power factor (default value: 0.97)
- For FRT control (see Figure 4-2):
 - Slope: defined as (change of reactive current) / (change of positive sequence voltage) on the linear operating characteristic of the grid-side converter (default value: 2.0 pu)
 - This is the multiple K given in section 2.3.
 - FRT deadband (voltage in pu): current I_q is injected only when the voltage is outside the deadband (default values: min 0.9 to max 1.1). For voltages in the deadband (close to 1.0 pu) only the active current component (I_d) is injected.
- **Control Priority:** The priority P (active) or Q (reactive) applies to the current when the limits are hit. With P priority, active current (I_d) has priority; with Q priority, reactive current (I_q) has priority.
- **Grid Side Converter (GSC) Current Limiter**
 - Total current limit (pu) (default value: 1.1)
 - Active current limit (pu) (default value: 1.0)
 - Reactive current limit (pu) (default value: 1.0)

3) Network Data

- **LV-MV Transformer:** This models the aggregate turbine/inverter transformer. A two-winding Y-delta three-phase transformer is used to convert the inverter low voltage to the collector system medium voltage, and to block zero-sequence current. The leakage impedance (R, X) is in pu and the default values are (0.01, 0.1). The magnetizing (excitation) shunt admittance is ignored.
- **Filter Admittance:** The filter is a capacitive shunt. Values are in pu. Default values are $G = 0$ and $B=0.01$ pu.
- **MVA Base Selection:** The data can be entered either a) using the total MVA of the plant as base or b) the system MVA as base (=100 MVA)

For more details of the data and options, CAPE users can refer to [16] and forthcoming updates.

4.3.2 Type-III WTG model

The Type-III model uses a simple phasor solution with a fixed current limit and a fixed impedance (R , X) for currents below the limit. The model first computes the current into the network from each generator bus with the generator internal impedance included. If any phase current exceeds the limit, it is reduced to the limit. The phase angle of each phase (A, B, C) is fixed at the value that CAPE has computed before imposing the current limit, and the relative magnitudes I_b/I_a and I_c/I_a are fixed, where I_a is the maximum phase current due to an unbalanced fault. Then the generator injects a constant injected current with an infinite shunt impedance.

The zero-sequence component is removed; negative sequence current still exists if the fault is unbalanced, but otherwise is not controlled.

If the currents for all three phases (A, B or C) are less than the limit, the generator behaves as a generic synchronous generator, which has a fixed EMF behind an internal impedance. It is a linear device: its own source impedance is $(R, X) = (\text{Change of Voltage})/(\text{Change of Current})*(-1)$, which is constant during a fault and chosen as steady-state, transient or subtransient.

Type-III also has a global “Crowbar” option in which every Type-III model behaves as a synchronous generator, without a current limit. With the crowbar option, CAPE automatically resets the maximum current limit to 9999.0 perunit, effectively removing the constraint everywhere in the network.

4.3.3 Voltage-Controlled Current Source (VCCS)

The tabular structure discussed in this report has been also implemented in CAPE. In a VCCS model, the generator voltage at the network (MV bus) determines the current and power-factor angle via tables of values. Only positive-sequence values are used. On the Generator Data form, the user can choose the “Voltage-Controlled Current Source” and enter the data in the table, as shown in Fig. 4-28. The current is lowest for a remote fault with 1.0 pu voltage at the generator. These points specify the current generated for any fault. The power factor angle is the phase lead of current from voltage; it is a negative number when the generator supplies lagging (inductive) current to the network.

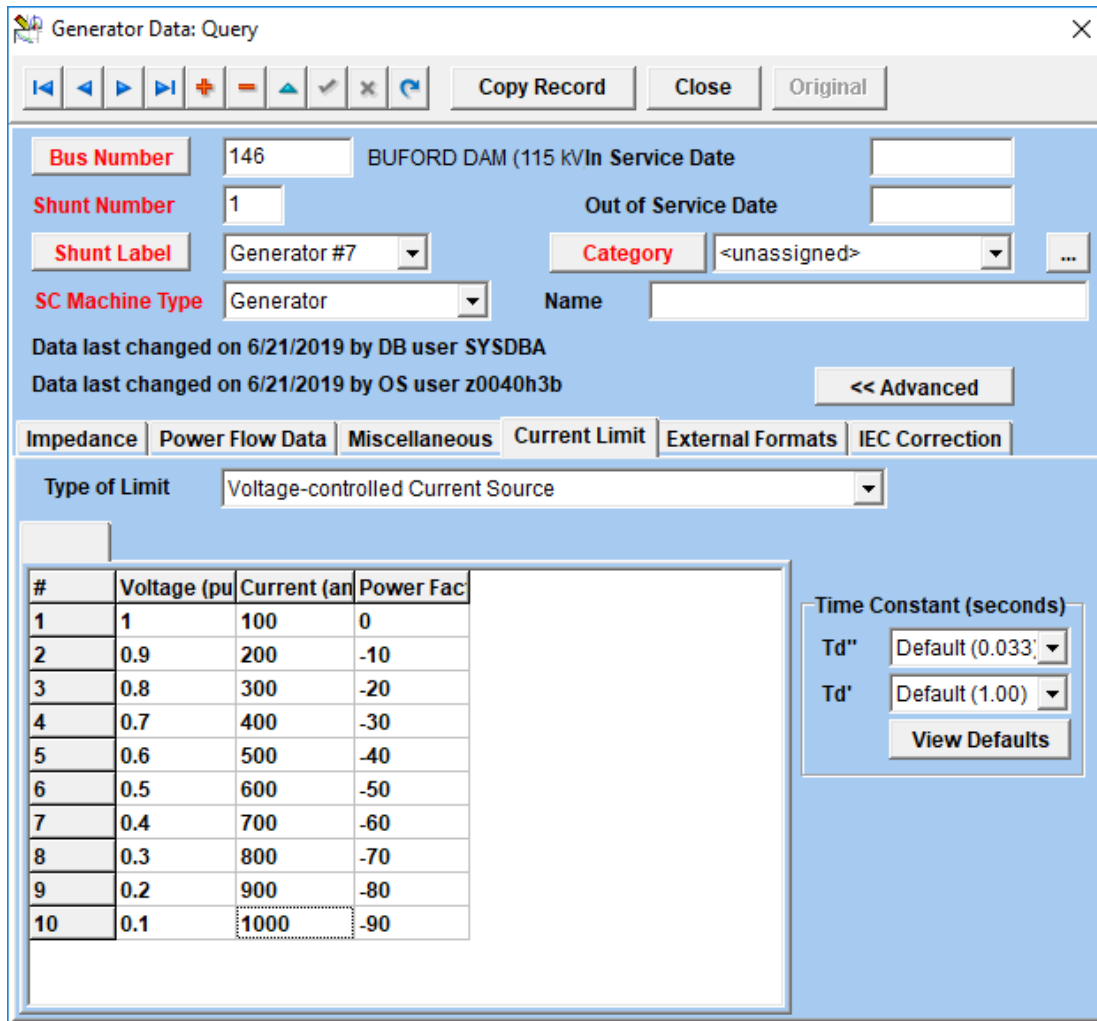


Fig. 4-28. VCCS Model in CAPE.

4.3.4 Iterative Algorithm

CAPE uses the following algorithm to calculate the steady-state fault current from the wind plants to the network, subject to the selected parameters previously discussed.

1. Loop through all the wind plants in the system.
2. For the first iteration, use the pre-fault bus voltages, which may consist of a load-flow profile or a classical flat profile at 1.0 pu.
3. Derive the pre-fault current (I_d , I_q) from the specified reference power (P , Q).
4. For subsequent iterations, compute the controlled fault currents from all Inverter Based Generator (IBG) plants and inject them into the network to obtain the network solution [17]. The bus voltage is the pre-fault voltage plus the incremental voltage due to faults and injected current.
5. Remove any wind plants isolated from the network by open breakers.
6. Start testing for convergence after 4 iterations. For each wind plant, find the difference in positive-sequence bus voltage at the MV bus, $|V_p(k) - V_p(k-1)|$ in

iteration (k). If the voltage difference exceeds the tolerance, the voltage for that wind plant has not yet converged. The default tolerance is $MXI_ITER_TOL = 0.01$ pu on the system base MVA.

7. Compute the positive-sequence voltage and current (V_p, I_p) at the LV grid-side converter.

If the inverter controls cannot produce a fault current consistent with the faulted network, the computed postfault voltage after any iteration step repeatedly leads or lags the voltage in successive steps. This happens, for example, when the wind plant is "islanded" by a three-phase fault, with no other source of current between the plant and the fault. If there is no source of infeed current between the generator and the fault, the iterative solution may not converge. Then the power-flow angle from the wind generator to the network cannot be determined. The extreme case is a solid fault on a radial line where no power is transferred to the network. In that case the apparent impedance $Z_p = (V_p/I_p)$ is constant and equal to the line impedance from the MV bus to the fault so that $\angle(P + jQ) = \angle(Z_p)$. The controlled angle due to the generator may be different. For the particular fault, the generator is defined to be "islanded" [18].

To improve the convergence of the model, CAPE has implemented the following logic upon discussions with EPRI.

1. CAPE does not attempt to solve an IBG isolated from all other sources. Before iterating the voltage, CAPE searches the unfaulted network for a connection between the IBG and any synchronous generator. If a connection exists, iterations proceed normally. If no connection is found, CAPE sets the generator current as zero, effectively removing the generator. This case can occur when a fault has been cleared by opening breakers.
2. The changes of phase angle $\arg(I_p)$ at successive iterations are smoothed.
3. The apparent impedance Z_p at the MV bus is computed with the fault applied in the network. If Z_p is constant in the first three iterations, the wind generator is considered to be islanded by the fault. Then CAPE keeps the voltage angle $\arg(V_p)$ at its pre-fault value so the controls and current limits are applied in a fixed (d-q) reference frame. The solution converges leaving a mismatch angle between the input and output currents at the MV bus.
4. If the solution has not converged in MXI_ITER_N iterations, the currents that did not converge are switched to an "Iq-injection" state for a further MXI_ITER_N iterations. At the LV node $I_d = 0$ and $I_q = (-1)^*$ (Chosen limit)

4.3.5 Reports

These reports help the user to understand how the wind plants respond to a fault. Fig. 4-29 shows an example of the "Bus Report" that identifies the wind plant at the bus as Type-III or IV.

```

-----
THREE_PHASE at bus "6 Bus_6"
-----
Substation Sub1
Bus      8 Bus_8      CO Base kV  34.50 Ph-Ph ( 19.92 @-30 deg A-Gnd)
Prefault 1.000 V (p.u.) @ -30.00

Voltage (p.u.)      > 0.88885 @ -7.4   0.00000 @ 0.0   0.00000 @ 0.0
Voltage (kV) Ph-Gnd > 17.7046 @ -7.4   0.00000 @ 0.0   0.00000 @ 0.0
Shunt Currents (Amps) incremental (I) and total (T) from >
Wind/Solar          I 1 1304.09 @ -21.6  0.00004 @ -8.4  0.00006 @ 116.6
Wind/Solar          T 1 1304.09 @ -21.6  0.00004 @ -8.4  0.00006 @ 116.6

Type-IV Normal
Converged in 5 steps; Ip pu to network ( 0.779 @ -21.6);
P, Q = ( 67.15, 16.99) MVA; PF deg 14.2

Line Currents (Amps) incremental from >
Sub1 Line: COLLECTOR
7 Bus_7          1 1304.15 @ 158.4  0.00000 @ 0.0  0.00000 @ 0.0 |

```

Fig. 4-29. CAPE bus fault report (excerpt).

A supplementary report (Fig. 4-30) contains all the data for a single wind plant.

```

Controlled generator (EPRI type-IV)
At bus 8 in Sub1 Bus_8      Base kV  34.50  Shunt #  1

System base      Machine base
S MVA            100.000      75.015
Desired reactive power (pu)  -0.075      -0.100
Des reactive power (MVAR)   -7.502      -7.502

.....

Operation Report for Controlled Generator 1 "Wind/Solar" at "8 Bus_8"

THREE_PHASE at bus "6 Bus_6"
CONTROL MODE      PF
CONTROL PRIORITY  Q
.....

Base      Bus Ckt  VP pu mag,deg      IP_MV mag,deg      Power MW
Syst      8 1      0.889 -7.36      0.779 -21.563      67.149
Mach      8 1      0.889 -7.36      1.039 -21.563      67.149

MVAR  MV deg(I/V)  VP_LV mag,deg      IP_GSC  GSC deg(I/V)
16.99 -14.199  0.93 -1.30      0.758 -16.61      -15.164
16.99 -14.199  0.93 -1.30      1.010 -16.61      -15.164

Generator status:
Type-IV Normal
Converged in 5 steps; Ip pu to network ( 0.779 @ -21.6);

```

Fig. 4-30. CAPE detailed report for one wind plant (excerpt).

For a network with many wind plants, a summary report shows which wind plants produce significant fault current. An example is shown in Fig. 4-31.

Summary of controlled generation					
MXI_ITER_TOL = 0.01000 perunit voltage; 41 Iterations					
Bus	Shunt #	P,Q MVA		Status	
14	1	0.00,	378.91	Type IV Switched to limited-Iq injection	Converged
15	1	0.00,	0.00	Type IV Switched to limited-Iq injection	Not converged
16	1	0.00,	0.00	Type IV Switched to limited-Iq injection	Not converged
17	1	0.00,	0.00	Type IV Switched to limited-Iq injection	Not converged
18	1	0.00,	0.00	Type IV Switched to limited-Iq injection	Not converged
19	1	0.97,	25.45	Type IV Normal	Converged
20	1	1.13,	25.13	Type IV Normal	Converged
21	1	1.25,	24.90	Type IV Normal	Converged
22	1	1.30,	24.79	Type IV Normal	Converged
23	1	0.37,	19.33	Type IV Normal	Converged
24	1	0.34,	18.03	Type IV Normal	Converged
25	1	0.00,	0.00	Type IV Switched to limited-Iq injection	Not converged
26	1	0.00,	0.00	Type IV Switched to limited-Iq injection	Not converged
27	1	0.00,	0.00	Type IV Switched to limited-Iq injection	Not converged
28	1	0.00,	0.00	Type IV Switched to limited-Iq injection	Not converged
29	1	0.00,	0.00	Type IV Switched to limited-Iq injection	Not converged
30	1	0.00,	0.00	Type IV Switched to limited-Iq injection	Not converged
THREE_PHASE at bus "27 EXAMPLE_27"					
17 active IBG machines					
99 inactive: remote fault (Vp ~ 1)					
Total	116 IBGs in bus set "Controlled_shunt_buses"				

Fig. 4-31. CAPE summary report for multiple wind plants.

4.3.6 Examples

EPRI Test System

An 8-bus test system is shown in Fig. 4-32. A Type-IV wind generator with GSU transformer is connected at bus 8; a separate synchronous generator is connected at bus 2. A three-phase fault is applied at various buses and the results for various control modes are shown and compared with the EPRI model results in Table 4-15 – Table 4-22. In the tables “mv” stands for medium voltage, and “lv” for low voltage. It is observed that the comparison results show close match between the CAPE and EPRI model.

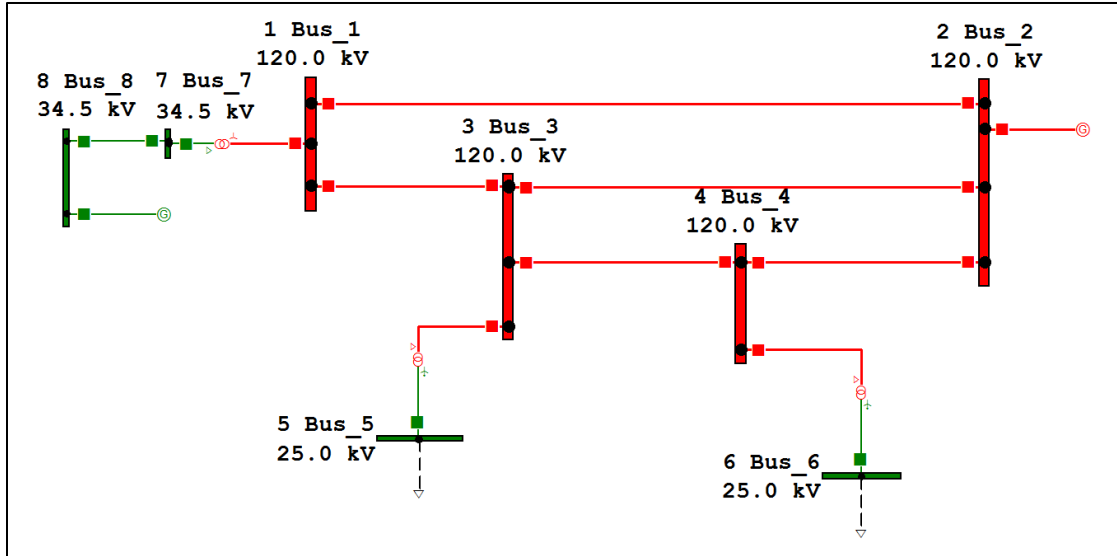


Fig. 4-32. EPRI 8-bus test system.
Table 4-15. FRT Control – CAPE Results

Fault bus	V mv (p.u.)	I mv (p.u.)	mv PF angle	V lv (p.u.)	I GSC (p.u.)	lv PF angle
3	0.434 \angle -1.14°	1.150 \angle -73.0°	-61.86°	0.543 \angle -6.48°	1.100 \angle -71.9°	-65.42°
4	0.614 \angle -7.4°	1.150 \angle -47.9°	-40.5°	0.702 \angle -0.87°	1.100 \angle -45.4°	-44.53°
5	0.805 \angle -6.18°	1.107 \angle -24.8°	-18.62°	0.857 \angle 0.61°	1.073 \angle -20.7°	-21.31°
6	0.862 \angle -8.54°	1.065 \angle -22.2°	-13.66°	0.903 \angle -2.13°	1.037 \angle -17.5°	-15.37°

Table 4-16. FRT Control – EPRI Results

Fault bus	V mv (p.u.)	I mv (p.u.)	mv PF angle	V lv (p.u.)	I GSC (p.u.)	lv PF angle
3	0.443 \angle -11.3°	1.150 \angle -73.3°	-62.0°	0.552 \angle -6.7°	1.100 \angle -72.1°	-65.4°
4	0.619 \angle -7.7°	1.150 \angle -47.5°	-39.9°	0.706 \angle -1.1°	1.100 \angle -45.0°	-43.9°
5	0.811 \angle -7.1°	1.102 \angle -25.3°	-18.1°	0.862 \angle -0.4°	1.069 \angle -21.1°	-20.7°
6	0.867 \angle -10.0°	1.062 \angle -23.2°	-13.2°	0.908 \angle -3.6°	1.035 \angle -18.5°	-14.9°

Table 4-17. Voltage Control – CAPE Results

Fault bus	V mv (p.u.)	I mv (p.u.)	mv PF angle	V lv (p.u.)	I GSC (p.u.)	lv PF angle
3	0.434 \angle -1.04°	1.1495 \angle -2.8°	-61.76°	0.543 \angle -6.36°	1.100 \angle -71.67°	-65.31°
4	0.711 \angle -2.02°	1.175 \angle -6.20°	-64.18°	0.823 \angle -9.19°	1.100 \angle -84.53°	-65.34°
5	1.00 \angle -17.35°	1.195 \angle -4.93°	-57.58°	1.109 \angle -14.56°	1.100 \angle -72.08°	-57.52°
6	1.00 \angle -13.00°	1.137 \angle -1.02°	-38.02°	1.082 \angle -8.62°	1.067 \angle -46.73°	-38.11°

Table 4-18. Voltage Control – EPRI Results

Fault bus	V mv (p.u.)	I mv (p.u.)	mv PF angle	V lv (p.u.)	I GSC (p.u.)	lv PF angle
3	0.443∠-11.3°	1.150∠-73.3°	-62.0°	0.552∠-6.7°	1.100∠-72.1°	-65.4°
4	0.721∠-22.8°	1.176∠-87.1°	-64.3°	0.833∠-20.0°	1.100∠-85.4°	-65.4°
5	1.000∠-16.7°	1.191∠-70.2°	-53.4°	1.104∠-13.5°	1.100∠-67.0°	-53.5°
6	1.000∠-14.4°	1.118∠-51.2°	-36.8°	1.080∠-10.0°	1.050∠-46.8°	-36.8°

Table 4-19. Q Control – CAPE Results

Fault bus	V mv (p.u.)	I mv (p.u.)	mv PF angle	V lv (p.u.)	I GSC (p.u.)	lv PF angle
3	0.437 ∠-42.8°	1.05∠-132.9°	-90.1°	0.542∠-43.9°	1.00∠-132.8°	-88.9°
4	0.312 ∠2.52°	1.00 ∠21.19°	18.67°	0.3059∠21.19°	1.0005∠22.94°	1.75°
5	0.667 ∠-5.82°	1.00 ∠2.8°	8.62°	0.6698∠2.80°	1.0022∠6.63°	3.83°
6	0.752 ∠-8.14°	1.00 ∠-0.49°	7.65°	0.7548∠-0.49°	1.0028∠3.82°	4.31°

Table 4-20. Q Control – EPRI Results

Fault bus	V mv (p.u.)	I mv (p.u.)	mv PF angle	V lv (p.u.)	I GSC (p.u.)	lv PF angle
3	0.444∠-44.1°	1.055 ∠-135.4°	-91.3°	0.549∠ -45.4°	1.00 ∠ -135.4°	-90.0°
4	0.313∠2.2°	1.000 ∠20.8°	18.6°	0.307∠20.8°	1.00 ∠22.6°	1.8°
5	0.675∠-6.7°	1.000 ∠ 1.8°	8.5°	0.677∠1.8°	1.002 ∠5.7°	3.9°
6	0.756∠-9.5°	1.000 ∠ -0.9°	7.6°	0.759 ∠-1.9°	1.003 ∠2.4°	4.3°

Table 4-21. PF Control – CAPE Results

Fault bus	V mv (p.u.)	I mv (p.u.)	mv PF angle	V lv (p.u.)	I GSC (p.u.)	lv PF angle
3	0.435∠-43.95°	1.054∠-135.2°	-91.23°	0.540∠-45.3°	1.000∠-135.2°	-89.87°
4	0.4605∠3.73°	1.113∠-10.35°	-14.08°	0.509∠15.65°	1.091∠-7.941°	-23.59°
5	0.779∠-6.07°	1.072∠-20.14°	-14.07°	0.822∠1.014°	1.045∠-15.94°	-16.95°
6	0.865∠-8.55°	1.067∠-22.62°	-14.07°	0.906∠-2.159°	1.039∠-17.93°	-15.78°

Table 4-22. PF Control – EPRI Results

Fault bus	V mv (p.u.)	I mv (p.u.)	mv PF angle	V lv (p.u.)	I GSC (p.u.)	lv PF angle
3	0.444 ∠-44.0°	1.055 ∠-135.3°	-91.3°	0.550 ∠-45.3°	1.000 ∠-135.3°	-90.0°
4	0.464 ∠3.3°	1.111 ∠-10.8°	-14.0°	0.513 ∠15.1°	1.090 ∠-8.3°	-23.4°
5	0.789 ∠-7.1°	1.071 ∠-21.1°	-14.0°	0.832 ∠-0.1°	1.044 ∠-16.8°	-16.8°
6	0.871 ∠-10.2°	1.062 v-24.2°	-14.0°	0.913 ∠-3.9°	1.033 ∠-19.5°	-15.6°

4.4 ETAP model implementation

4.4.1 WTG Type-I and II

WTG is modeled as an induction generator. It should be noted that zero sequence current does not exist in all WTG types due to the line-to-line connection of WTG.

4.4.2 WTG Type-III with crowbar

WTG is modeled as an induction generator. Users can also assign the crowbar and chopper resistance. In case of the IEC short-circuit program, there are additional parameters available for the user to specify as defined by the latest IEC 60909 to adjust the fault current.

4.4.3 WTG Type-III without crowbar or Type-IV

WTG is modeled as a voltage dependent current source. In this model, short-circuit current is limited based on two curves as detailed next. First, maximum positive sequence current ($I_{SC, \max}$) injected to the system is limited by a curve as shown in Fig. 4-33 where the user can adjust the indicated parameters. If WTG maximum short-circuit current is fixed within the short-circuit region, user can set $I_{SC, \max}$ and $I_{SC, \min}$ to the same value as $I_{SC, \max}$. It is important to note that, if the fault voltage falls within the operating region as defined in Fig. 4-33, the current injection maintains normal operating power factor and power injection rather than the one defined for short-circuit conditions. In case of toggling between short-circuit and normal operating regions, ETAP locks the current to the operating region (I_{op}).

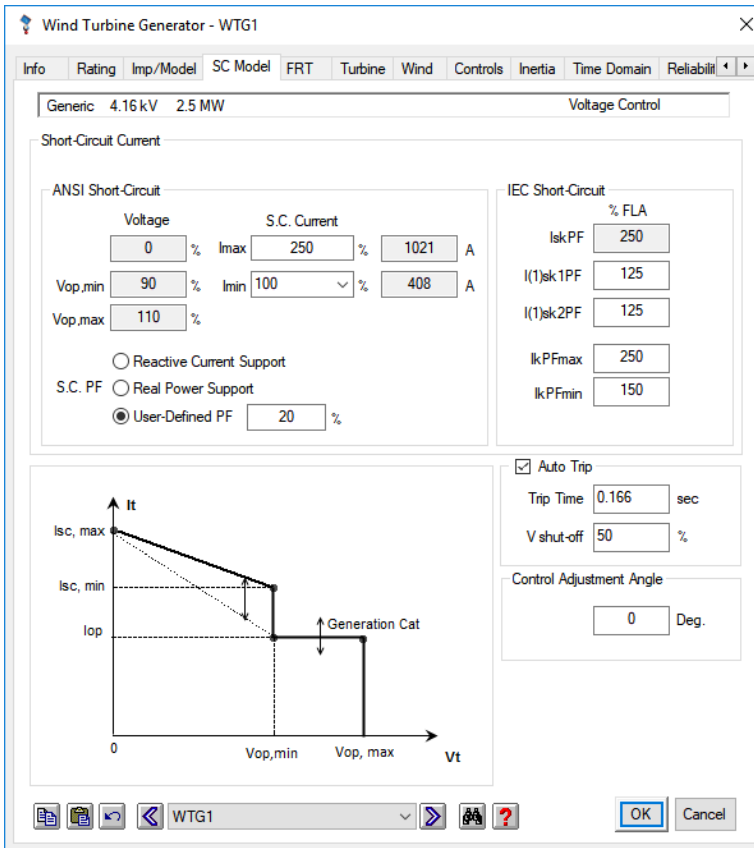


Fig. 4-33. ETAP WTG short-circuit model.

Three modes of operation are supported: 1- Reactive Current Support, 2- Real Power Support and 3- User defined PF. In reactive current support mode of operation, the reactive current (I_q) injection is calculated based on the user-defined FRT curve as shown in Fig. 4-34. If the amount of injected reactive current (I_q) is below $I_{SC, max}$ as defined in Fig. 4-33, active current (I_d) is injected provided that the active power during fault does not exceed the pre-fault active power and total injected current ($|I_d + jI_q|$) does not exceed $I_{SC, max}$.

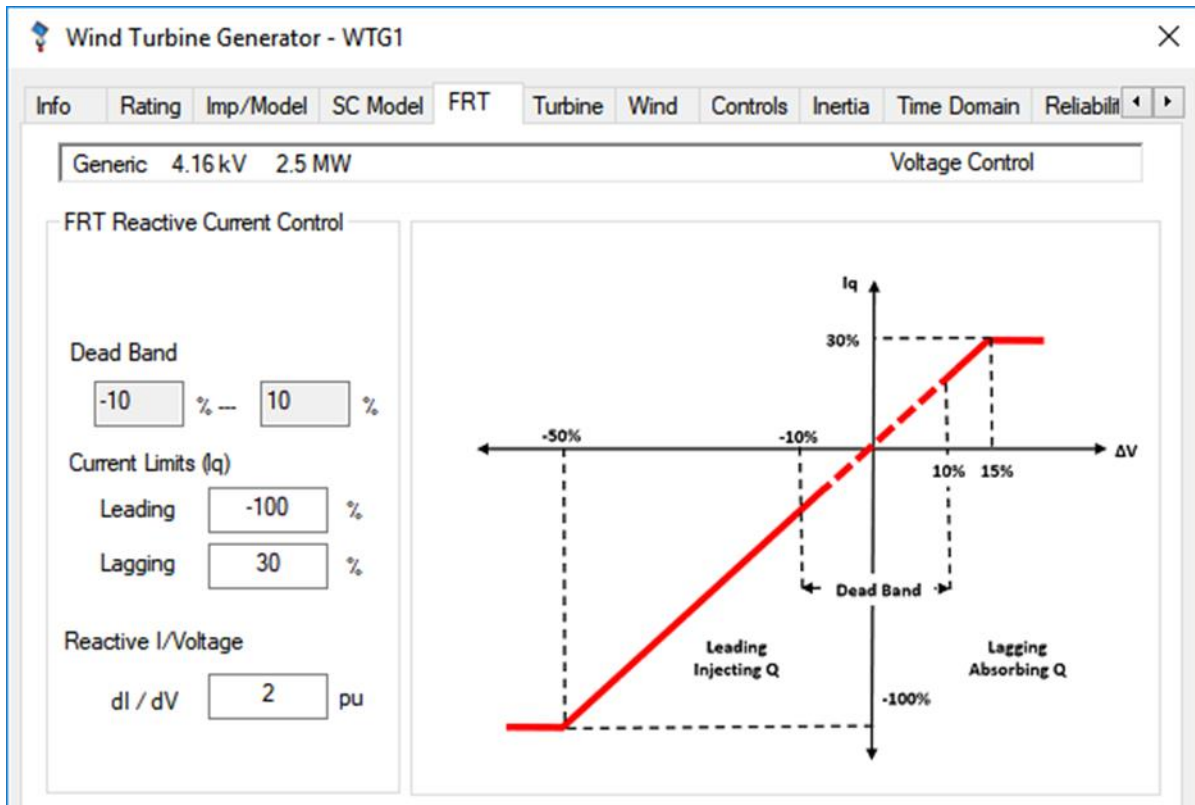


Fig. 4-34. ETAP WTG FRT.

In real power support mode of operation, the active power current (I_d) injection is calculated first based on the pre-fault active power limited to $I_{SC, max}$. If I_d is less than $I_{SC, max}$, reactive current injection is determined based on the FRT curve provided that total injected current does not exceed $I_{SC, max}$.

In user-defined power factor mode of operation, I_d is determined based on pre-fault active power while I_q is determined based on I_d and user defined power factor. The total injected current ($|I_d + jI_q|$) should not exceed $I_{SC, max}$. If it exceeds, both I_d and I_q are reduced with the same proportion to meet the user-defined power factor and $I_{SC, max}$ limit. It is important to note that $I_{SC, max}$ is a function of voltage as shown in Fig. 4-34 in all cases.

In all three modes of operation, there is a possibility that injected current cannot flow into the system due to system characteristic and limitations in transferring certain amount of active or reactive power. This obviously happens more often in case of higher active power injection as compared to the reactive. In this scenario, the injected WTG current results in considerable voltage angle shift at the terminal of WTG. This results in continuous angle rotation of the injected current and the WTG terminal voltage leading to non-convergence of solution. What actual WTG controller does in such scenarios depends on the controller algorithm and may vary from one to another. To resolve such issues in ETAP short-circuit analysis, a logic is implemented to determine which WTGs are potentially capable of injecting current with a specified angle and which are not. This is done by performing pre-short-circuit analysis excluding all current injection sources such as WTGs Type-III and IV. If voltage at the WTG terminal is less than a pre-set threshold, this means that the path of current injection is most probably blocked by the

fault. For such WTGs, ETAP utilizes positive sequence pre-fault voltage angle of WTG terminal as a reference instead of the voltage during fault. Second, during the iterative short-circuit analysis, if the injected current, especially angle, does not converge within a few iterations (starts rotating) for certain WTGs or inverters, they are added to the list of current injecting elements not capable of following their short-circuit set points. For these elements, regular current injection is applied, except that similar to the previous case, the reference for determination of angle is replaced from the fault positive sequence voltage to pre-fault positive sequence voltage. This allows the current injection method to converge. As shown in Fig. 4-33, user defined control adjustment angle can be employed by the user to adjust the short-circuit result to the actual WTG controller performance, if known.

User has an option to block negative sequence current or specify a negative sequence impedance for Type-III; however, negative sequence current is blocked for Type-IV. In case of IEC short-circuit, similar to Type-III with crowbar, there are additional parameters available for the user to adjust the fault current as per the latest IEC 60909.

5. CONCLUDING REMARKS

As the penetration of wind farms increases, there is an urgent need to update commercial steady-state short-circuit programs to accommodate the unconventional fault response of WTGs, especially Type-III and Type-IV. Considering the fact that this response is dictated by the proprietary controls implemented by the WTG-manufacturers, this report describes two approaches to define the short-circuit models.

First, a tabular approach is proposed that defines the current output and power factor angle of the machine at different terminal voltages, both positive and negative sequence, at different time-frames, for various control modes the manufacturer may have. This is the most general approach, and the manufacturers have agreed to provide such data. Software developers have shown that this approach can be integrated in their existing short-circuit programs by treating the WTG as a nonlinear element with output characteristics defined by the values in the tables.

Second, generic EMT models [22] can be used to validate against available field data. Phasor domain models are developed by EPRI based on these validated models. These are also integrated by software developers. Though there is no guarantee that the fault response of these models matches all makes and models of WTGs, they can be judiciously used as an educated approximation by users.

The report describes the software implementation of the proposed approaches by three major software developers in the USA. Simulation results on small test-systems are provided for illustration. The report also documents data provided by Siemens (through their detailed control logic for Type IV WTGs), Vestas, GE, and one more manufacturer (name not disclosed) in the proposed tabular format. In addition, data generated by black box models of Type-III and Type-IV WTGs are provided by running these models in the PSCAD environment. These data from diverse sources underscore the need for the control-agnostic modeling approach proposed in this report.

Finally, it is noted that this work is foundational in nature. Further testing of the software models on actual utility systems with varying penetration of renewable sources and standardization of fault response by grid codes and/or industry standards (e.g. IEEE P2800) are expected to contribute to refinement of the software-models implemented in the vendors' products.

6. REFERENCES

- [1] Fault Current Contribution from Wind Plants – IEEE PSRC/Machinery/T&D Committees Report. Available online: “<http://www.pes-psrc.org/kb/published/reports/Fault%20Current%20Contributions%20from%20Wind%20Plants.pdf>”
- [2] German Grid Code, VDE-ARN 4120, 2018-11, “<https://www.vde-verlag.de/standards/0100493/vde-ar-n-4120-anwendungsregel-2018-11.html>”.
- [3] Amirnaser Yazdani and Reza Iravani, *Voltage-Sourced Converters in Power Systems: Modeling, Control, and Applications*, New Jersey: Wiley-IEEE Press, 2010.
- [4] T. Kauffmann, U. Karaagac, I. Kocar, H. Gras, J. Mahseredjian and E. Farantatos, "Phasor domain modeling of Type-III wind turbine generator for protection studies," Proc. 2015 IEEE PES General Meeting, Denver, CO, 26-30 July 2015.
- [5] U. Karaagac, T. Kauffmann, I. Kocar, H. Gras, J. Mahseredjian and E. Farantatos, "Phasor domain modeling of Type-IV wind turbine generator for protection studies," Proc. 2015 IEEE PES General Meeting, Denver, CO, 26-30 July 2015.
- [6] T. Kauffmann, U. Karaagac, I. Kocar, S. Jensen, J. Mahseredjian, E. Farantatos, “An Accurate Type-III Wind Turbine Generator Short-circuit Model for Protection Applications”, IEEE Transactions on Power Delivery, 2017.
- [7] E. Farantatos, T. Kauffmann, U. Karaagac, I. Kocar, and J. Mahseredjian, “Phasor Domain Modeling of Electronically Coupled Generators for System Protection Studies”, Proc. of 5th International Workshop on Integration of Solar Power into Power Systems, Brussels, Belgium, Oct. 2015.
- [8] “Impact of Renewables on System Protection: Short-Circuit Phasor Models of Converter Interfaced Renewable Resources and Performance of Transmission Line Distance Protection”, EPRI, Palo Alto, CA: 2015. 3002005765.
- [9] “Impact of Renewables on System Protection: Wind/PV Short-Circuit Phasor Model Library and Guidelines for System Protection Studies”, EPRI, Palo Alto, CA: 2016. 3002008367.
- [10] “Short-Circuit Phasor Models of Converter Based Renewable Energy Resources for Fault Studies”, EPRI, Palo Alto, CA: 2017. 3002010936
- [11] R. Walling and M. Reichard (GE Energy), “Short-circuit Behavior of Wind Turbine Generators”. Proceedings of Annual Conference for Protective Relay Engineers, College Station, TX, March 30- April 2, 2009.
- [12] V. Brandwajn and W.F. Tinney, “Generalized Method of Fault Analysis,” IEEE Trans. On Power Apparatus and Systems, pp. 1301-06, June 1985.
- [13] W.K. Chan, *Linear Networks and Systems: Algorithms and Computer-Aided Implementations*, Singapore, World Scientific, 1994.
- [14] Fault Current Contribution from Wind Plants – IEEE PSRC/Machinery/T&D Committees Report. Available online: [http://www.pes-psrc.org/Reports/Fault Current Contributions from Wind Plants.pdf](http://www.pes-psrc.org/Reports/Fault%20Current%20Contributions%20from%20Wind%20Plants.pdf)
- [15] Malati Chaudhary, S. M. Brahma, S. J. Ranade, “Short-circuit Analysis of Type-II Induction Generator and Wind Farm,” *Proc. 2012 IEEE Transmission and Distribution Conference & Exposition*, April 2012, Orlando, Florida.

- [16] "Type-IV Wind/Solar Generator Models" presented at 2018 CAPE Users' Group Meeting, Electrocon International, Inc.; June 2018.
- [17] Fernando L. Alvarado, Sao Khai Mong, and Mark K. Enns, "A Fault Program with Macros, Monitors, and Direct Compensation in Mutual Groups," *IEEE Transactions on Power Apparatus and Systems*, vol. PAS-104, No. 5, pp. 1109-1120; May 1985.
- [18] Goksu, O.; Teodorescu, R.; Bak, C.L.; Iov, F.; Kjaer, P.C., "Instability of Wind Turbine Converters During Current Injection to Low Voltage Grid Faults and PLL Frequency Based Stability Solution," *IEEE Transactions on Power Systems*, vol.29, no.4, pp.1683,1691; July 2014.
- [19] ANAFAS ANALISE DE FALTAS VERSIO 6.5.1 MANUAL DO USUARIO, CEPEL - Centro de Pesquisas de Energia Eletrica, Rio de Janeiro, Brasil; Marco, 2014.
- [20] Sergio P. Romero et. al. (CEPEL), "Representacao de Geradores Eolicos Sincronos com Conversor de Frequencia por Fontes de Corrente Controladas em um Programa de Calculo de Curtos Circuitos," XI Symposium of Specialists in Electric Operational and Expansion Planning, Brasil; March 17-20 2009.
- [21] IEC 61400-27-1:2015 - Wind turbines - Part 27-1: Electrical simulation models - Wind turbines.
- [22] U. Karaagac, J. Mahseredjian, R. Gagnon, H. Gras, H. Saad, L. Cai, I. Kocar, A. Haddadi, E. Farantatos, S. Bu, K. W. Chan, and L. Wang, "A generic EMT-type model for wind parks with permanent magnet synchronous generator full size converter wind turbines," *IEEE Power and Energy Technology Systems Journal*, vol. 6, no. 3, pp. 131–141, Sep. 2019.

APPENDIX A: DATA GENERATED WITH PSCAD USING BLACK-BOX MODELS – TYPE-III AND IV

The fault current characteristics of Type-III and Type-IV WTGs are obtained considering the power system shown in Fig. A.1-1. The WTG is connected to the 33 kV level at Bus-1. The total load at Bus-3 is $7.835+j15.025$ MVA (5.6484 pu on 3 MVA, 132 kV base), which, at 132 kV, draws 74 A current. Faults are simulated at two different locations:

1. Bus-2 at the point of interconnection (POC) of WTG, and
2. Bus-4 as remote fault.

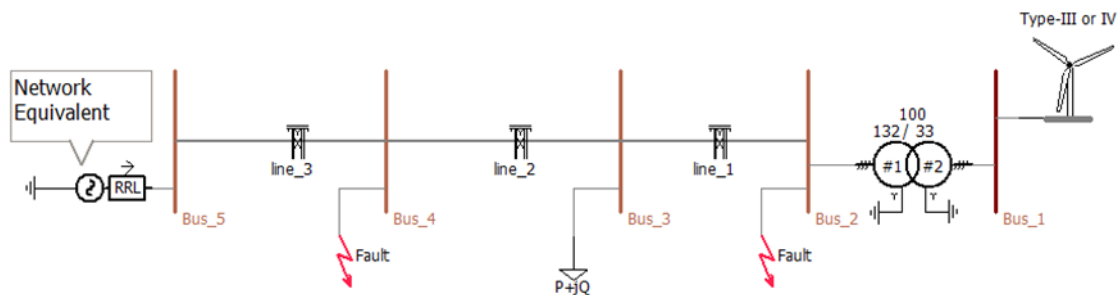


Fig. A1-1 Power system simulated to generate test data.

The voltage-drop magnitudes at the terminal of the wind farm during faults are varied by changing the resistance of fault for both fault locations. The values of fault resistances are thus determined based on the required voltage range at the terminals of the WTG rather than practical considerations. The machine responds to the value of the positive/negative sequence voltage at its terminal; how this voltage is created should not affect its output.

The waveforms of voltages and currents are measured at the terminal of the WTG at Bus-1 (33kV). The corresponding phasors are extracted using Fast Fourier Transform (FFT), and the positive and negative sequence voltages and currents are computed.

The WTG was simulated in PSCAD using a black-box model provided by the manufacturer of the respective WTGs. Thus, the model closely emulates an actual WTG of the particular manufacturer with its controllers. In addition to black-box models by vendors, a generic Type-IV wind turbine as described in IEC Standard 61400-27-1 [21] was also tested in a similar fashion.

A.1 Type-III wind turbine results

The Type-III WTG is rated at 3 MW, 0.69 kV, 60 Hz. The 0.69 kV/33 kV step-up transformer is internal to the WTG model. In the simulations, no over/under voltage protection is activated; however, crowbar protection is enabled.

A.1.1 Fault results on Bus 2

A.1.1.1 Three phase to ground (ABC-G) fault

The detailed rms measurements for a three-phase-to-ground fault (ABC-G fault) occurring on Bus-2 are given in Table A1-1. Note that in the tables and figures of this appendix, the phase angle difference between positive/negative sequence voltage and positive/negative sequence current is provided and plotted. This is opposite to the definition of the power factor angle at the description in section 3 and the implementations in section 4. Also note that the reported phase angles are unreliable when the relevant magnitude is close to zero

Table A1-1. Measured voltages and currents at different time-frames (ABC-G fault on Bus 2) – Type-III Positive sequence:

After one cycle			After two cycles			After five cycles		
Magnitude [pu]		Angle [deg]	Magnitude [pu]		Angle [deg]	Magnitude [pu]		Angle [deg]
Vp	Ip	$\angle V_p - \angle I_p$	Vp	Ip	$\angle V_p - \angle I_p$	Vp	Ip	$\angle V_p - \angle I_p$
0.0730	2.0652	51.3135	0.0064	1.8064	36.3473	0.0043	1.3416	176.4989
0.1352	2.1580	15.4842	0.0917	1.9109	-32.2384	0.0971	1.0105	-14.4292
0.2229	2.1764	3.5423	0.1942	1.9616	-21.5206	0.2009	1.0644	84.8482
0.3130	2.1696	0.0556	0.2993	1.9091	-8.0428	0.3009	1.2503	94.4748
0.3977	2.1074	-1.4313	0.3978	1.8011	1.2506	0.3954	1.2438	97.4460
0.5005	1.9952	-2.1375	0.5157	1.6583	9.7195	0.5104	1.0845	93.8617
0.5962	1.8749	-2.8738	0.6207	1.5166	13.4573	0.6157	0.9325	81.6207
0.7001	1.7109	-3.6389	0.7324	1.3626	15.1805	0.7244	0.8215	62.6247
0.7802	1.5488	-3.8910	0.8153	1.2352	14.8837	0.8071	0.9238	24.1965
0.8874	1.3243	-5.6467	0.9128	1.1486	2.1885	0.9104	1.0325	4.2822
0.9425	1.1706	-6.7397	0.9565	1.0646	-2.1343	0.9559	1.0035	-1.7065

A.1.1.2 Single phase to ground (A-G) fault

The detailed rms measurements for an A-G fault occurring on Bus-2 are given in Table A1-2. The voltage of the faulted phase was varied from target value of 0 pu (actual 0.0057 pu) to target value of 1 pu (actual 0.9547 pu).

Table A1-2. Measured voltages and currents at different time-frames (A-G fault on Bus 2) – Type-III

Positive sequence:

After one cycle			After two cycles			After five cycles		
Magnitude [pu]		Angle [deg]	Magnitude [pu]		Angle [deg]	Magnitude [pu]		Angle [deg]
Vp	Ip	$\angle V_p - \angle I_p$	Vp	Ip	$\angle V_p - \angle I_p$	Vp	Ip	$\angle V_p - \angle I_p$
0.8054	1.1888	12.0715	0.7876	1.1760	21.8530	0.7789	0.9209	35.4431
0.8154	1.2030	10.1268	0.7979	1.1924	19.6035	0.7897	0.9266	32.7271
0.8270	1.2074	8.6089	0.8105	1.1846	18.3179	0.8030	0.9139	31.2061
0.8394	1.2080	7.0407	0.8243	1.1726	17.0125	0.8176	0.9012	28.7639
0.8520	1.2104	5.4620	0.8386	1.1522	15.5151	0.8327	0.8825	26.4088
0.8690	1.2028	3.7161	0.8584	1.1349	13.4458	0.8535	0.8692	22.9081
0.8865	1.1917	1.6888	0.8791	1.1087	11.2699	0.8752	0.8657	18.5833
0.9082	1.1763	-0.9331	0.9046	1.0892	7.8513	0.9019	0.8593	13.6866
0.9274	1.1525	-2.9314	0.9255	1.0924	1.3338	0.9235	1.0527	1.9856
0.9568	1.1038	-5.9754	0.9581	1.0518	-2.5559	0.9574	1.0145	-2.1162
0.9712	1.0703	-11.6987	0.9718	1.0385	-11.9985	0.9712	1.0357	-12.3578

Negative sequence:

After one cycle			After two cycles			After five cycles		
Magnitude [pu]		Angle [deg]	Magnitude [pu]		Angle [deg]	Magnitude [pu]		Angle [deg]
Vn	In	$\angle V_n - \angle I_n$	Vn	In	$\angle V_n - \angle I_n$	Vn	In	$\angle V_n - \angle I_n$
0.1835	0.3953	-101.9109	0.2002	0.3426	21.8530	0.2025	0.2052	-84.3172
0.1762	0.3885	-103.0388	0.1943	0.3223	19.6035	0.1965	0.1874	-85.3231
0.1680	0.3765	-103.3094	0.1868	0.3107	18.3179	0.1891	0.1816	-84.8178
0.1591	0.3636	-103.5879	0.1784	0.3002	17.0125	0.1806	0.1811	-84.5670
0.1501	0.3474	-103.4706	0.1693	0.2838	15.5151	0.1714	0.1726	-83.1794
0.1377	0.3226	-103.0460	0.1561	0.2680	13.4458	0.1581	0.1663	-82.6685
0.1244	0.2949	-102.0601	0.1411	0.2433	11.2699	0.1430	0.1530	-83.6256
0.1067	0.2578	-100.6410	0.1201	0.2194	7.8513	0.1220	0.1378	-82.1929
0.0894	0.2152	-98.7936	0.0992	0.1911	1.3338	0.0993	0.1863	-88.4719
0.0564	0.1364	-94.6230	0.0603	0.1174	-2.5559	0.0604	0.1142	-88.1405
0.0300	0.0628	-95.7003	0.0311	0.0600	-11.9985	0.0312	0.0584	-89.8842

A.1.2 Fault results on Bus 4

Faults were created using the same procedure at Bus-4 to simulate a remote fault. As expected, the machine responds simply to the voltages at its terminals, irrespective of the location of fault. The comparison of results obtained for faults on Bus 2 and Bus 4 is captured in Figures A.1-2 to A.1-5.

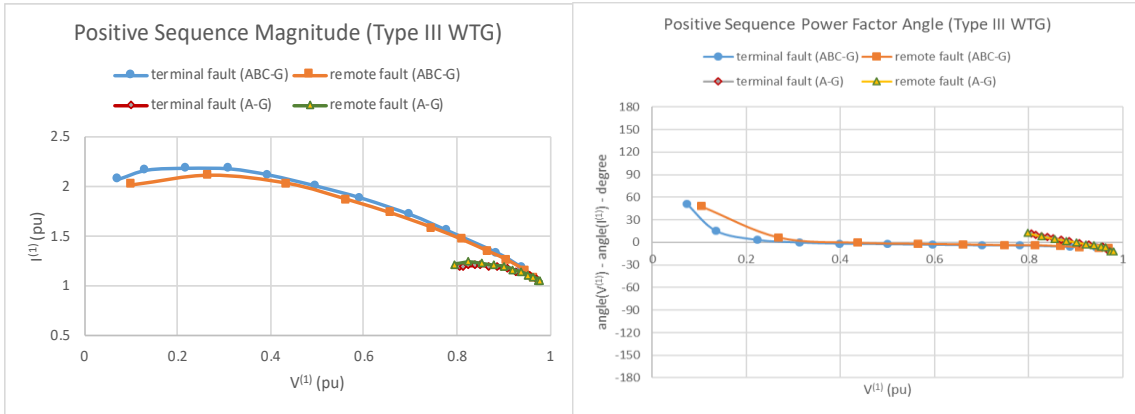


Fig. A.1-2. Positive sequence magnitudes and power factor angle after one cycle.

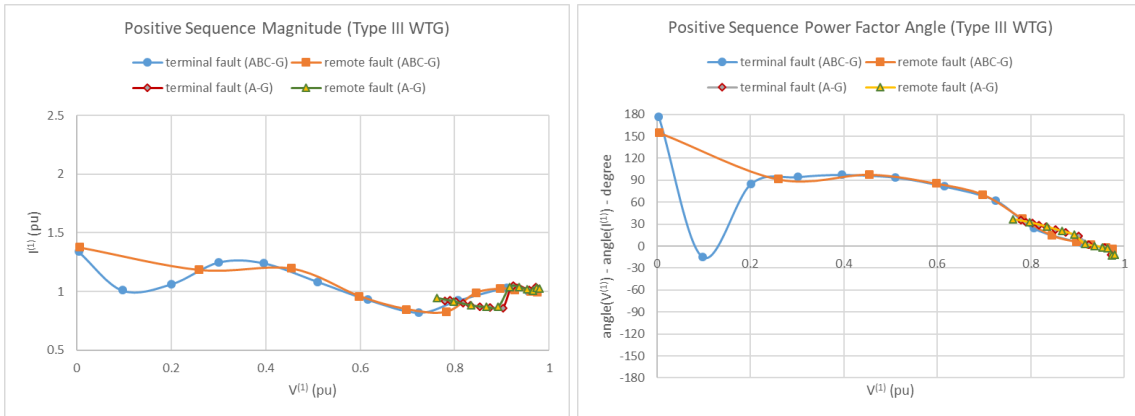


Fig. A.1-3. Positive sequence magnitudes and power factor angle after five cycles.

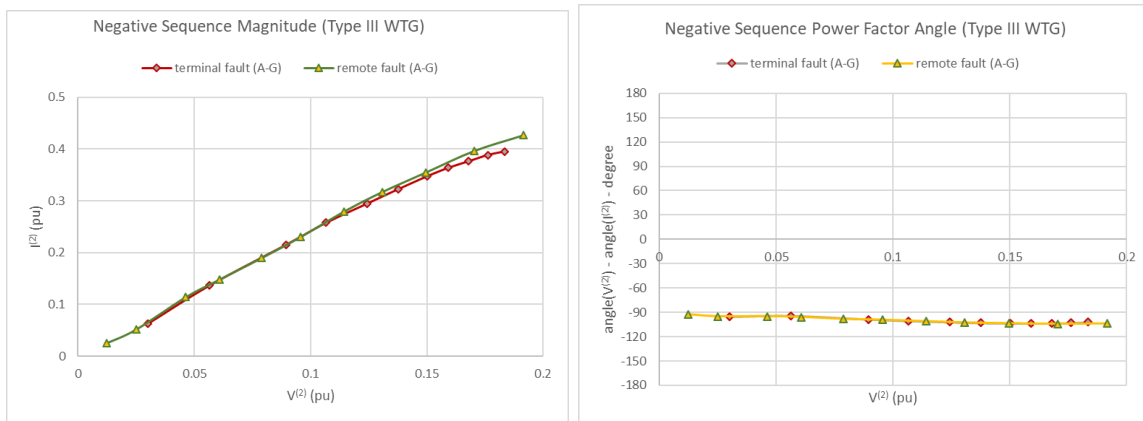


Fig. A.1-4. Negative sequence magnitudes and power factor angle after one cycle.

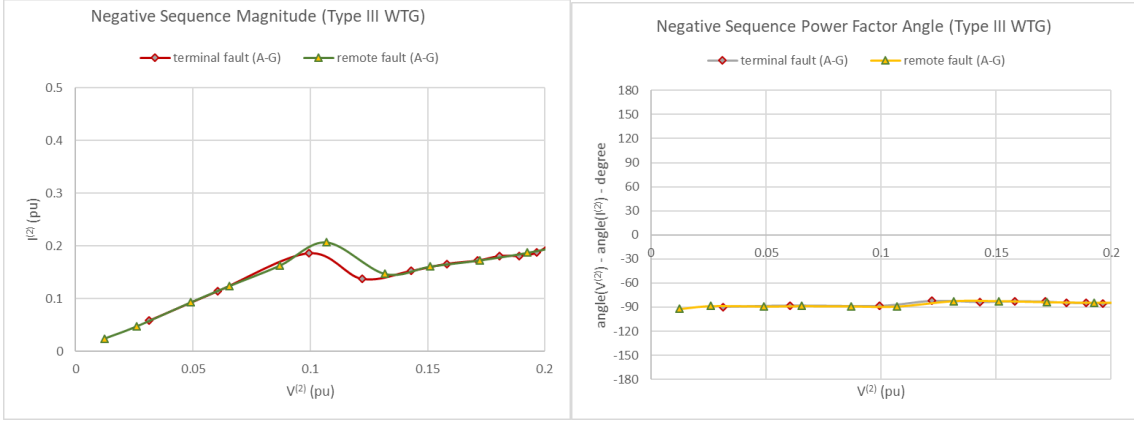


Fig. A.1-5. Negative sequence magnitudes and power factor angle after five cycles.

A.2 Type-IV wind turbine results

Type-III WTG was now replaced by a black box model of a Type-IV WTG rated 3MW, 0.69 kV, 50Hz. The process of obtaining the data remained the same as described for Type-III. Note that in the tables and figures of this appendix, the phase angle difference between positive/negative sequence voltage and positive/negative sequence current is provided and plotted. This is opposite to the definition of the power factor angle at the description in section 3 and the implementations in section 4.

A.2.1 Fault results on Bus 2

A.2.1.1 Three phase to ground (ABC-G) fault on Bus 2

Table A.2-1. Measured voltages and currents at different time-frames (ABC-G fault on Bus 2) – Type-IV

Positive sequence:

After one cycle			After two cycles			After five cycles		
Magnitude [pu]		Angle [deg]	Magnitude [pu]		Angle [deg]	Magnitude [pu]		Angle [deg]
Vp	Ip	$\angle V_p - \angle I_p$	Vp	Ip	$\angle V_p - \angle I_p$	Vp	Ip	$\angle V_p - \angle I_p$
0.0017	1.5032	11.3759	0.0018	1.3393	-23.8641	0.0017	1.2243	-56.1471
0.0957	1.2101	-72.6864	0.0953	1.1511	-70.8030	0.0947	1.2170	-65.8739
0.1896	1.3279	-66.7268	0.1882	1.2295	-65.2884	0.1891	1.2063	-56.2835
0.2896	1.3377	-60.0078	0.2880	1.2234	-57.1261	0.2903	1.1954	-42.9504
0.3830	1.3175	-53.8239	0.3821	1.1854	-49.5959	0.3855	1.1901	-31.9491
0.4624	1.2784	-48.1442	0.4622	1.1450	-43.0035	0.4664	1.1902	-23.8160
0.5540	1.2135	-40.4777	0.5539	1.0943	-34.8521	0.5589	1.1961	-15.9335
0.6674	1.1795	-30.5519	0.6645	1.0971	-25.1147	0.6695	1.2042	-8.9194
0.7454	1.1564	-23.3822	0.7420	1.1101	-18.6473	0.7440	1.1991	1.9127
0.8410	1.1324	-9.7024	0.8402	1.0846	-3.9147	0.8448	1.0886	13.6934
0.9391	0.9618	0.8607	0.9390	0.9564	1.2257	0.9391	0.9580	1.5209

A.2.1.2 Single phase to ground (A-G) fault on Bus 2

Table A2-2. Measured voltages and currents at different time-frames (A-G fault on Bus 2) – Type-IV Positive sequence:

After one cycle			After two cycles			After five cycles		
Magnitude [pu]		Angle [deg]	Magnitude [pu]		Angle [deg]	Magnitude [pu]		Angle [deg]
V _p	I _p	∠V _p - ∠I _p	V _p	I _p	∠V _p - ∠I _p	V _p	I _p	∠V _p - ∠I _p
0.7380	1.2531	0.1205	0.7577	1.2279	1.5047	0.7502	1.2212	10.8088
0.7512	1.2378	2.1663	0.7699	1.2035	3.3940	0.7626	1.2011	11.0117
0.7647	1.2182	2.3199	0.7825	1.1822	3.6631	0.7761	1.1819	11.1170
0.7802	1.1951	2.4999	0.7971	1.1582	3.9318	0.7918	1.1604	11.2714
0.7961	1.1716	2.6734	0.8120	1.1347	4.1926	0.8079	1.1399	11.4333
0.8111	1.1497	2.7929	0.8259	1.1133	4.3994	0.8228	1.1209	11.5661
0.8303	1.1217	2.9307	0.8436	1.0864	4.6285	0.8419	1.0974	11.7560
0.8576	1.0820	2.9785	0.8686	1.0506	4.6921	0.8684	1.0627	11.5580
0.8787	1.0525	2.7762	0.8875	1.0243	4.0964	0.8877	1.0326	9.3175
0.9084	1.0103	2.2529	0.9136	0.9900	2.9755	0.9141	0.9948	5.8448
0.9432	0.9558	0.6955	0.9435	0.9539	0.7275	0.9436	0.9539	0.8068

Negative sequence:

After one cycle			After two cycles			After five cycles		
Magnitude [pu]		Angle [deg]	Magnitude [pu]		Angle [deg]	Magnitude [pu]		Angle [deg]
V _n	I _n	∠V _n - ∠I _n	V _n	I _n	∠V _n - ∠I _n	V _n	I _n	∠V _n - ∠I _n
0.1722	0.2009	-125.6739	0.2592	0.1289	-10.4573	0.2444	0.1285	-40.6602
0.1693	0.1986	-124.2687	0.2551	0.1293	-11.6577	0.2412	0.1269	-38.7271
0.1660	0.1915	-122.1463	0.2503	0.1259	-9.8172	0.2373	0.1253	-36.4810
0.1621	0.1825	-119.4695	0.2443	0.1221	-7.8175	0.2323	0.1233	-34.1208
0.1580	0.1728	-116.2934	0.2375	0.1191	-5.7153	0.2267	0.1214	-31.7069
0.1541	0.1631	-112.9845	0.2305	0.1165	-3.6596	0.2209	0.1195	-29.5881
0.1490	0.1500	-107.8248	0.2204	0.1136	-1.2175	0.2124	0.1168	-26.8405
0.1411	0.1304	-98.2873	0.2033	0.1100	2.3316	0.1978	0.1133	-22.6103
0.1342	0.1136	-88.2471	0.1871	0.1069	5.0144	0.1836	0.1089	-17.4931
0.1220	0.0918	-66.2123	0.1574	0.1017	7.8760	0.1570	0.1017	-9.9637
0.0918	0.0861	-6.5357	0.0942	0.0903	2.4157	0.0952	0.0901	-0.3451

A.2.2 Fault results on Bus 4

Faults were created using the same procedure at Bus-4 to simulate a remote fault. As expected, the machine responds simply to the voltages at its terminals, irrespective of the location of fault. The comparison of results obtained for faults on Bus 2 and Bus 4 is captured in Figures A.2-1 to A.2-4.

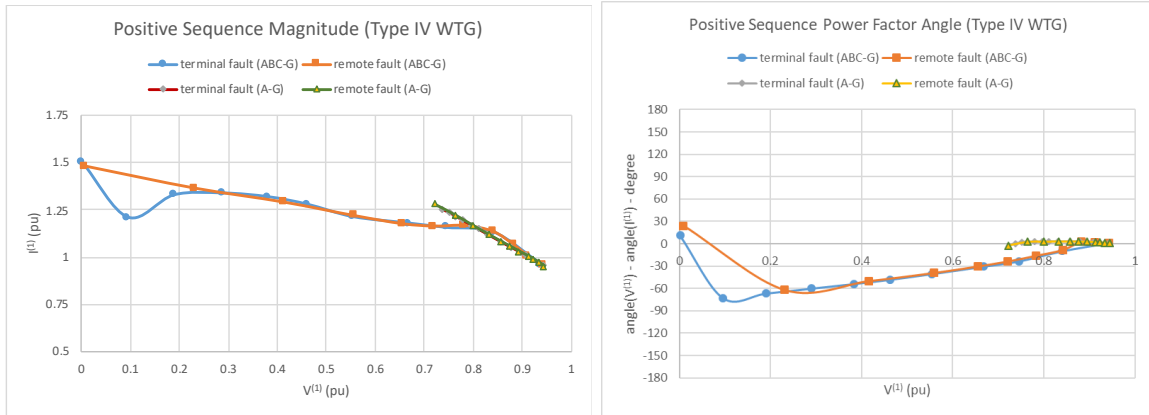


Fig. A.2-1. Positive sequence magnitudes and power factor angle after one cycle.

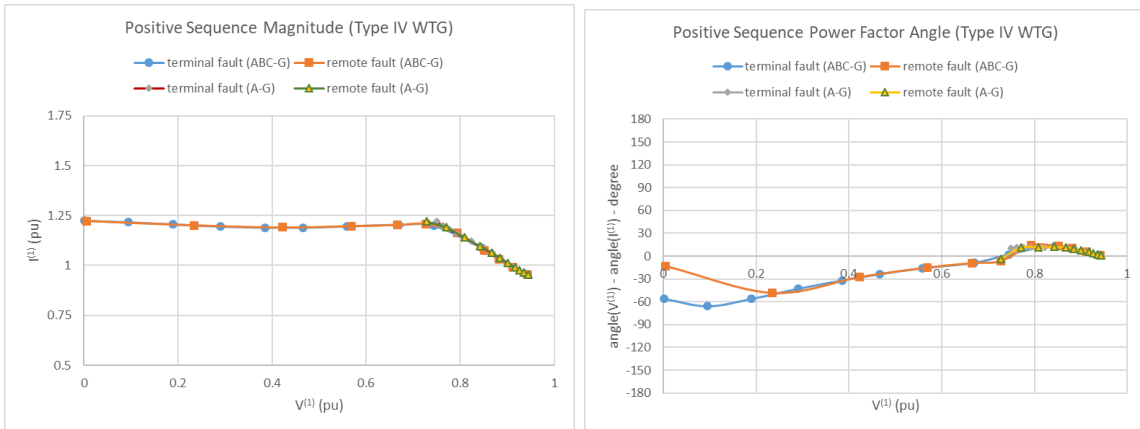


Fig. A.2-2. Positive sequence magnitudes and power factor angle after five cycles.

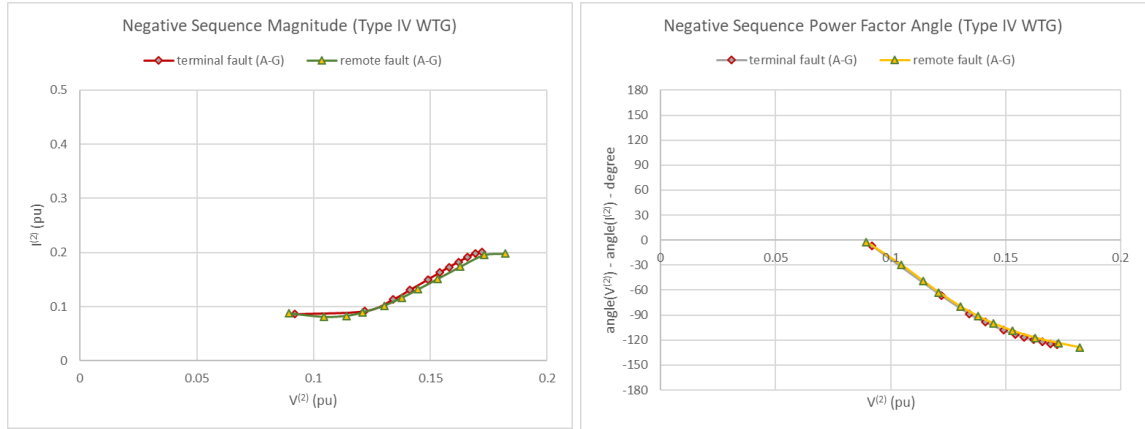


Fig. A.2-3. Negative sequence magnitudes and power factor angle after one cycle.

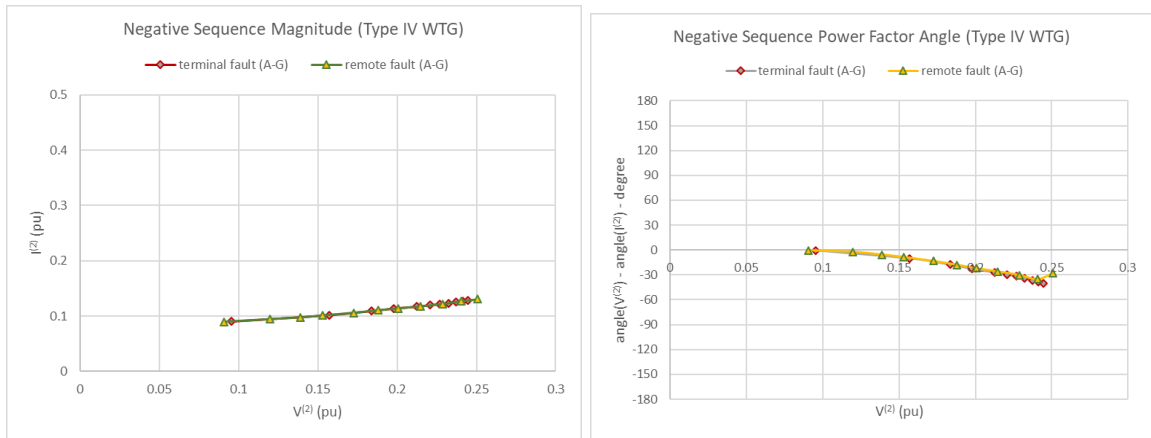


Fig. A.2-4. Negative sequence magnitudes and power factor angle after five cycles.

A.2.3 Generic Type-IV WTG based on IEC standard 61400-27-1 (2015)

This section presents another Type-IV wind farm simulated in PSCAD using the controls described in IEC Standard 61400-27-1 [21]. The single WTG in the wind farm is rated at 0.9kV, 6MW, 50Hz. The ratings of the internal transformer are adjusted to match with the WTG ratings. The controller is set to PV and ac voltage modes.

The performance of this WTG is captured in plots shown in Figure A.2-5 and A.2-6.



Fig. A.2-5. Magnitudes and power factor angle of Type-IV WTG modeled as per IEC Standard 61400-27-1, after one cycle.

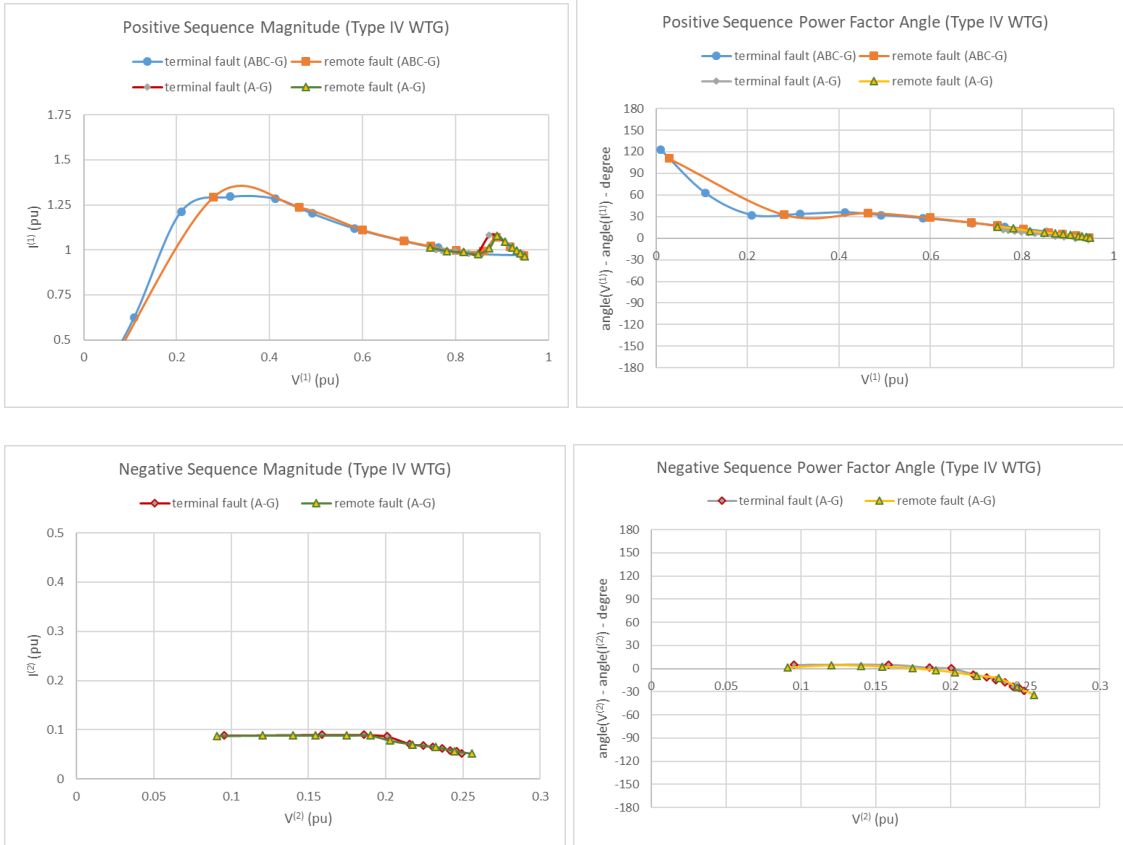


Fig. A.2-6. Magnitudes and power factor angle of Type-IV WTG modeled as per IEC Standard 61400-27-1, after five cycles.

APPENDIX B – DATA PROVIDED BY OEM – TYPE-IV WTG

This document provides the short-circuit current information, provided by an OEM (name not disclosed as requested by the OEM due to confidentiality), as needed to model a Type-IV WTG for balanced faults based on the tabular format described in section 3.

The currents in the table are provided in PU at converter rated power and valid for a 2.3MW WTG. Please note these short-circuit currents are valid after 50ms from fault inception. These data points also assume that pre fault grid voltage was at 1.0 pu and WTG was delivering full active power. Maximum short-circuit current of 2.3MW WTG during initial 50ms is 1.65 pu for 3 phase balanced fault.

Only the yellow highlighted columns are needed for the modeling in commercial programs. d-axis and q-axis currents are provided to show the split between active and reactive components of the total current.

Table B-1. OEM Data for Type-IV WTG Voltage-Controlled Current Source Model

Voltage in pu	d-axis current in pu	q-axis currnt in pu	total current in pu	powerfactor angle
1.000	1.000	0.000	1.000	0.00
0.900	1.000	-0.200	1.020	-11.31
0.700	0.922	-0.600	1.100	-33.06
0.500	0.458	-1.000	1.100	-65.38
0.300	0.458	-1.000	1.100	-65.38
0.100	0.458	-1.000	1.100	-90.00

APPENDIX C – SIMULATION AND ANALYSIS OF SEQUENCE FAULT VOLTAGE-CURRENT CHARACTERISTICS OF A TYPE-III GE WTG

C.1 Simulation of Faults

EMT Simulations were performed representing one particular combination of generator, converter, converter controls and parameter set that are commonly used for a particular GE WTG. The magnitude and angle of fault current from the turbines may vary substantially with changes to converter control parameters that are tuned to meet grid code requirements associated to active and reactive current injection during fault conditions and/or to achieve system stability on a project specific basis. Additionally, initial active power output, electrical machine characteristics and grid strength can affect the results reported. Therefore, the tables shown below may be considered as one example of the nature of fault currents that can be seen. The one-line diagram of the simulated system is shown in Figure C.1.

Three-phase-to-ground and single-phase-to-ground faults were simulated for two different pre-fault power output levels (100% and cut-in wind speed operation) and various fault inception point of wave timing. Results are shown for faults with a short-circuit ratio (SCR) of 2.0 simulating a weak grid, where reciprocal of SCR is the grid impedance (Z_{Grid}). Fault impedance, Z_{fault} is varied to get the desired fault voltage, referred to as residual voltage (V_{res}) for 10 different scenarios from 1 thru 10 – residual voltage is higher for scenario 10 than scenario 1. All results presented in this document are in per unit (pu) with 34.5 kV as the base voltage, typical collector system voltage, and based on machine MW as base MVA. WTG transformer has 5.75% impedance. Grid impedance, Z_{Grid} , is primarily inductive with a very small resistive component.

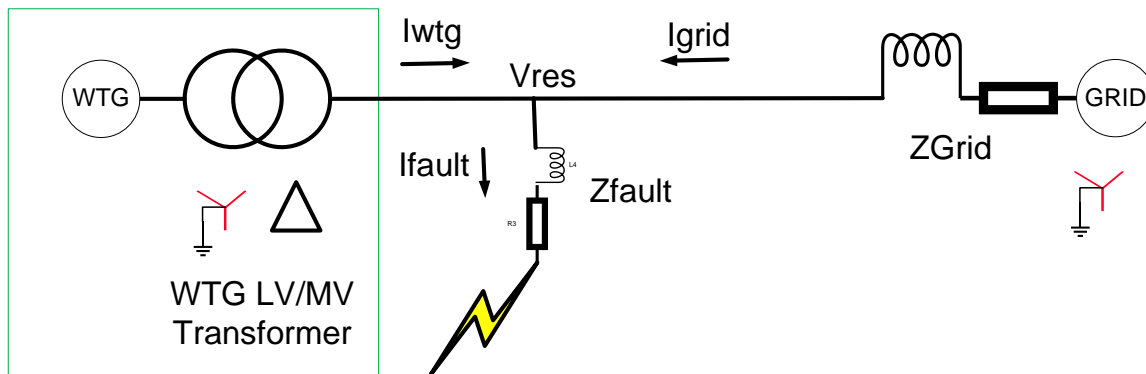


Figure C.1 – One-line diagram of the simulated system.

C.2 Faults Performance Characteristics

WTG terminal voltage (V_{res}) and current (I_{wtg}) behavior for three-phase-to-ground and single-phase-to-ground faults are shown in Table C.1 through Table C.3 for 100% of prefault power output conditions and for Short-Circuit Ratio (SCR) of 2. Prefault (1 cycle prior) information is shown along with the information at the fault inception (0 cycle) and after 1-6 cycles of fault in steps of 1 cycle.

Table C.1: Three-phase-to-ground Fault Positive Sequence Voltage-Current for SCR 2

Time (Cycle)	Parameter	Residual Voltage Scenario									
		1	2	3	4	5	6	7	8	9	10
-1	Voltage (pu)	1.10	1.10	1.10	1.10	1.10	1.10	1.10	1.10	1.10	1.10
	Current (pu)	0.91	0.91	0.91	0.91	0.91	0.91	0.91	0.91	0.91	0.91
	Angle (Deg)	7.70	7.70	7.70	7.70	7.70	7.70	7.70	7.70	7.70	7.70
0	Voltage (pu)	1.10	1.10	1.10	1.10	1.10	1.10	1.10	1.10	1.10	1.10
	Current (pu)	0.91	0.91	0.91	0.91	0.91	0.91	0.91	0.91	0.91	0.91
	Angle (Deg)	7.69	7.70	7.70	7.70	7.70	7.70	7.70	7.70	7.70	7.70
1	Voltage (pu)	0.00	0.13	0.25	0.39	0.53	0.65	0.75	0.84	0.93	1.02
	Current (pu)	1.59	1.33	1.17	1.16	1.14	1.03	0.93	0.91	0.94	0.92
	Angle (Deg)	–	-62.31	-56.01	-51.54	-49.88	-48.04	-33.92	-18.58	-7.52	-0.26
2	Voltage (pu)	0.00	0.09	0.20	0.31	0.43	0.62	0.75	0.87	0.96	1.04
	Current (pu)	0.41	0.45	0.78	0.82	0.75	1.30	1.31	1.22	1.06	0.98
	Angle (Deg)	–	-71.11	-46.88	-42.43	-41.67	-34.18	-29.15	-25.77	-17.67	-4.73
3	Voltage (pu)	0.00	0.13	0.26	0.39	0.53	0.68	0.81	0.92	0.99	1.05
	Current (pu)	1.22	1.20	1.38	1.42	1.31	1.44	1.41	1.20	1.00	0.97
	Angle (Deg)	–	-84.84	-59.09	-54.13	-52.58	-47.69	-41.53	-34.40	-21.67	-5.77
4	Voltage (pu)	0.00	0.13	0.25	0.38	0.53	0.68	0.82	0.95	1.02	1.05
	Current (pu)	1.33	1.29	1.41	1.33	1.33	1.35	1.25	1.22	1.06	0.97
	Angle (Deg)	–	-81.14	-52.05	-54.92	-52.89	-46.75	-44.52	-38.51	-24.99	-6.67
5	Voltage (pu)	0.00	0.12	0.23	0.38	0.52	0.66	0.81	0.95	1.02	1.06
	Current (pu)	1.21	1.24	1.28	1.20	1.22	1.36	1.29	1.23	1.09	0.97
	Angle (Deg)	–	-78.92	-51.20	-65.27	-59.05	-42.08	-40.84	-37.08	-25.29	-7.43
6	Voltage (pu)	0.00	0.12	0.24	0.38	0.53	0.65	0.80	0.95	1.03	1.06
	Current (pu)	1.20	1.15	1.21	1.15	1.18	1.37	1.33	1.26	1.10	0.97
	Angle (Deg)	–	-83.61	-58.28	-76.48	-63.98	-40.17	-37.79	-35.04	-24.68	-8.12

Table C.1 shows that, for a given residual voltage scenario and for the specific converter parameters and grid conditions represented in the simulation, the variation of positive sequence fault current magnitude between cycles 3 and 6 after fault initiation is within $\pm 10\%$ of the median value. Also, the variation of angle between positive

sequence fault voltage and positive sequence fault current between cycles 3 and 6 is within ± 10 degrees of the median value.

Table C.2: Single-phase-to-ground Fault Positive Sequence Voltage-Current for SCR 2

Time (Cycle)	Parameter	Residual Voltage Scenario									
		1	2	3	4	5	6	7	8	9	10
-1	Voltage (pu)	1.10	1.10	1.10	1.10	1.10	1.10	1.10	1.10	1.10	1.10
	Current (pu)	0.91	0.91	0.91	0.91	0.91	0.91	0.91	0.91	0.91	0.91
	Angle (Deg)	7.70	7.70	7.70	7.70	7.70	7.70	7.70	7.70	7.70	7.70
0	Voltage (pu)	1.10	1.10	1.10	1.10	1.10	1.10	1.10	1.10	1.10	1.10
	Current (pu)	0.91	0.91	0.91	0.91	0.91	0.91	0.91	0.91	0.91	0.91
	Angle (Deg)	7.76	7.72	7.71	7.71	7.71	7.70	7.70	7.70	7.70	7.70
1	Voltage (pu)	0.75	0.79	0.88	0.91	0.94	0.96	0.99	1.01	1.04	1.07
	Current (pu)	1.19	1.12	1.06	0.99	0.94	0.90	0.89	0.90	0.92	0.92
	Angle (Deg)	-13.00	-15.29	-22.70	-20.45	-16.76	-12.08	-6.95	-1.68	2.29	4.87
2	Voltage (pu)	0.76	0.77	0.81	0.87	0.92	0.97	1.00	1.03	1.06	1.08
	Current (pu)	0.82	0.68	1.31	1.33	1.27	1.16	1.08	1.02	0.97	0.94
	Angle (Deg)	-34.86	-35.27	-4.74	-5.99	-8.07	-9.69	-7.74	-4.92	-1.02	3.37
3	Voltage (pu)	0.81	0.84	0.82	0.86	0.92	0.96	1.02	1.04	1.06	1.08
	Current (pu)	1.23	1.18	1.41	1.40	1.26	1.15	1.08	1.01	0.96	0.93
	Angle (Deg)	-18.31	-17.63	-9.01	-8.03	-8.66	-7.61	-9.82	-6.09	-1.55	3.14
4	Voltage (pu)	0.78	0.81	0.86	0.91	0.95	0.98	1.02	1.06	1.07	1.09
	Current (pu)	1.36	1.36	1.34	1.37	1.23	1.15	1.01	1.00	0.96	0.93
	Angle (Deg)	-13.58	-12.67	-12.71	-13.29	-12.52	-11.16	-10.35	-8.22	-2.14	2.80
5	Voltage (pu)	0.79	0.83	0.87	0.92	0.97	1.01	1.04	1.06	1.07	1.09
	Current (pu)	1.29	1.31	1.33	1.36	1.24	1.15	1.06	1.00	0.96	0.93
	Angle (Deg)	-17.60	-16.42	-15.96	-15.13	-16.01	-15.73	-12.65	-7.69	-2.59	2.54
6	Voltage (pu)	0.80	0.84	0.88	0.92	0.97	1.02	1.05	1.06	1.08	1.09
	Current (pu)	1.16	1.19	1.26	1.30	1.20	1.10	1.04	0.99	0.95	0.92
	Angle (Deg)	-20.86	-19.45	-16.80	-14.79	-15.89	-17.76	-15.48	-8.30	-3.08	2.28

Table C.2 shows that, for a given residual voltage scenario and for the specific converter parameters and grid conditions represented in the simulation, the variation of positive sequence fault current magnitude between cycles 3 and 6 is within $\pm 10\%$ of the median value. Also, the variation of angle between positive sequence fault voltage and positive sequence fault current between cycles 3 and 6 is within ± 5 degree of the median value, except for scenarios with positive sequence residual voltage levels close to 1 pu (scenarios 6 to 10).

Table C.3: Single-phase-to-ground Fault Negative Sequence Voltage-Current for SCR 2

Time (Cycle)	Parameter	Residual Voltage Scenario									
		1	2	3	4	5	6	7	8	9	10
-1	Voltage (pu)	0.00	0.00	0.00	0.00	0.00	0.00	0.00	0.00	0.00	0.00
	Current (pu)	0.00	0.00	0.00	0.00	0.00	0.00	0.00	0.00	0.00	0.00
	Angle (Deg.)	-	-	-	-	-	-	-	-	-	-
	Resistance (pu)	-	-	-	-	-	-	-	-	-	-
	Reactance (pu)	-	-	-	-	-	-	-	-	-	-
0	Voltage (pu)	0.00	0.00	0.00	0.00	0.00	0.00	0.00	0.00	0.00	0.00
	Current (pu)	0.00	0.00	0.00	0.00	0.00	0.00	0.00	0.00	0.00	0.00
	Angle (Deg.)	-	-	-	-	-	-	-	-	-	-
	Resistance (pu)	-	-	-	-	-	-	-	-	-	-
	Reactance (pu)	-	-	-	-	-	-	-	-	-	-
1	Voltage (pu)	0.21	0.19	0.19	0.17	0.14	0.12	0.09	0.07	0.06	0.03
	Current (pu)	0.77	0.69	0.62	0.54	0.45	0.37	0.28	0.20	0.12	0.05
	Angle (Deg.)	141.78	143.88	121.34	120.76	122.64	125.15	129.04	136.46	148.53	153.25
	Resistance (pu)	0.22	0.22	0.16	0.16	0.17	0.18	0.21	0.27	0.39	0.48
	Reactance (pu)	0.17	0.16	0.26	0.26	0.26	0.26	0.26	0.25	0.24	0.24
2	Voltage (pu)	0.23	0.20	0.19	0.17	0.14	0.12	0.10	0.08	0.05	0.03
	Current (pu)	0.78	0.67	0.56	0.49	0.43	0.36	0.28	0.19	0.11	0.05
	Angle (Deg.)	111.76	110.79	130.40	132.51	140.10	148.14	149.94	155.06	157.13	152.49
	Resistance (pu)	0.11	0.11	0.22	0.23	0.25	0.29	0.30	0.36	0.47	0.42
	Reactance (pu)	0.27	0.28	0.25	0.25	0.21	0.18	0.18	0.17	0.20	0.22
3	Voltage (pu)	0.25	0.23	0.18	0.17	0.15	0.13	0.10	0.08	0.06	0.03
	Current (pu)	0.77	0.68	0.61	0.50	0.40	0.32	0.26	0.17	0.10	0.05
	Angle (Deg.)	122.96	123.41	133.47	134.37	133.92	139.42	149.67	149.69	147.05	144.57
	Resistance (pu)	0.18	0.19	0.20	0.23	0.26	0.32	0.34	0.42	0.51	0.46
	Reactance (pu)	0.27	0.29	0.21	0.24	0.27	0.27	0.20	0.24	0.33	0.33
4	Voltage (pu)	0.24	0.21	0.20	0.18	0.16	0.14	0.12	0.09	0.06	0.03
	Current (pu)	0.75	0.66	0.58	0.50	0.39	0.31	0.22	0.16	0.09	0.04
	Angle (Deg.)	123.95	126.19	128.39	130.42	132.29	132.62	140.39	147.06	140.52	136.93
	Resistance (pu)	0.18	0.19	0.21	0.23	0.27	0.30	0.41	0.48	0.53	0.48
	Reactance (pu)	0.26	0.26	0.27	0.28	0.30	0.33	0.34	0.31	0.43	0.44
5	Voltage (pu)	0.24	0.22	0.20	0.18	0.17	0.14	0.12	0.09	0.06	0.03
	Current (pu)	0.75	0.66	0.58	0.50	0.39	0.31	0.22	0.15	0.08	0.04
	Angle (Deg.)	121.89	122.96	126.93	129.48	128.06	124.25	131.51	143.94	132.96	130.96
	Resistance (pu)	0.17	0.18	0.21	0.23	0.26	0.26	0.36	0.49	0.54	0.48
	Reactance (pu)	0.27	0.28	0.28	0.28	0.33	0.39	0.41	0.36	0.58	0.56
6	Voltage (pu)	0.25	0.22	0.20	0.18	0.16	0.14	0.12	0.10	0.06	0.03
	Current (pu)	0.72	0.65	0.57	0.49	0.40	0.30	0.21	0.14	0.08	0.04
	Angle (Deg.)	121.89	123.52	129.82	133.92	133.90	127.45	127.10	143.88	129.58	126.77
	Resistance (pu)	0.18	0.19	0.23	0.26	0.28	0.29	0.35	0.55	0.53	0.49
	Reactance (pu)	0.29	0.29	0.28	0.27	0.29	0.38	0.46	0.40	0.64	0.65

Table C.3 shows that, for a given residual voltage scenario and for the specific converter parameters and grid conditions represented in the simulation, the variation of negative sequence fault current magnitude between cycles 3 and 6 is within ± 0.025 pu of the median value. Also, the variation of angle between negative sequence fault voltage and negative sequence fault current between cycles 3 and 6 is within ± 10 degree of the median value, except for scenarios with positive sequence residual voltage close to 1 pu (scenarios 6 to 10).

Using negative sequence voltage and negative sequence current for the specific converter parameters and grid conditions represented in the simulation, it can be observed that the generator has a behavior approximated to a negative sequence resistance and reactance of 0.2pu and 0.28 pu respectively. This is observed for faults with negative sequence voltages greater than 0.15 pu.

Comparison of 100% pre-fault output and low power conditions (cut-in wind speed) shows that:

1. 100% pre-fault cases results in higher positive sequence current contributions in shallow faults due to the larger load current.
2. No significant impact of pre-fault loading on negative sequence response was observed.

Higher values of SCR result in comparable positive and negative sequence response during the fault period, also affected by converter control parameters. The performance after fault clearing is considerably affected by system strength even for a given converter control parameter set.

APPENDIX D – DATA PROVIDED BY VESTAS – TYPE-IV WTG

Data provided by Vestas for the Type-IV WTG are shown in tables below¹:

For 3-phase faults:

Positive Sequence																				
WTG Terminal Voltage (pu)	0		0.1		0.2		0.3		0.4		0.5		0.6		0.7		0.8		0.9	
	Current (pu)	Power Factor	Current (pu)	Power Factor	Current (pu)	Power Factor	Current (pu)	Power Factor	Current (pu)	Power Factor	Current (pu)	Power Factor	Current (pu)	Power Factor	Current (pu)	Power Factor	Current (pu)	Power Factor	Current (pu)	Power Factor
Initial Maximum current (peak, pu)	1.52	0.638	1.524	0.79	1.52	0.86	1.515	0.919	1.508	0.912	1.499	0.897	1.515	0.924	1.565	0.923	1.548	0.981	1.485	0.999
After 1 cycle (pu)	0.8966	-0.033	0.912	0.448	0.969	0.3211	0.968	0.396	0.971	0.359	0.94	0.431	0.989	0.763	1.148	0.93	1.224	0.985	1.111	0.999
After 2 cycles (pu)	0.3899	0.028	0.612	0.391	1.083	0.335	1.083	0.36	1.084	0.355	0.907	0.439	0.92	0.767	1.14	0.932	1.254	0.987	1.115	0.999
After 5 cycles (pu)	0.394	0.065	0.611	0.418	1.074	0.326	1.075	0.355	1.076	0.362	0.896	0.432	0.946	0.77	1.146	0.935	1.26	0.987	1.117	0.999
Negative Sequence																				
WTG Terminal Voltage (pu)	0		0.1		0.2		0.3		0.4		0.5		0.6		0.7		0.8		0.9	
	Current (pu)	Power Factor	Current (pu)	Power Factor	Current (pu)	Power Factor	Current (pu)	Power Factor	Current (pu)	Power Factor	Current (pu)	Power Factor	Current (pu)	Power Factor	Current (pu)	Power Factor	Current (pu)	Power Factor	Current (pu)	Power Factor
Initial Maximum current (peak, pu)	0.072	-0.257	0.08	0.164	0.068	-0.2565	0.0709	-0.252	0.0661	-0.139	0.0591	-0.245	0.0689	0.208	0.061	-0.595	0.0255	-0.485	0.0137	-0.236
After 1 cycle (pu)	0.0405	-0.016	0.053	-0.0558	0.1209	-0.0795	0.125	-0.064	0.1267	-0.067	0.112	-0.0644	0.0571	-0.139	0.025	-0.286	0.013	-0.216	0.011	-0.094
After 2 cycles (pu)	0.013	0.983	0.0088	-0.0517	0.0018	0.246	0.0061	0.528	0.0093	0.374	0.007	0.8364	0.0147	0.241	0.009	0.949	0.005	0.231	0.001	0.332
After 5 cycles (pu)	0.0005	0.41	0.001	0.745	0.0002	-0.075	0.0003	-0.976	0.0002	0.721	0.0003	-0.676	0.0008	-0.737	0.0008	-0.736	0.0001	0.165	0.0003	0.143

For Line to Line to Ground Fault:

Positive Sequence																				
WTG Terminal Voltage (pu)	0		0.1		0.2		0.3		0.4		0.5		0.6		0.7		0.8		0.9	
	Current (pu)	Power Factor	Current (pu)	Power Factor	Current (pu)	Power Factor	Current (pu)	Power Factor	Current (pu)	Power Factor	Current (pu)	Power Factor	Current (pu)	Power Factor	Current (pu)	Power Factor	Current (pu)	Power Factor	Current (pu)	Power Factor
Initial Maximum current (peak, pu)	1.507	0.72	1.503	0.815	1.499	0.837	1.496	0.877	1.491	0.92	1.487	0.9208	1.486	0.94	1.482	0.931	1.493	0.996	1.494	0.995
After 1 cycle (pu)	0.908	0.963	0.893	0.99	0.881	0.998	0.875	0.998	0.88	0.986	0.893	0.987	0.888	0.987	0.906	0.993	0.982	0.997	1.083	0.999
After 2 cycles (pu)	0.586	0.96	0.594	0.995	0.612	0.999	0.63	0.977	0.715	0.978	0.795	0.95	0.751	0.973	0.744	0.992	0.808	0.997	0.945	0.999
After 5 cycles (pu)	0.586	0.976	0.594	0.985	0.611	0.999	0.632	0.991	0.724	0.983	0.802	0.952	0.766	0.976	0.77	0.986	0.838	0.997	0.965	0.999
Negative Sequence																				
WTG Terminal Voltage (pu)	0		0.1		0.2		0.3		0.4		0.5		0.6		0.7		0.8		0.9	
	Current (pu)	Power Factor	Current (pu)	Power Factor	Current (pu)	Power Factor	Current (pu)	Power Factor	Current (pu)	Power Factor	Current (pu)	Power Factor	Current (pu)	Power Factor	Current (pu)	Power Factor	Current (pu)	Power Factor	Current (pu)	Power Factor
Initial Maximum current (peak, pu)	0.073	-0.984	0.077	-0.965	0.082	-0.985	0.086	-0.952	0.069	-0.997	0.093	-0.937	0.072	-0.887	0.066	-0.834	0.062	-0.68	0.041	-0.604
After 1 cycle (pu)	0.053	-0.991	0.046	-0.997	0.04	-0.985	0.038	-0.988	0.042	-0.932	0.047	-0.88	0.042	-0.824	0.032	-0.732	0.015	-0.629	0.014	-0.483
After 2 cycles (pu)	0.019	-0.991	0.02	-0.99	0.022	-0.974	0.027	-0.951	0.021	-0.918	0.034	-0.869	0.02	-0.814	0.016	-0.727	0.019	-0.608	0.018	-0.435
After 5 cycles (pu)	0.021	-0.991	0.021	-0.991	0.02	-0.976	0.02	-0.955	0.019	-0.921	0.018	-0.873	0.016	-0.816	0.013	-0.728	0.011	-0.608	0.007	-0.437

¹ For the purpose of the data given in these tables, negative power factor, though provided by the manufacturer, may simply be the result of calculation for negligibly small currents.

APPENDIX E – TYPE-III WTG MODEL PARAMETERS

Table E- 1. Parameters of the Wind Generator Model Fault 1 (230 kV).

Parameters	Value	Units
Wind park		
Number of wind turbines	66	
Frequency	60	Hz
Collector grid nominal voltage	34.5	kV
Transmission grid nominal voltage	230	kV
Zig-zag transformer on collector grid		
R0	0.1265	Ω
L0	0.3831	mH
Single wind turbine parameters		
Wind turbine generator type	Type-III	DFIG
Wind turbine rated power	1.667	MVA
Wind turbine active power	1.5	MW
Generator nominal voltage	0.575	kV
Filter reactive power	75	kVar
Equivalent collector grid		
Resistance	0.1265	Ω
Inductance	0.3831	mH
Capacitance	7	mF
Operating conditions		
Number of wind turbines in service	66	
Pre-fault Q	-0.01236	pu
Wind speed	7.1885	m/s
Wind park transformer		
Connection type	DACY	
Nominal power	100	MVA
Turbine-side voltage	34.5	kV
Grid-side voltage	230	kV
Winding R	0.003	pu
Winding X	0.12	pu
Wind turbine transformer		
Connection type	DACY	
Nominal power	1.75	MVA
Turbine-side voltage	34.5	kV
Converter-side voltage	0.575	kV
Winding R	0.002	pu
Winding X	0.06	pu

DFIG		
Number of poles	6	
Stator winding resistance Rs	0.033	pu
Stator leakage inductance Lls	0.18	pu
Magnetizing inductance Lmd	2.9	pu
Magnetizing inductance Lmq	2.9	Pu
Rotor resistance Rr	0.026	pu
Rotor leakage inductance Llr	0.16	pu
Inertia constant Hgen	0.9	s
Wind park controller		
V-control Kv	2	
Q-control Kp	0	
Q-control Ki	0.15	ms
Rotor-side converter control		
Fault current limit	1.1	pu
Fault d-axis current limit	1	pu
Fault q-axis current limit	1	pu
FRT voltage deviation	0.1	pu
Grid-side converter control		
Fault current limit	0.4	pu
Fault q-axis current limit	0.25	pu
Fault d-axis current limit	0.25	pu

Table E- 2. Parameters of the Wind Generator Model for Fault 2 (115 kV).

Parameters	Value	Units
Wind park		
Number of wind turbines	11	
Frequency	60	Hz
Collector grid nominal voltage	34.5	kV
Transmission grid nominal voltage	115	kV
Zig-zag transformer on collector grid		
R0	0.1265	Ω
L0	0.3831	mH
Single wind turbine parameters		
Wind turbine generator type	Type-III	DFIG
Wind turbine rated power	1.667	MVA
Wind turbine active power	1.5	MW
Generator nominal voltage	0.575	kV
Filter reactive power	75	kVar
Equivalent collector grid		
Resistance	0.1265	Ω
Inductance	0.3831	mH

Capacitance	7	mF
Operating conditions		
Number of wind turbines in service	11	
Pre-fault Q	0.17	pu
Wind speed	11.5475	m/s
Wind park transformer		
Connection type	DACY	
Nominal power	15	MVA
Turbine-side voltage	34.5	kV
Grid-side voltage	115	kV
Winding R	0.005	pu
Winding X	0.18	pu
Wind turbine transformer		
Connection type	DACY	
Nominal power	1.75	MVA
Turbine-side voltage	34.5	kV
Converter-side voltage	0.575	kV
Winding R	0.002	pu
Winding X	0.06	pu
DFIG		
Number of poles	6	
Stator winding resistance Rs	0.033	pu
Stator leakage inductance Lls	0.18	pu
Magnetizing inductance Lmd	2.9	pu
Magnetizing inductance Lmq	2.9	Pu
Rotor resistance Rr	0.026	pu
Rotor leakage inductance Llr	0.16	pu
Inertia constant Hgen	0.9	s
Wind park controller		
V-control Kv	2	
Q-control Kp	0	
Q-control Ki	0.15	ms
Rotor-side converter control		
Fault current limit	1.1	pu
Fault d-axis current limit	1	pu
Fault q-axis current limit	1	pu
FRT voltage deviation	0.1	pu
Grid-side converter control		
Fault current limit	0.4	pu
Fault q-axis current limit	0.25	pu
Fault d-axis current limit	0.25	pu